TABLE OF CONTENTS

LIST OF TABLES

LIST OF FIGURES

LIST OF ABREVIATIONS

ANSI	American National Standards Institute
CEP	Closed Earpiece Device
CR	Criterion Level
CSA	Canadian Standards Association
DC	Direct Current
ECE	Earcanal Entrance
ER	Exchange Rate
ETS	École de technologie supérieure
HPD	Hearing Protection Device
ICAR	Infrastructure commune en acoustique pour la recherche ÉTS-IRSST
IEC	International Electrotechnical Commission
IEM	Inner-Ear Microphone
IRSST	Institut de recherche Robert-Sauvé en santé et en sécurité du travail
ISLM	Integrating Sound Level Meter
ISO	International Organization for Standardization
MEC	Microphone-to-Eardrum Correction
NIHL	Noise-Induced Hearing Loss
NIOSH	National Institute for Occupational Safety and Health
NRR	Noise Reduction Rate

OED	Open-Ear Device
OEM	Outer-Ear Microphone
OSHA	Occupational Safety and Health Administration
PSEM	Personal Sound Exposure Meter
REAT	Real-Ear Attenuation at Threshold
REL	Recommended Exposure Limit
RMS	Root Mean Square
SLM	Sound Level Meter
SPL	Sound Pressure Level
WHO	World Health Organization
WID	Wearer-Induced Disturbance

LIST OF SYMBOLS AND UNITS OF MEASUREMENTS

$L_{eq,T}$	Equivalent sound pressure level over a period of time T [dBA]
$L_{eq,8h}$	Equivalent sound pressure level over 8 h [dBA]
L_c	Equivalent constant noise level allowed for 8 h work shift [dBA]
$L_{ex,T}$	Sound level energy-averaged over a period of time T [dBA]
p_0	Reference sound pressure of 20 μ [Pa].
p	Sound pressure [Pa]
γ^2	Coherence function [—]
f	Frequency [Hz]
L_p	Acoustic pressure level [dB]
t	Measurement time duration [h]
T	Reference time duration [h]

INTRODUCTION

The assessment of noise exposure is a core element of any hearing conservation program. It relies on a set of well-known measurement procedures, often standardized such as with CSA Z107.56 - CSA (2013), and the use of specialized equipment such as sound level meters (SLM) and personal noise dosimeters (PND). Nevertheless, the information that is acquired by this equipment and these methods often fails to properly estimate the exact amount of noise energy reaching each individual's ear: the measurements are conducted over a short period of time, which may not represent the effective exposure nor take into account the large variability of noise levels that the worker may be exposed to during an entire work shift. Moreover, when hearing protection devices (HPD) are worn, noise exposure estimates are commonly done by subtracting the attenuation provided by the protector from the external noise measurement levels. While apparently straightforward, this procedure is known to be very approximate and to lead to high uncertainties and variabilities, detailed hereafter, given that many factors can have a large influence on the attenuation that is expected from these HPDs. For example, earcanal geometry, insertion depth and day-to-day usage can all affect the level of attenuation provided during a work shift. Consequently, a reliable estimation of the effective noise exposure levels remains a huge challenge, given the high variability of the ambient noise levels, which are hardly measured with traditional SLM or PND, and the large variability in the HPD attenuation values. These large variabilities result, in turn, in the large uncertainties traditionally associated with personal noise exposure assessment.

To reduce these uncertainties in the measurements, in-ear noise dosimetry (IEND) is gaining attention. IEND is capable of providing more reliable estimates of what is occuring directly inside the earcanal. However, at the present, most IEND systems fail to take into account the necessary corrections needed to convert the sound pressure levels (SPL) measured at a specific location within the earcanal, to "equivalent free-field" levels, as prescribed by occupational

noise exposure standards (such as CSA Z107.56 - CSA (2013)), as these corrections may vary significantly from one individual to another.

Another relevant aspect that has to be considered when performing such IEND measurements, is that their measurements can be dramatically affected by any noise emitted by the wearer, such as vocal sound, coughing, throat-clearing, etc. Therefore, a reliable IEND system should be able to detect and estimate the noise generated by the wearer (later referred to as Wearer Induced Disturbances, WID) and distinguish them from the noise exposure of ambient sounds.

This master's thesis presents the implementation of a low computational method to perform in-ear noise dosimetry under an earplug or in the open ear. This method addresses the two limitations previously mentioned, by making the necessary individual corrections to the Sound Pressure Level (SPL) measured inside the earcanal and by detecting and calculating the WID contributions.

The IEND algorithms are based on the doctoral work of Bonnet *et al.* (2019a), École de technologie supérieure (2018) and Bonnet *et al.* (2018a, 2019b); and their implementation in specifically designed prototypes are presented in this master's thesis. Figure 0.1 shows the similarities and specific objectives of the work of Bonnet *et al.* as well as those presented in the current master's thesis. This diagram clearly illustrates that while Bonnet *et al.* focussed on the theoretical development of an improved IEND method, this master's thesis work deals with the practical aspects of the development of the method, from prototype construction to real-time acquisition/processing as well as experimental validation. Important to notice that the term "real-time" used all over this document is intended to convey the idea of "on the fly" operation rather than that specific meaning normally employed in software engineering.

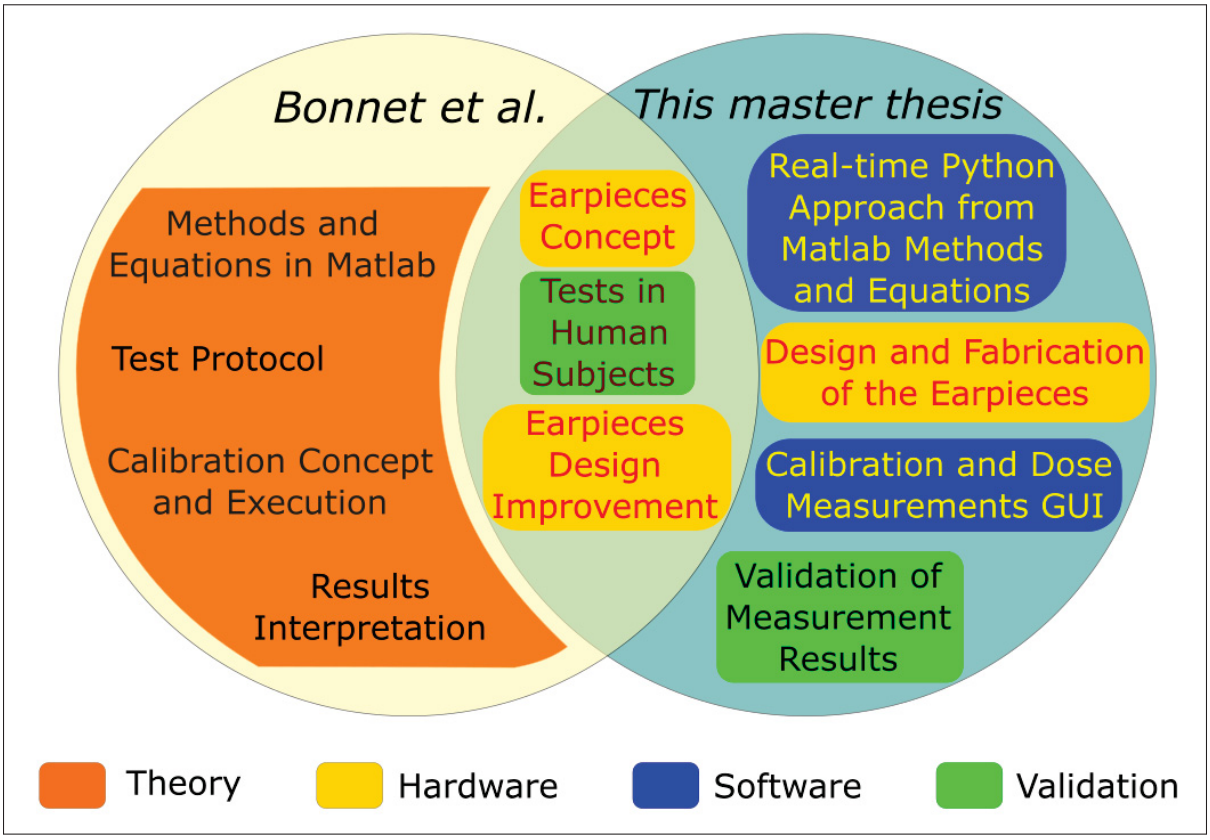

Figure 0.1 Venn diagram showing specific and overlapping areas of prior doctoral work from Bonnet and the current master's thesis
Orange area represents the theoretical aspects, green area, the validation aspects and the blue and yellow areas refer respectively to software and hardware implementations done within the current master's thesis

The approach developed by Bonnet *et al.* consists in measuring the noise levels in the earcanal of individuals in typical workplace conditions such as with unprotected ears or with ears protected by earplugs or earmuffs. The developed method utilizes two miniature microphones located respectively inside and outside the earcanal. This makes it possible to take into account individual characteristics (shape and length of the earcanal) when estimating acoustical correction factors required to convert the measured in-ear SPLs to equivalent free-field values.

These correction factors are extremely important, as the damage risk criteria (i.e. the risk of suffering Noise-Induced Hearing Loss (NIHL) because of excessive noise exposure) are

established based on "free-field equivalent" levels in most Occupational Health and Safety (OHS) regulations.

The measurement approach developed by Bonnet *et al.* (2019b,a) relied on algorithms developed in Matlab (MathWorks, Natick, MA, USA) scripts and was validated through experimental measurements on human subjects. First, the developed method establishes a relation between the SPL values read along the earcanal and the values at the eardrum itself, the so-called Microphone to Eardrum Correction (MEC), then it establishes a relation between the eardrum levels and the "free-field equivalent". Secondly, as part of the developed method, a low computational algorithm (Bonnet *et al.* (2019b)) was designed to perform in-ear noise dosimetry measurements under an earplug while excluding the WIDs.

Objectives

The overall objective of this master's thesis is to develop a real-time measurement system and algorithms for measuring in-ear sound exposure levels of workers exposed to noise, wearing HPDs or not, in real work conditions. This would also make possible the simultaneous monitoring of the effective noise exposure received by a given individual.

To achieve this objective the algorithms previously developed by Bonnet *et al.* for IEND need to be implemented into a real-time portable system featuring an earpiece equipped with two miniaturized microphones.

More specifically, the sub-goals of this master's project are as follows:

1. **Hardware development**

    a. Design, develop and construct two prototypes of dosimetric earpieces: one for use under an earplug and the other for an open ear. These two earpieces are expected to perform measurements at the entrance and inside the earcanal to enable the assessment of in-ear noise exposure in various noise conditions.

2. **Software development**

    a. Develop a portable real-time measurement system implementing all the algorithms required by the earpiece equipped with two miniaturized microphones;

        - Develop a graphical user interface (GUI) for the data acquisition system;
        - Develop and implement the acoustical calibration procedures required for reliable noise-dose measurements;
        - Implement the correction factors computation, linking the sound pressure levels measured with the two miniaturized microphones first to the effective levels at

the eardrum, then to the "free-field equivalent" levels prescribed in current OHS legislation;

- Implement and fine-tune the algorithm developed by Bonnet *et al.* that identify the WIDs;
- Implement noise dose calculation routines, taking into account or not the WIDs.

3. Experimental validation

a. Conduct experimental tests and validate the acoustic transparent earpiece (later referred to as Open Ear Device, OED) supporting noise measurements inside the earcanal without any induced occlusion effect. This device may be used in combination with earmuff-type protectors.

b. Conduct experimental tests and validate the dosimetric earplug (later referred to as Closed Earpiece, CEP), supporting noise measurements inside the earcanal while the ear is occluded by passive means.

Methodology

To achieve the general goal and specific sub-goals previously mentioned, both the hardware and software components of a complete measurement system needed to be designed from scratch.

As for the hardware, the required earpieces were designed to include the two miniature microphones required by the method developed by Bonnet *et al.* for the in-ear noise measurements. The audio signals were then acquired with a portable sound card specially designed for in-ear measurements (Nadon & Voix (2018)). As for the software, algorithms developed by Bonnet *et al.* (2019a) for Microphone to Eardrum Correction (MEC) calculation and Wearer Induced Disturbances (WID) detection were programmed in Python language (with specific libraries) on a low-powered wearable Intel (Intel Corporation, Santa Clara, CA, USA) mini-PC (ATOM

Z3735F processor, 2GB DD3 memory) running on Windows 10 (Microsoft Corp., Redmond, Washington, WA) operating system (OS) and featuring the portable sound card.

The detailed methodology of this master's thesis includes three distinct but complementary activities:

Prototyping development and implementation. First, two different earpiece prototypes were designed for this project: an Open Ear Device (OED) and a Closed Earpiece (CEP). The present work shows detailed and consistent information about the hardware concept, design and construction as well as the evolution of the prototyping development. These aspects are all covered in Section 2.

Software requirements and implementation. Second, this work also aims to describe in detail the implementation of the software and algorithms, further discussed in Section 3. Since the algorithms implemented were initially validated using Matlab algorithms from Bonnet *et al.* (2019a, 2018a, 2019b), the newly developed real-time algorithms using the Python software (Python Software Foundation, Wilmington, DE) are compared to the results in Matlab as a means of validation.

Experimental validation. Third, the strategies to test and validate all needed algorithms are exposed in the Section 4 - Validation tests. The first part of the validation tests concerns the individual correction factor MEC, which is used in both prototypes, OED and CEP. The final validation pertains to the detection of wearer-induced disturbances (WID), which are meant to be detected and separated from the in-ear noise coming from the wearer's environment. The WID detection algorithm applies to the CEP device specifically, since the impact of WIDs is expected to be more important inside a protected ear due, notably, to the occlusion effect.

Originality

This master's thesis is fundamentally based on the theory developed in the doctoral work of Bonnet *et al.*, however it is original and unique in the following:

1. The innovative and unique design and development of OED and CEP earpieces. These prototypes can perform MEC identification, implementing for the first time individual corrections while also being able to identify WIDs.

2. Low computational method that guarantees real-time in-ear noise dosimetry for protected and unprotected ears that simultaneously considers the necessary individual SPL corrections inside the earcanal as well as the detection and exclusion of the WIDs.

3. Real-time monitoring on a portable platform that allows the user to have an instantaneous overview of the current noise exposure and to store these for future verification and analysis.

These characteristics taken separately make this work exclusive and unique in its kind and combined they show the originality of this methodology compared to the solutions currently available on the market, which will be presented further.

Beyond having developed a valuable tool for assessing noise dose in the workplace, this project also paid attention to the practical and relevant aspects of ergonomics and robustness to improve the tool's usability for the wearer.

Contributions

This master's thesis contains several major contributions relating to three categories:

Prototyping and hardware development: a completely new hardware system was developed from scratch, featuring two instrumented earpieces (a transparent measurement earpiece and a dosimetric earplug) as well as a portable data acquisition and signal-processing platform equipped with a mini-PC, customized audio sound card and a battery power pack. The entire process of developing the two functional prototypes of earpieces and the portable platform was CAD-designed, 3D-printed, wired and assembled by the master's student.

Software implementation: all the algorithms previously developed by Bonnet in his doctoral work (Bonnet (2019)) were coded in Python, implemented on the mini-PC processor and optimized for real-time processing. A functional GUI was designed taking into account the needs of potential end-users of this measurement system.

Experimental validation: comprehensive testing of the resulting measurement system was conducted in a controlled environment against laboratory equipment and proved that the system's performance meets specifications and requirements.

In short, the project was successful in transforming a new and original theoretical approach into a fully functional prototype of an in-ear noise dose measurement device. Since then, the two devices developed and used during this master's thesis have been made available to IRSST, as originally planned in the project "Projet de recherche concertée ♯ 2013-0017 "Développement d'une méthode de mesure de l'exposition sonore effective intra-auriculaire pour une utilisation en milieu de travail" and will be used by IRSST researchers for field trials.

Furthermore, a provisional US patent application was filed on May 9th, 2018, under No. 62/669,177, covering both the measurement method and the developed earpieces for in-ear

dosimetry, under the title "Méthode de mesure de l'exposition sonore effective intra-auriculaire sous un protecteur auditif de type "bouchon"" (École de technologie supérieure (2018)). This provisional patent is about to be filed worldwide under a PCT application and the company EERS Global Technologies approached ÉTS in early 2018 to obtain a full license for the developed technology to pursue its line of advanced hearing protectors.

Finally, the technical aspects of this work have been documented in a scientific conference proceedings paper that shall be presented by the Master's student at the upcoming 26th International Congress of Sound and Vibration (ICSV26) conference (Nogarolli *et al.* (2019)).

Organization of the Master's thesis

This master's thesis is organized as follows:

The literature review in Chapter 1 presents the problem context and the possible solutions that have led to the conclusions of this work. The elements exposed in this section provide the basis for the methodology that was adopted herein.

Chapter 2 describes the hardware implementation. The system requirements are defined for both the computer platform and signal acquisition. Mechanical design constraints are also defined and prototyping fabrication is demonstrated.

Software elements are specified in Chapter 3. The chosen programming language and libraries as well as the developed software codes and algorithms are presented in great detail. A guide is also provided on how to use the above-mentioned programs.

Chapter 4 covers the system tests and also presents their results. A comparison method is then applied to validate these results with the theoretical implementation in Matlab.

Finally, the conclusion and recommendations chapter is presented showing the summary of what has been achieved so far, the limitations of the present thesis and future recommendations.

CHAPTER 1

LITERATURE REVIEW

A fairly extensive literature review on personal dosimetry was proposed by Bonnet. In this document, only a summary is thus given, followed by a focus on the existing measurement methods and systems to perform dosimetry. Finally, the methods and algorithms specifically developed by Bonnet are presented, as it represent the starting basis of the work presented in this thesis.

The literature review is divided into six different sections:

1. Problem statement;
2. Legislation and measurement procedures for noise exposure;
3. Review of existing measurement methods and systems;
4. Measurement of individual noise exposure: Bonnet's approach;
5. Earcanal geometry;
6. Summary of literature review.

1.1 Problem statement

It is estimated that a considerable number of more than 16 % of all workers in Quebec are exposed to high noise levels and hence are very likely to suffer from hearing problems in the future. Additionally at least 2.5 % of them are about to suffer from immediate consequences of occupational deafness according to Vigneault (2007). Another study among 3431 Canadians (Feder *et al.* (2017)) pointed out that over 42 % of them worked in such noisy environments in 2012 and 2013, or in the past years.

Considering this scenario, measures to correct this problem must be taken into consideration. The assessment of noise exposure level at the workplace is one of the first important action towards efficient solutions for solving this problem. However, several aspects have to be considered when assessing noise exposure.

The first one is that the noise levels estimations in the workplace are normally performed in steady conditions, or more specifically, at specific times and locations, which may not be very representative of the real exposure, given the large and considerable variations that may occur during a work-shift.

A second aspect is that current noise measurements are not made directly inside the ear-canal, but are rather performed near the subject's ears. Extra complexities are then added when the subject is wearing hearing protection devices (HPD) since in this case, noise exposure is typically obtained by subtracting the hearing protection attenuation from the external noise to obtain an estimate of the noise exposure. Although HPDs are made to provide a wide range of attenuation, known as Noise Reduction Rating (NRR), in order to be able to block certain amount of noise, there are still lot of unpredictability in the real attenuation obtained in the workplace as the it depends on various parameters such as earcanal geometry, insertion depth, usage, morphological problems in the earcanal, among many others (Berger (2003)).

As a result, obtaining realistic estimates of the noise exposure requires that the:

- environmental noise must be clearly identified;
- attenuation of the HPD must be accurately determined.

Given all the variability associated to the assessment of the environmental noise and the HPD attenuation, it is believed that an efficient way to establish the level of noise a worker is exposed to is to take continuous SPL measurements directly in the earcanal.

1.2 Legislation and measurement procedures for noise exposure

Noise exposure limits are defined by some standards regulations such as Canada Labour Standards Regulations (2019) aiming preserving the hearing health of the employees. Employers are required to follow these regulations and are being responsible to guarantee that no employee is submitted to noise exposure levels above those indicated by the regulating agencies. Appendix I - Table I-1 and Table I-2 show examples of maximum exposure level according to different legislations.

Controlling noise at the source is usually the most effective way of preventing harmful noise, but is sometimes not feasible nor realistic in some circumstances, for practical reasons or economical ones. A popular solution to protect workers against those high levels of noise exposure is to use hearing protection devices. They exist in various forms and sizes and may provide specific attenuation for many different applications and conditions.

Even though those devices are designed to provide a minimum attenuation during work operation, this attenuation can not be guaranteed for the reasons already exposed previously. In some cases not only the lack of protection is a problem, but over protection (that is, too much attenuation) may also be detrimental. The latter can expose the worker to other additional risks at work, such as miscommunication or also the impossibility of hearing vital warning sounds. Again, in order to estimate the auditory risks a worker may be subjected to, it is primordial to assess correctly the ambient noise levels as well as the attenuation those HPDs effectively provide. Unfortunately, those two conditions are rarely met in real life.

The way noise exposure or dose measurements are usually performed in the workplace is by means of either sound level meters (SLM) or personal noise dosimeters (PND). These measurement devices, explained in more details later, are used to measure the noise a worker is exposed by using microphones located near the subject's head. When a HPD is worn, an estimate of the noise exposure can be made by subtracting its attenuation rating from the noise level measured with the SLM or the PND.

This may lead to exposure level numbers that are not always very representative and reliable as this procedure takes just one picture of the current exposure levels, not considering that the subject may always be in movement, that the incident noise may vary and that the real attenuation of the HPD may change significantly over time.

It turns out that there is a lot of unpredictability when performing noise measurements and it becomes very clear that the HPD plays a big role in the whole measurement process. It was demonstrated by Nélisse *et al.* (2010) that the protection performance of HPDs can vary significantly over time during a certain work shift.

In order to solve such problems, some manufacturers developed personal dosimeters that can be incorporated in the protection devices thus being able to offer the necessary protection while taking continuous measurements over time (SVANTEK (2019); Honeywell (2019)) underneath the protector, directly in the earcanal. The advantages of such system are already known but there are still some important questions to be answered regarding the measurement of SPL directly in the occluded ear.

One these questions is related to the the wearer's own noise (e.g speech). Such noises can have an important influence on the sound pressure levels in the occluded earcanal. Hence, some techniques must be employed to identify and separate those unwanted disturbances and then make the correct reading of the out-coming values from the instrumentation.

On the other hand it is not well established in the current literature what risks those noise levels can present, although it is believed that they can be less harmful than those external ones due to biological protection mechanisms.

The CSA Z107.56-13 (CSA (2013)) recommendation presents some methods to be applied in the workplace for assessing the noise exposure. The proposed noise measurement procedures assume a certain know-how from the users regarding the basic concepts on measurement of the sound pressure levels as well as the noise equivalent levels. These methods are based on sampling techniques and can be used to determine the exposure noise levels in the workplace.

Noise Exposure $L_{ex,T}$ is the sound level energy-averaged over a period of time T, generally 8 hours, which corresponds the daily noise exposure an individual is submitted over a work shift and is calculated from measurements of $L_{eq,t}$ in the workplace.

Equivalent continuous sound level $L_{eq,t}$ is defined as the steady sound pressure level which, over a given period of time t, which has the same total energy as the actual fluctuating noise. Thus, the $L_{eq,t}$ is in fact the RMS sound pressure level with the measurement duration used as the averaging time. It is calculated as shown in equation .

$$L_{eq,t} = 10.\log_{10}\left(\frac{1}{t}\int_0^t \frac{p^2(t)}{{p_0}^2}dt\right), \tag{1.1}$$

where:

t is the measurement duration;

$p(t)$ refers to the sound pressure;

p_0 is reference sound pressure of 20μ [Pa].

The relation between L_{eq},t and L_{ex},T is given in the equation 1.2.

$$L_{ex,T} = L_{eq,t} + 10.\log_{10}\left(\frac{t}{T}\right), \tag{1.2}$$

The most common unit of acoustic measurement for sound is the decibel (dB). Additionally, a frequency weighting parameter is defined. It aims to correlate measured sound pressure levels measurements with assessments in humans.

Thus, noise exposure is commonly assessed using A-weighting, a filtering process used to account for the relative loudness perceived by the human ear, as the ear is less sensitive to low audio frequencies. Also, it is used because it considers the sound level in the spectrum range where humans are more prone to suffer any damage in the hearing system.

On the other hand, C-weighting expressed in dB(C) scale, is the total amount of sound including frequencies beyond the range of human hearing. It is sometimes used for specifying peak or impact noise levels, such as gunfire. It can be compared to unweighted dB readings (no filtering) used for the same purpose and therefore there is not much difference perceived between both. A-weighting as well as C-weighting curves are depicted in the Coherence function - Figure I-1. When A-weighting is used, the L_{eq} is typically noted L_{Aeq} and expressed as dBA or dB(A) (Berger (2003)).

The dB(A) sound level meter applies to the mid-range frequencies and for sound pressure level normally bellow 100 dB as opposed to the dB(C) sound level meter that measures low and high frequencies and higher volume levels (a rock concert for example).

The exposure level measurement depends on certain criteria. One defines the criterion level, L_c, as the equivalent constant noise level allowed for an 8-hour work shift. In most cases in Canada this value is 85 dB(A) except in Quebec where it is 90 dB(A).

As the sound level increases above the criterion level (L_c), the allowed exposure time must be decreased. This allowed maximum exposure time is calculated using an exchange rate, also called a "dose-trading relation" or "trading ratio." As explained by Canadian Center of Occupational Health and Safety (CCOHS (2019)) the exchange rate is the amount by which the permitted sound level may increase if the exposure time is halved. Two types of exchange rates are currently in use: 3 dB exchange rate and 5 dB exchange rate. These two exchange rates, with criterion levels of 85 dB(A) and 90 dB(A), would give two different sets of exposure guidelines. The 3 dB exchange rate is more stringent. For example, the maximum permitted duration for a 100 dB(A) noise exposure with the 3 dB exchange rate is 15 minutes. while with the 5 dB exchange rate, it is around an hour.

A Canadian and worldwide jurisdiction table for both criterion level and exchange rate is provided in Appendix I - Table I-1 and Table I-2 respectively.

The CSA (2013) standard recommends the measurement methods for all types of noise: continuous noise, pure sounds and impulse noise. However, it is worth noting that the implementation proposed in this thesis does not include the impulse or impact noises because of the limitations of the miniature microphones used.

1.3 Review of existing measurement methods and systems

1.3.1 Sound level meter and noise level meter

A sound level meter is a device used for acoustic measurements to assess noise or sound levels by measuring the sound pressure with a microphone. It is often referred to as a sound pressure level (SPL) meter, decibel (dB) meter, noise meter or noise dosimeter. A noise dosimeter is normally a wearable and portable device aimed to measure personal noise exposure for occupational purposes at workplace. The measured level must then comply with Health and Safety regulations.

Such devices are able to measure and store sound pressure levels (SPL) and process them over time in order to provide a cumulative noise-exposure reading for a specific period of time, which is a working day or week.

With sound level meters, industrial hygienists and workplace safety professionals can measure sound pressure levels in multiple locations to ensure that environmental conditions don't go beyond the recommended exposure limits (REL). Some sound level meter devices can be permanently installed for continuous monitoring of sound pressure levels at a workplace. On the other hand, dosimeters are generally placed on the shoulder for practical reasons and positioned relatively close to the worker's ear. Results from technique make clear that it is only valid if subjects do not move too much in front the source or if the acoustic field is sufficiently diffuse.

These instruments are specified by different standards and techniques, derived from International Organization for Standardization (ISO) like the IEC 61672-1:2002 (IEC (2002)).

There are many considerations to take into account when selecting the right equipment. For instance the type and class, give indication of the accuracy of the equipment as specified by the American National Standards Institute (ANSI (1996)) or International Electrotechnical Commission (IEC (2002)) guidelines. Also, the type of measurements to be made (impulse vs steady noise, high levels, etc.) will also influence the selection of the equipment.

Sound level meters and dosimeters are divided in two classes per IEC standard. Instruments from class 1 have a wider frequency range and a tighter tolerance than a lower cost, class 2 units. Class 1 instruments are mostly used for research and law enforcement. Similarly, ANSI specifies sound level meters as three different Types 0, 1 and 2.

These are described per Occupational Safety and Health (OSHA (2019a)) and it defines the performance and accuracy tolerances according to three levels of precision: Types 0, 1, and 2. The first one (Type 0) is used in laboratories, Type 1 is used for precision measurements in the field and Type 2 is used for general-purpose measurements.

In terms of precision, ANSI Type 2 sound level meters and dosimeters are considered to have an accuracy of $\pm$ 2 dB(A), while a Type 1 instrument has an accuracy of $\pm$ 1 dB(A). The minimum requirement by OSHA for noise measurements is the Type 2 meter and is normally adequate for general purpose noise surveys. The Type 1 meter is preferred for the design of cost-effective noise control solutions.

The way noise measurements are normally conducted with SLMs is by positioning the instrument in the center level position of the worker's head, but without the presence of that one. In fact the presence of the worker (head, body, shoulder, etc.) can cause some unwanted effects in the measurement such as sound absorption, diffraction and reflections and may fail to account for the device's placement effects and inter-individual differences in the wearers' ear geometries, which can greatly complicate the near acoustic field and therefore compromises the measure.

A conventional SLM is able to make instantaneous noise measurements only. It is very practical for places with continuous noise levels but not efficient for workplaces with impulse, intermittent or variable noise levels, therefore making hard to evaluate an average exposure to noise over a work shift a worker is submitted.

SLMs with time integration capabilities (most modern SLMs have these capabilities) are also called Integrating Sound Level Meters (ISLM). They can be used to to provide the L_{eq}, t as the time integration can be done automatically by the device. It must comprise the A-weighting factor since IEC 61672-1:2002 (IEC (2002)) mandates the inclusion of an A-frequency-weighting filter in all sound level meters.

Since time-integrated levels can be obtained, ISLM is very similar to the dosimeter and is used for determining the equivalent sound level over a defined period of time. A substantial difference is that an ISLM does not provide personal exposure because it is hand-held, and not intended to be worn attached to the body. The ISLM provides the equivalent sound levels at a specific location and it provides a single reading of a given noise, even if the current noise levels changes continually. It generally makes use of a user-defined exchange rate and time integration constant.

1.3.2 Personal noise dosimeters

In order to overcome those problems mentioned above concerning SLM devices, one solution is to use a noise dosimeter. A noise dosimeter is a small and lightweight device equipped with a microphone and attached to the worker's body. Typically, it is attached to worker's shoulder, close to the ear. It acquires and process the noise data in a continuous manner, providing the an averaged number, the L_{eq}, t. It is suitable for places where the noise substantially varies in intensity and duration and time span and/or when the worker moves constantly. A noise dosimeter allows to measure the noise exposure of a worker per requirements of CFR 1910.95 (OSHA (2019b)) or EU Directive 2003/10/EC (EU-OSHA (2003)). As the SLM devices, noise dosimeters have also to meet specifications defined by OSHA (2019a) and IEC (2002). Noise

dosimeters can be set with some parameters like criterion level, exchange rate and threshold level.

Criterion level (L_c) is the continuous equivalent 8-hour A-weighted sound level (dBA) maximum allowable accumulated noise level that results in 100% dose. Exchange or Doubling Rate (ER) is the decibel level that would double or halve the sound exposure. For instance with a 5 dB exchange rate the sound exposure doubles with every 5 dB increase, and the sound exposure is halved every 5 dB decrease. Provincial or territory noise based standards specify both CL and ER as informed in the Table I-1 and Table I-2.

Threshold cut off level is a reference value where the noise levels below the threshold are integrated as zero decibel. This will affect measurements like L_{eq} and Dose values for instance.

Noise dosimeters used to be bulky devices and worn attached to the body by a belt. Because the microphone usually stayed close to the ear while the cable was connected to the instrument, many issues were found on its utilization such as cable reliability and disturbances on the workers activities. Nowadays, those devices can be very small and are able to not only measure simple noise exposure, but to perform many other functions similar to of full-sized sound level meters, including full octave band analysis (for example the doseBadge2 from NoiseMeters Inc. (2019)).

1.3.3 Recent technologies

The recent technological evolution of electronic components and processors brought new possibilities in the field of noise exposure measurements. Specially in this area, many improvements were achieved and permitted new functions and features to be incorporated in those devices such as wireless communication and monitoring, increased data storage, GPS receiver for indicating the exact measurement position, etc..

Some examples of portable dosimeters are the Edge 5 (TSI Incorporated (2018)) , the Spark Series (Larson-Davis (2019)) and a wireless model like Dosebadge from Cirrus Research LLC (2019).

More recently, some advances in the field of noise measurement comes from Tympan (2019) as they claim: "Tympan is the first Open Source Hearing Aid development platform. We are committed to open source design principles, and we firmly believe that in doing so we can accelerate research studies and facilitate translation of novel algorithms into widespread use".

Besides its open-source (hardware and software) distribution, many important features can be outlined such as 180MHz / 32bit processor, low-power 32 bit codec, Bluetooth capable, on board dual microphone, battery operated and microSD card slot for audio recording and data logging. However it is not provided with the earpieces for personal in-ear monitoring.

Although all the options above provide an excellent means for assessing the noise dose at work-place, they don't consider the use in conjunction with HPDs. Their recommendations say that the noise measurements are to be taken normally at the worker's shoulders level, thus definitely not allowing the measurement inside the earcanal under the protected earplug. Because of this limitation, measured levels are not very precise and only give a certain estimation of the exposure level, since, again, the SPL inside the earcanal has to be estimated by subtracting the NRR of the HPD from the measured noise levels by the NRR given by the HPD.

This motivated some researchers to suggest some improvements on the earplug's attenuation measuring methods (Voix & Laville (2009)) but they were still not perfect with some uncertainties as raised by Nélisse *et al.* (2012).

Many systems emerged to offer new possibilities for noise dosimetry in what concerns the integration of such measurement tools for measurements under the HPD (earplugs or earmuffs). It is worth mentioning the efforts from some vendors that developed some measurement systems, where the personal dosimeter can be worn during the work shift. As an example to be mentioned is the Quietdose (Howard-Leight by Honeywell (2019)) shown in the Figure 1.1.

Figure 1.1 Quietdose personal dosimeter from Honeywell
Adapted from Howard-Leight by Honeywell (2019)

A great feature of this devices is while protecting also allows the noise dose measurement to be accomplished under the earplug. Unfortunately this system was discontinued by the vendor and is no longer available in the market. Additionally, there is another system available, the SV102A+ (SVANTEK (2019))that is able to perform in-ear dosimetry under an earplug as shown in the Figure 1.2.

Figure 1.2 Svantek SV102A+ personal dosimeter
Adapted from SVANTEK (2019)

The table 1.1 shows a brief comparison among the options so far and the proposed approach.

Table 1.1 Personal dosimeter equipment basic comparison

Feature	**Svantek SV102A+**	**Honeywell QUIETDOSE**	**What we are proposing**
Worn under earplug	✓	✓	✓
Worn under earmuff	✓	✗	✓
Store measurements	✓	✓	✓
Open-ear measurement	✓	✗	✓
Acoustical corrections towards the eardrum	✗	✗	✓
WID detection	✗	✗	✓

Some authors (Bessette & Michael (2012); Theis *et al.* (2012); Mazur & Voix (2012)) have recently worked on a so called dosimetric earplugs, which are able to measure continuously the noise exposure under the earplug. However these systems do not account for individual correction factors when interpreting the in-ear SPL measurements. Furthermore, the microphone

inside the earcanal is not located specifically at the eardrum position,but is rather positioned at certain distance from it, for obvious safety reasons.

General group corrections (ISO (1999)) or data collected on a mannequin (Mazur & Voix (2012)) have been proposed to convert the measured SPL levels inside the occluded ear to free-field or diffuse-field values. A more precise method has recently been proposed by Bonnet *et al.* (2018a) to convert the in-ear measured SPLs to the tympanum, thus providing reliable results by including automatically individual's dedicated correction factors.

A second important aspect that comes into play is the wearer's self-noise (walking, speech, etc.). As pointed out by some researchers (Ryherd *et al.* (2012); Nélisse *et al.* (2012)) these noises may greatly influence the noise exposure. Even when utilizing the A-frequency weighting, those noise events can effect the lower part of the spectrum and consequently change the exposure measurements that is reported by the instrumentation. On the other hand it is not well established in the current literature what risks those noise levels can present, although it is believed that they can be less harmful than those external ones due to biological protection mechanisms (Mukerji *et al.* (2010)).

1.4 Measurement of individual noise exposure: Bonnet's approach

The methods and algorithms used all along in this thesis for the noise exposure measurement come from the work of Bonnet *et al.* (2019b, 2018a). As they form the backbone of the present work, they are summarized in the next sections.

1.4.1 MEC for OED and CEP

The method is based on the use of two microphones, as illustrated in Figure 1.3. This figure points out specific microphone locations inside the earcanal for the calculation and consequently the identification of the Microphone-to-Eardrum Corrections (MEC) for both OED (Open Ear Device) and CEP (Closed EarPiece) devices. The MEC is the transfer function that allows to convert SPL measured in the earcanal to SPL at the eardrum.

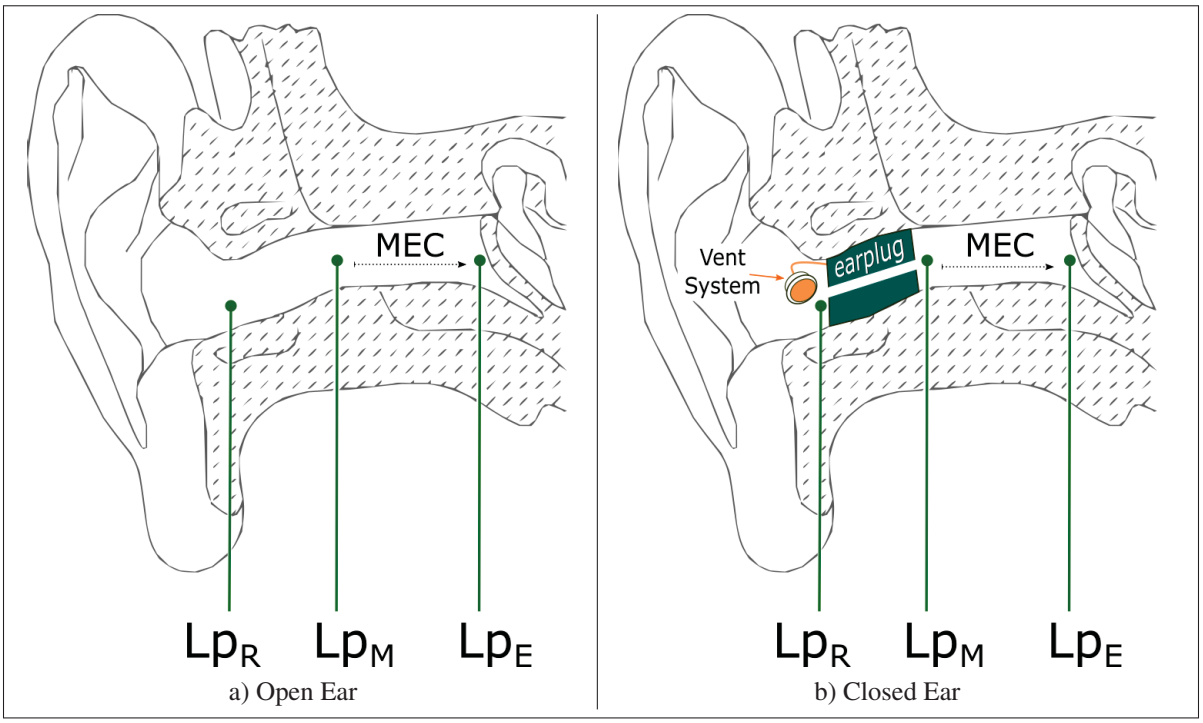

Figure 1.3 SPL points to calculate MEC
Reproduced and adapted with the permission of Bonnet *et al.* (2019a, p. 4-6)

L_{p_R} refers to the SPL at external microphone (OEM) whereas L_{p_M} refers to the SPL at the internal one (IEM). L_{p_E} refers to the SPL at the eardrum. MEC is therefore the difference $(L_{p_R} - L_{p_M})$ between sound pressure levels.

The MEC identification is based on the study of Bonnet *et al.* (2019a), where MECs were measured on 10 participants and presented in 1/12th octave band frequencies. From these results, a unique curve was generated, representing the average MEC for this population sample.

Using this average MEC curve as a template, coupled to OEM and IEM measurements, Bonnet et *al.* has shown that is it possible to obtain individual correction factors allowing to convert SPL in the earcanal to SPL at the eardrum for a specific subject.

With respect to the CEP devices, it was shown that a leak or a vent had to be used in order to obtain reliable correction factors, due to the attenuation of the CEP device. This is of major

importance for the present work as the design of such a leak/vent was a challenging task, as explained later in the thesis in the subsection 2.5.4.

Wearer's induced disturbances (WID) detection

A method is proposed by Bonnet *et al.* (2019b) to detect and exclude WIDs (wearer's induced disturbances such as speech, coughing, sneezing, microphonics, etc.) for dosimetry purposes. This method takes into consideration the sound pressure level measured inside the ear and its relation to surrounding ambient noise.

It is based on the fact that a strong correlation or coherence exists between the OEM and IEM microphone signals during the sound transmission from the OEM to IEM through the earplug. When the internal microphone's signal is perturbed by WIDs, such as speech, this coherence decreases significantly in the frequency range of the disturbance signal.

The correlation between two signals at specific frequencies is called the coherence function and is given by γ^2 (Randall (1987)). It is defined as:

$$\gamma^2(f) = \frac{|G_{xy}(f)|^2}{G_{xx}(f)\, G_{yy}(f)}, \tag{1.3}$$

where:

$G_{xy}(f)$ is the Cross-spectral density between two signals $x(t)$ measured by the OEM and $y(t)$ measured by the IEM;

$G_{xx}(f)$ *and* $G_{yy}(f)$ are the autospectrum of $x(t)$ and $y(t)$ respectively.

The coherence or $\gamma^2(f)$ measures the degree of linear relationship between the two signals or data sets at any given frequency or band center frequency. It is commonly used to estimate the power transfer between input and output of a linear system. It can vary from 0 (not correlated at all) to 1 (totally correlated).

For a given time frame i at specific frequencies, the coherence function can be calculated and averaged over a desirable frequency range. One can define the parameter Δ as shown in equation 1.4.

$$\Delta_i = -10 \log_{10} \left(\frac{\Sigma_{f_p=f_{\min}}^{f_p=f_{\max}} \gamma_i^2(f_p)}{N} \right), \tag{1.4}$$

where:

$f_{\mathbf{min}}$ *and* $f_{\mathbf{max}}$ are respectively the lowest and highest bands of the desired frequency range to be determined;

N is the number of frequency bands within this range.

Δ_i always returns a positive number and is expressed in dB. This variable indicates how correlated the two signals are. Δ is close to 0 in the spectrum range and for a specific time-frame where no WIDs are present. In the event of WIDs, Δ increases. Bonnet has shown that both Eq. 1.3 and Eq. 1.4 are best used when implemented as fractional band calculations more specifically in $1/12^{\text{th}}$ octave band frequencies.

For WID detection purposes, the use of 300 ms time-frames are proposed by Bonnet. Indeed, over 80% of the within-speaker gaps between words or phrases in the speech (pauses), are between 200 ms and 1000 ms (Campione & Véronis (2002)).

Δ is calculated for every time-frame and is compared to a defined threshold value of $\Delta_{\text{th}} = 0.75$. If the result is lower than this threshold, the WID is not considered to contribute to the SPL at the IEM.

1.5 Earcanal geometry

In order to initiate the development of the earpieces presented in this thesis, a good understanding of the ear-canal geometry was required.

The basic starting point of the mechanical development was the earcanal geometry given by Stinson & Lawton (1989) and a three-dimensional (3D) geometry extracted from a magnetic resonance imaging (MRI) conducted on a human subject in a recent study Benacchio *et al.* (2018).

The earcanal's cross-sectional dimensions of the subject tested in Benacchio *et al.* (2018) are represented in Figure 1.4.

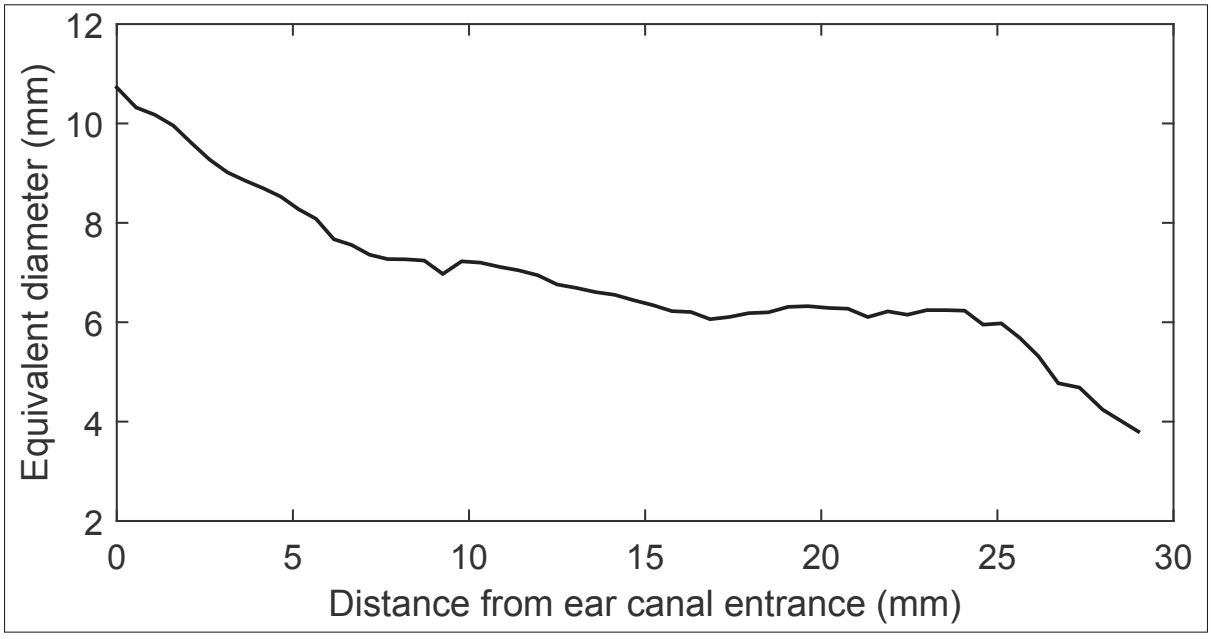

Figure 1.4 Earcanal geometry from the entrance to the eardrum - from the left to the right respectively
Taken from Bonnet *et al.* (2019a, p. 2)

This 3D rendering pinna scan (Benacchio *et al.* (2018)) shown in the Figure 1.5 was used in this project as it helped finding suitable geometry parameters for progressing the design concept and support modeling of the in-ear devices.

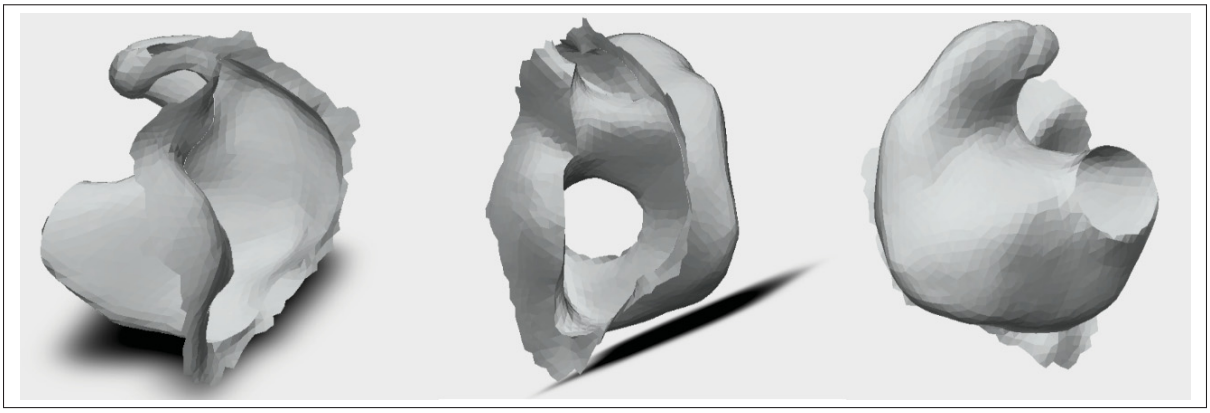

Figure 1.5 Pinna geometry used as initial model

An interaction study of the 3D rendering model of the device inside the pinna geometry model (see Figure 2.10) took place and demonstrated to be an important step toward a feasible and practical solution.

The geometry of the earcanal can be compared to a tube, which is open in one extreme and closed in the other by the eardrum. Its typical length ranges from 23-28 mm (Ballachanda (2013)). For safety reasons the maximum distance of 14 mm from the earcanal entrance (ECE) to the IEM position is defined.

1.6 Summary of the literature review

Section 1.1 situates the reader about the current evidences based on some studies, that workers in Canada and over the world are being exposed to high level of noise doses. Those studies also drawn the attention to the fact that this is serious problem and measures to decrease this statistics must me undertaken. In order to estimate those exposition level conditions, noise exposure measurements at the workplace has been largely employed by the industry in general. In some cases those levels exceed the limits imposed by regulations and therefore the use of HPDs by workers become mandatory in such cases. Although this is an important measure towards the resolution of those problems, such measurements still have some weaknesses and they must be improved to guarantee better noise exposure assessments and reliable outcomes.

It concerns basically to the methodology they have used to perform such measurements such as microphone positioning and earplug attenuation. In most cases, the microphone is attached to the body and not in the earcanal, where the sound is clearly perceived. Also, the NRR values informed by the HPDs are not always reliable and thus the correct noise dose result does not reflect the reality. In conclusion this section exposes the real situation workers are being submitted in terms of noise exposure and also alerts the reader of the risks they get in long term.

Section 1.2 situates the reader on the legislation available that defines the limits for those exposure levels. Some standards like CSA Z107.56 (CSA (2013)) contain some methods that are to be applied in the workplace for the measurement of occupational noise exposure. It defines in details the procedures and calculations that are to be performed in the work environment. These calculations aim to have a single number the L_{eq}, which is the averaged sound energy over a certain period of time. To have these numbers, three type of equipment are covered by these regulations: sound level meters, integrating sound level meters and noise level meters or dosimeters. To sum up, this section reviews the procedures and calculations for noise exposure and give the guidelines for implementing it in the real-time algorithms chosen for this purpose in this work.

Section 1.3 explains the type of instrumentation that can be used for noise exposure measurements. They are classified according to their type and classes, which tells essentially how accurate the device is and for what application it is employed. The sound level meters are utilized in some work cases when the work can be easily divided into defined activities and the SPL are relatively stable during the measurement period. The ILSMs, on the other hand, are essentially the same but they are able to additionally provide the L_{eq},t measurement. Noise dosimeters measure the noise dose according to some jurisdictions and therefore use some standard parameters like criterion level and exchange rate as a initial setup in order to provide the correct noise dose values. These parameters are region dependent and may have differences even in the same country. None of those equipment can measure the dose under the earplug or earmuff, since they are mostly used attached to the body, close to the worker's ear preferably.

They are normally referred as personal noise dosimeters. Some systems already on the market made a huge progress in developing earplugs incorporating a dosimeter. Nonetheless, they do not envision corrections considering the individual earcanal morphology and the influence that the subject individual noise contribution can have in the noise dose readings. By and large, this section gives a complete overview about the instrumentation that must be selected for assessing noise exposure. It provides the necessary background towards the right choice for the type of equipment that is going to be built here in this master's thesis. Moreover, it helped to identify a lack in the instrumentation available in the market in the present moment.

Section 1.4 makes the reader aware about the methods and equations that were used throughout the software implementation. The microphone-to-eardrum correction is presented for both prototypes the OED and CEP. It provides the theory which was exposed in the work of Bonnet et al. According to his findings this correction attempts to give an exact picture of the noise perceived at the eardrum position. Another proposal from Bonnet *et al.* is the correct identification of the wear induced disturbances, in other words, the noise generated by the wearer during the noise exposure measurements. The suggested methodology uses the coherence principle that is applied between two time signals to identify and separate those WIDs from the final results. In closing, this section provided the necessary understanding of the methods and equations that must be implemented in the measurement system developed in this work.

Section 1.5 provides the reader with information about the morphology of the earcanal. From studies, a standard cross-section geometry is made available and was taken as a reference for simulations on the initial work of Bonnet *et al.* (2019a) and also helped on the understanding of the dimensions of the earcanal for the concept elaboration of the prototypes. Another important gain for this thesis was the MRI scan of a subject's pinna supported the 3D rendering model of the earpieces. In closing, this section, although short, was of fundamental importance for the concept, design and construction of the prototypes employed in this work.

CHAPTER 2

HARDWARE IMPLEMENTATION

The following sections present in details the hardware implementation conducted in this project. To simplify the reading of this section, many pictures were moved to the Appendix II.

2.1 ARP3 hardware platform

A portable hardware platform dubbed ARP3 (Auditory Research Platform 3) developed by the NSERC-EERS Industrial Research Chair in In-Ear Technologies (CRITIAS) was used throughout the development. The ARP3 platform is connected to a four channel sound card and a battery-pack for long-run tests (up to 8-hour data acquisition and processing). A basic diagram with all hardware parts is depicted in the Figure 2.1.

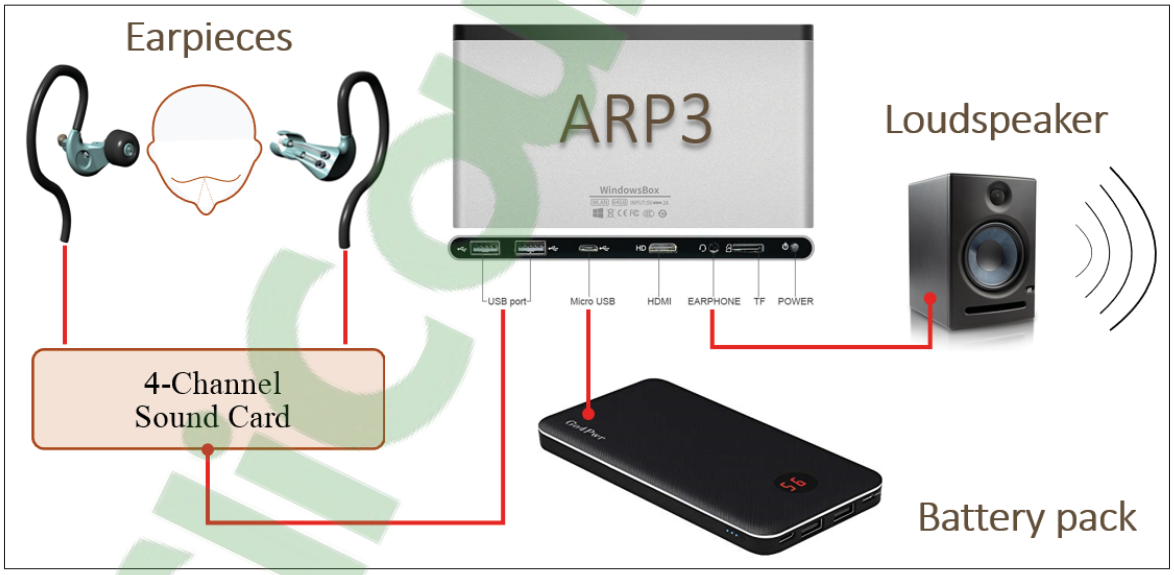

Figure 2.1 Hardware basic diagram

The ARP3 unit is based on the Intel ATOM Z3735F processor, 2GB DD3 memory and runs on Windows 10 operating system (OS). Moreover, in order to be able to process real-time acquisition data, this platform is specially configured to allow complex and fast algorithms to

run flawlessly. A four channel sound card was attached to the platform providing a connection bridge from the data coming from the earpieces (presented later) and the running algorithms. The entire assembly is depicted in the Figure 2.25. Python was chosen as the programming language for data acquisition and data processing on the final prototype system, and runs smoothly on the the ARP3 platform.

2.2 Miniature microphone and sound-guiding tube

The specifications for the microphone used in this project are:

- Very small mechanical dimensions;
- Flat frequency response;
- Compatibility with the ARP3 platform and sound card (bias voltage, electrical interface, etc.);
- Connection to a sound-guiding tube.

Taken into account these four main requirements, it was found that Knowles model FG23652-P16 microphone fulfilled all requirements (see Figure 2.2).

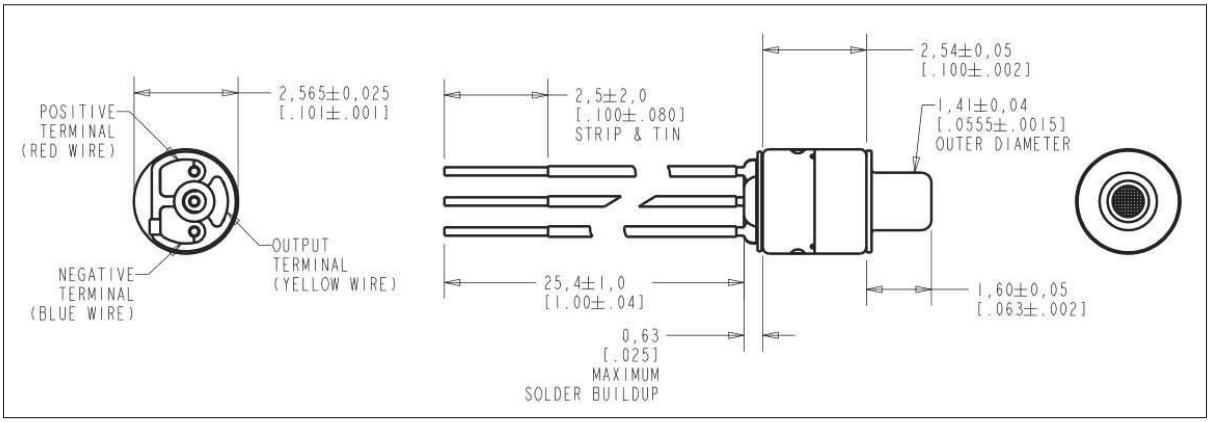

Figure 2.2 Knowles microphone model FG23652-P16
Taken from Knowles Corp. (2019)

The frequency response for this microphone model is given in Figure 2.3:

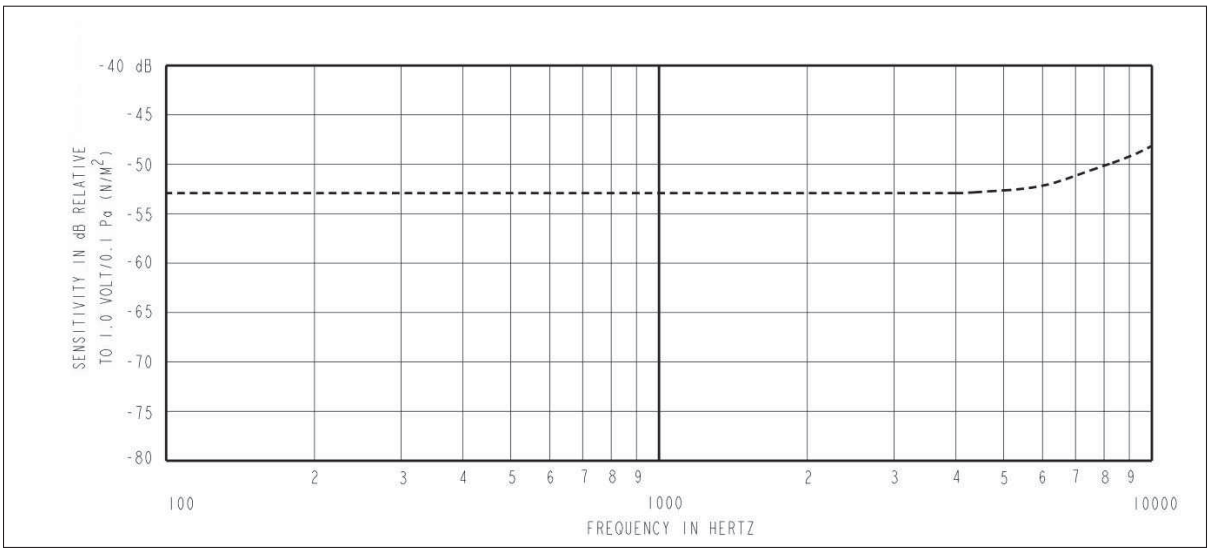

Figure 2.3 Knowles microphone model FG 23652-P16 frequency response
Taken from Knowles Corp. (2019)

Electrical wires shown in Figure II-5 were used on this device, which supports positive and negative voltage connections and an output pin. Considering that two microphones were needed for the operation of each earpiece device, a mini-DIN 6-pin connector was chosen for the elec-

trical attachment to the sound card. Figure II-2, Figure II-3 and Figure II-4 provide details of the pin-out for hardware connection implementation.

The sound-guiding probe tube is a special plastic tube connected to the microphone which allow measuring the SPL in the ear canal. Its internal diameter is 0.8mm and its external diameter is 1mm. Its construction material has unique properties, providing high attenuation for the sound waves that reaches the tube and thus making it ideal for the application in this study.

2.3 Sound card

The sound card is responsible for acquiring the analog signals from the microphones on either IEM or OED, This card was developed and used by Vincent Nadon in his thesis: *"Development of a method and algorithms for the combined measurement – inside the ear with a hearing protector – of the noise exposure dose and the induced hearing fatigue as measured with otoacoustic emissions"* (Nadon (2015), Nadon & Voix (2018)). The main features of this sound card can be summarized as follow:

- 4 audio channel inputs;
- 16/24/32bit and 44.1 KHz sampling rate;
- Bias voltage for the microphones;
- Interface with the ARP3.

2.3.1 Extra adjustments - sound card

The sound card described in the section 2.3 was developed to fulfil some features who were specific to the work of Nadon. Therefore, in the application proposed here, some hardware modifications had to be carried out on the card in order to make it compatible with our specifications. The main modifications that were realized are summarized as follows:

- Filter bypass;
- Gain adjustment;
- Shottky diode in series.

Filter bypass

The referred sound card implements a high-pass filter hardware made out resistors and capacitors, which leads to an "undesired" attenuation for frequencies from 40 Hz to 600 Hz in the acquired audio signal. A workaround had to be utilized using a series of jumper wires on the PCB in order to provide a flat response from the microphone signals, and thus obtaining the expected coherence function measurements (frequency range from 200 Hz to 1500 Hz) - see Figure V-1 in appendix V.

Gain adjustment

As indicated by Bonnet *et al.* (2019b), the sound pressure levels (under the earplug) that are intended to be measured by this device during its operation, ranges up to 105 dB(A). It is then required that the sound card and respective microphones could be able to operate within this range accordingly. As seen in section 2.2, the microphones are supposed to correctly operate within this specific SPL range, up to 140 dB(A) per the manufacturer specifications. However, the sound card hardware was initially set up to provide a specific gain for the devices connected to it. Some tests were conducted and indicated that the provided gain, for the hardware configuration adopted in this work, led to saturations in the signal (a "clip" in the wavefile), which in turn distorts the input signals, as can be seen in the Figure 2.5.

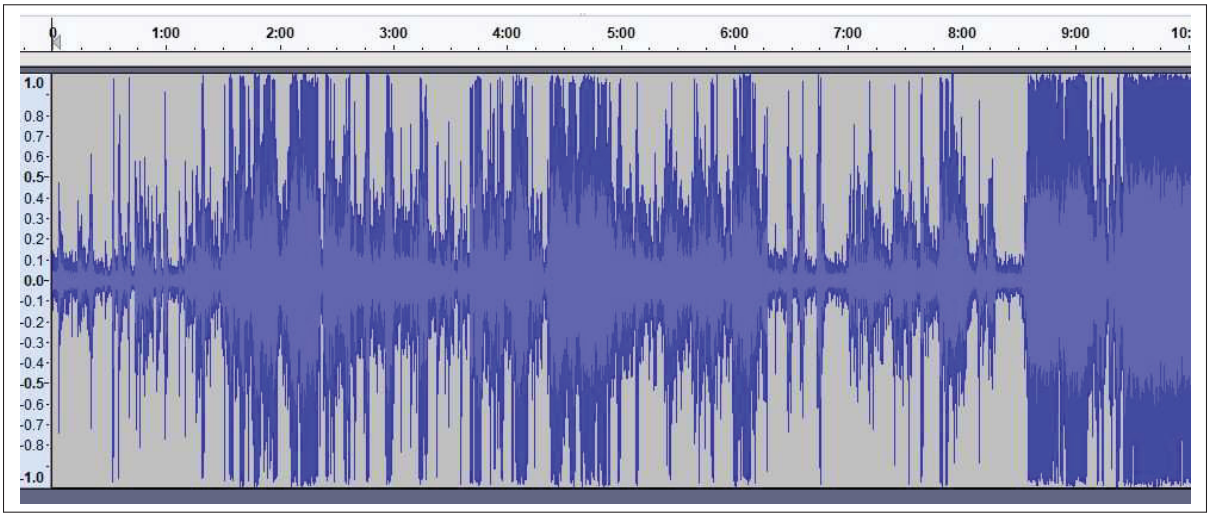

Figure 2.4 Example of a 10 minute audio waveform for testing the gain

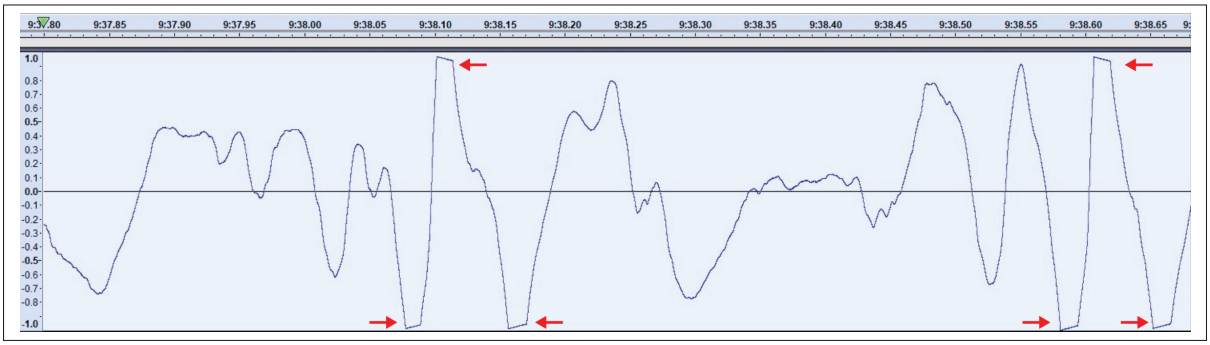

Figure 2.5 Red arrows in the audio signal showing distortions

A modification was then carried out by removing all resistors shown in the Figure V-2 in Appendix V in order to correct this behaviour. Figure 2.4 shows a typical audio file used for verification.

Schottky diode in series

Another necessary modification in the sound card, suggested by Nadon, is the inclusion of a Schottky diode (example: Diode Schottky 80V 500mA Surface Mount SOD-123) in series with the existing one, for better symmetry in the input signal as shown in the Figure V-3. The

purpose of this workaround was to remove any DC voltage offset from the input signal to avoid any kind of distortion as well.

2.4 Battery pack

Although the ARP3 device and the sound card have shown to be able to function for about 2-hours of continuous measurements with the ARP3 internal battery, this was deemed not enough in case longer tests had to be performed in the field. Thus, an external battery pack was added to provide extended autonomy.

The battery pack specifications are given below:

- Output capacity: 20.000 mA/h;
- Output Current: 3.4A (max.);
- Size: 155 x 79 x 23 mm;
- Weight: 14 oz (397g).

The referred model is the Poweradd Pilot X7 and is presented in Figure 2.6.

a) Overview b) Battery Connections

Figure 2.6 Battery pack
Taken from Ipoweradd (2019)

2.5 Prototypes

Two different prototypes were designed for this project: an Open Ear Device (OED) and a Closed Earpiece (CEP). This section gives an overview of their hardware concept, design and construction, and the time development evolution.

2.5.1 3D printing

All prototype cores developed in this work were fabricated in-house using a stereo-lithography (SLA) printer from Formalabs (Model: Form2).

It offers many possibilities in terms of materials for printing as shown in Figure 2.7. In our case, three resin types namely clear, black and flexible were available and they were tested by printing specific prototypes and evaluating their mechanical characteristics . The evaluation goal was to test in practical terms, parameters like hardness/softness, strength and durability.

a) Formlabs Printer

b) Formlabs Printing Materials

Figure 2.7 Formlabs printer and resin options
Adapted from Formlabs (2019)

Prototypes made with the flexible resin were too soft for our application. Indeed, in a quick test they did not demonstrated any mechanical stability when inserted in the earcanal. On the other hand, the clear and the black resin types showed to give very stable prototypes.

Figure 2.8 shows examples of prototypes taken right after the printing process.

Figure 2.8 Examples of printed prototypes

In terms of comfort (hardness/softness), especially for he OEDs, there was no remarkable differences observed between prototypes built with the clear and the black resin types. Prototypes made of the black material seemed to be less breakable over time and necessarily more durable than the clear ones. Thus the preferred material for printing was the black resin type FLGPBK02.

2.5.2 Earpiece development: overview

Both prototypes were first designed using Solidworks (Dassault Systèmes SOLIDWORKS Corp., Waltham, MA, USA) 3D CAD tool and were produced in-house with the help of a Formlabs (Formlabs Inc., Somerville, MA, USA) 3D resin printer. Once printed, two Knowles (Knowles Corp., Itasca, IL, USA) miniature microphones model FG23652-P16 were added to each device for SPL measurements in the earcanal. Figure 2.9 shows different iterations of prototypes created for this project showing the time evolution toward the final design.

The first device developed and implemented was the OED. Special care was taken to design it to provide the least cross-sectional area as possible in the earcanal in order to be as acoustically transparent as possible, as per recommendation of ISO (2002) - item 3.7. The device itself showed to be mechanically very stable and resistant after several test in human subjects.

In Figure 2.9, instead of placing the microphones directly inside the device as in the first iteration, it was decided to enclose the microphones in the device's main body directly (Figure II-9) for an additional protection of the electrical wires, and thus creating a more robust device. This modification also helped reducing the cross-sectional area, a feature needed to achieve an almost acoustically transparent solution.

The initial CEP design used the same mechanical main body of the OED as in Figure II-9. The main difference is in the eartip part, which is very similar to some conventional off-the-shelf earpieces. Two microphones were also used for this assembly and only one sound-guiding tube was first envisioned for conducting the sound from the earcanal to the respective internal microphone.

An application for patent at the US Patent and Trademark Office (USPTO) including the prototype concept was filed (École de technologie supérieure (2018)).

The next sections present the development of the OED and CEP in more details.

2.5.3 Open Ear Device (OED)

The first prototype that was developed what the Open Ear Device (OED). During the development process, many versions of the prototypes were designed, implemented and tested until a "working" one was finally accepted. Figures below show examples of many versions created during the project showing their time evolution.

As can be seen in Figure 2.9, the very first device brought the concept of the "Open Ear Device". However it was far behind of a real and practical solution in terms of both technical requirements and comfort. Although a perfect acoustical transparency for the OED was not fully achieved, mainly because of limitations on the current technological tools and materials, the final design itself showed to be mechanically very stable, resistant after several tests on human subjects and was deemed comfortable enough by the subjects.

Prototype construction improvements took into account important characteristics such as fit, comfort, measurement requirements (microphone and wiring assemblies) and accuracy. Changes and improvements were made until an acceptable solution was reached by the team members. In order to help optimizing the prototype design, the 3D rendering of a pinna scan was used (Figure 2.10). An interaction study of the 3D model of the device inside the pinna geometry model took place and demonstrated tobe an important step toward a feasible, practical and comfortable solution.

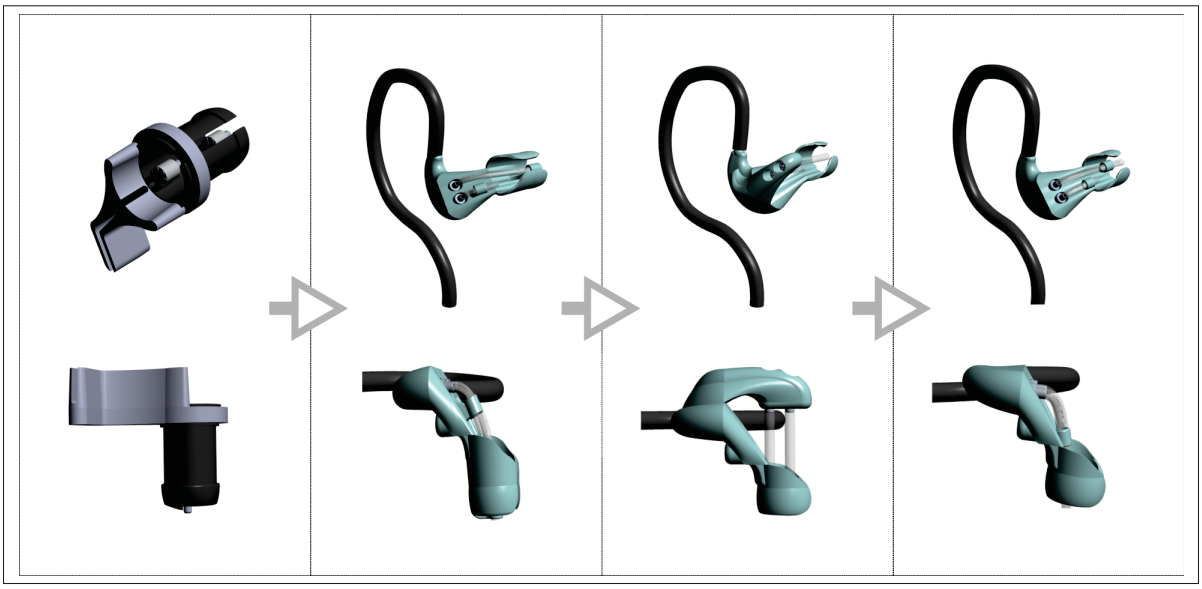

Figure 2.9 Open-ear device prototype evolution

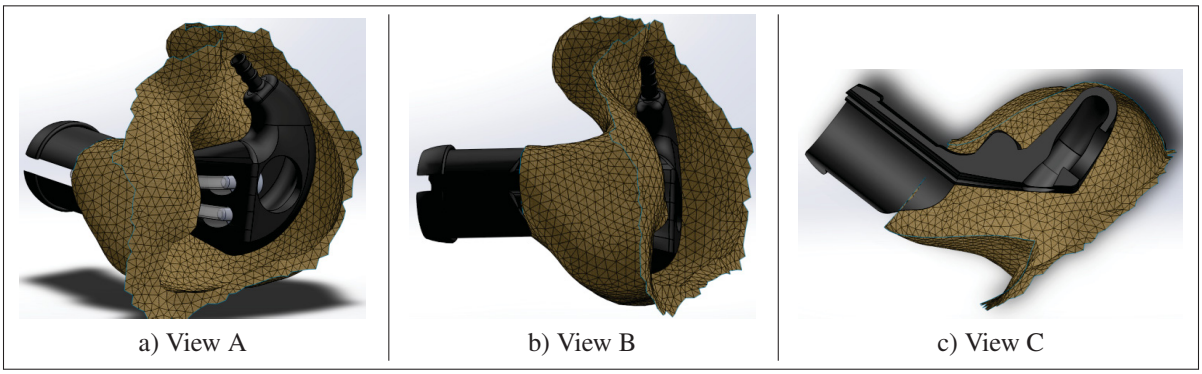

a) View A b) View B c) View C

Figure 2.10 Earpiece as assembled in the pinna

Beside the microphones, cables and connectors, the earpiece itself consists of three mechanical parts shown in Appendix II: ear hook (Figure II-8), main body (Figure II-9) and upper body (Figure II-10). The ear hook is an off-the-shelf piece that is made of soft plastic from Sonomax (EERS Global Technologies Inc., Montreal, Canada) V4 earpiece and helps to hold the device in the ear during operation. It also serves as means of conducting the electrical wire that connects the microphones to the sound card.

The last two ones (main body + upper body), although separate 3D pieces, are printed out as one single unit. The reason behind this was to use the same main body in both the OED and CEP devices.

It is to be noted that the left and right ear earpieces differ from each other in their development and construction since they are mirrored. The hole made in the middle of the main body component is meant to be used to access the wiring connections from the cable to the microphones.

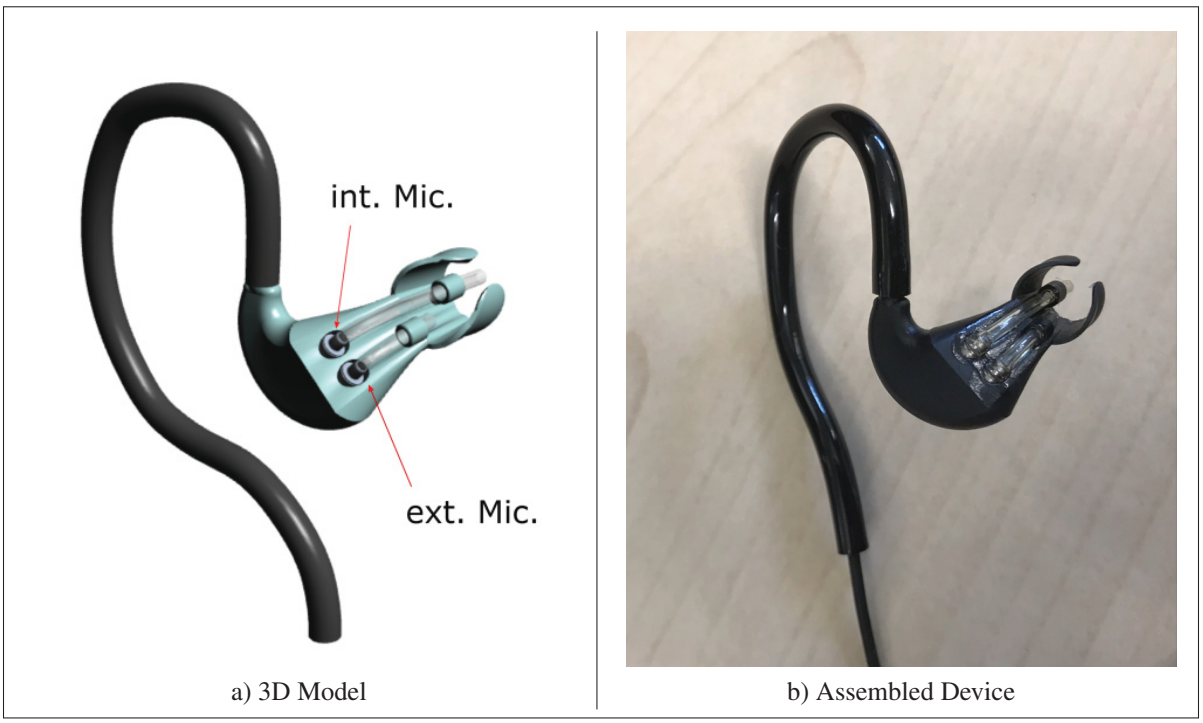

a) 3D Model b) Assembled Device

Figure 2.11 OED prototype

The upper body is designed to be inserted in the earcanal. It is also responsible to give some mechanical stability for the whole earpiece while in operation as well as holding the sound-guiding tubes in place.

The final 3D design and assembly of the OED is shown in the Figure 2.11.

The fabrication of this device is very similar the CEP one and follows the same procedure presented later in section 2.5.5.

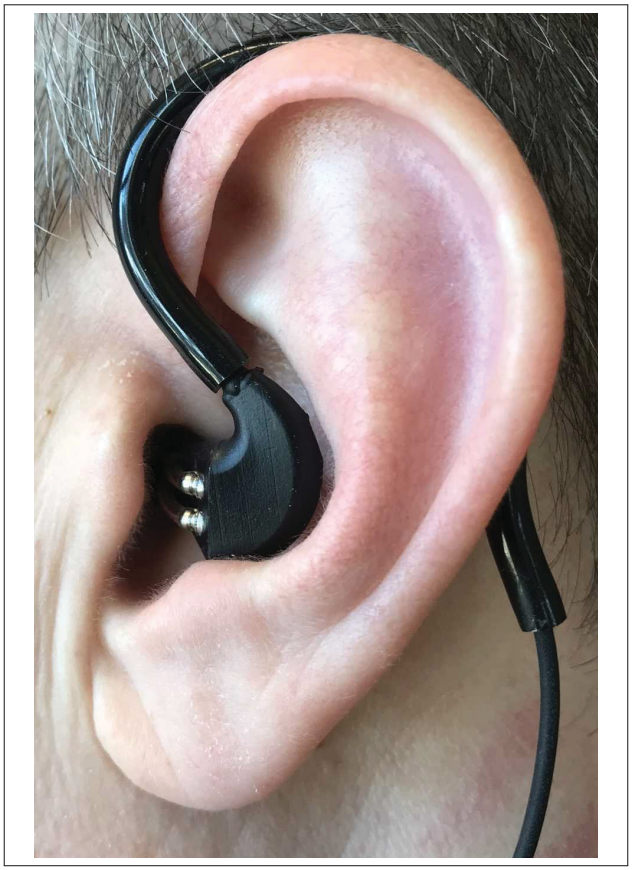

Figure 2.12 Open device as worn by a subject

After assembling the prototype, including the microphones, cables and connectors, it is ready to be worn as shown in Figure 2.12 and the necessary sound measurements can be started.

2.5.4 Closed Earpiece Device (CEP)

The development of the OED allowed to acquire the necessary knowledge for the design of the closed earpiece. The CEP was also required to be used for the MEC function identification process (see Bonnet *et al.* (2018b)). As explained by Bonnet, the measurements with the initial design unfortunately showed the difficulty of obtaining a stable and reliable MEC, and modifications had to be made to the design. The design was improved by adding a controllable leak mechanism (vent) that could be sealed properly after performing the MEC identification. The evolution of this device along the project is illustrated as follows:

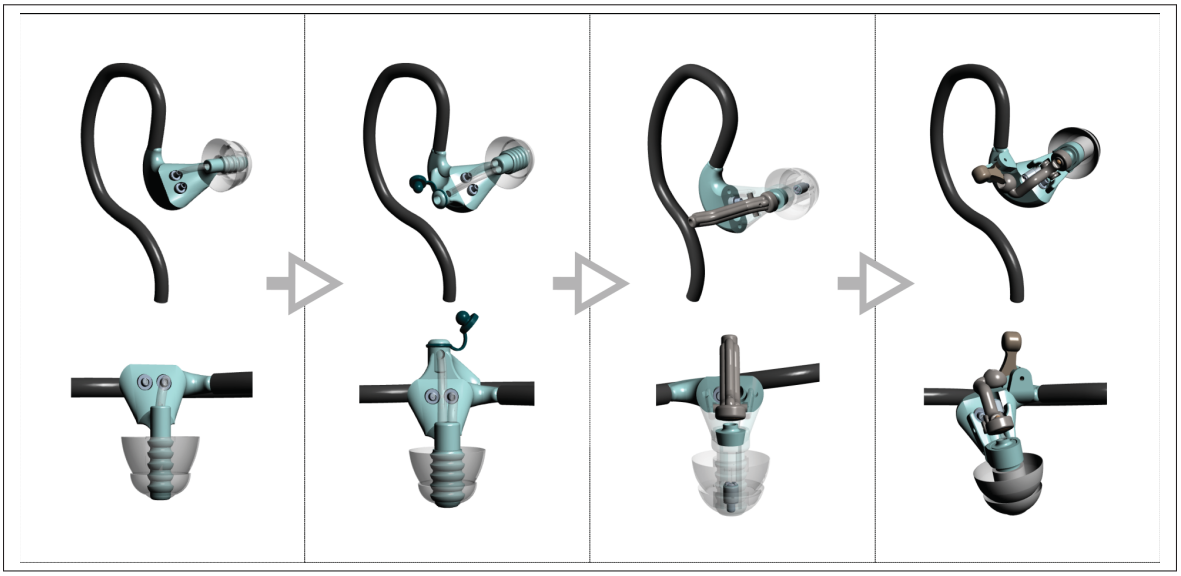

Figure 2.13 Closed-earpiece prototype time evolution

As in the OED, the earpiece device consists of thee mechanical parts shown in Appendix II: ear hook (Figure II-8), main body (Figure II-9) and upper body (Figure II-11).

The main body and upper body, although separate 3D pieces, form a single unit after printing. Two microphones were also used for this assembly and only one sound-guiding tube was first envisioned for conducting the sound from the earcanal to the respective internal microphone.

According to Bonnet *et al.* (2019a) the MEC function identification can be performed with this device as well. As explained by Bonnet *et al.*, a controllable leak had to be created in order to identify the MEC correctly. It was done using another tube (together with the internal one) added to the design. A first attempt on doing so was through a silicone cap, which failed mainly because of the tube length and associated resonance frequencies that would create unwanted interferences. Figure 2.14 shows this specific design in more details.

Figure 2.14 Details of a temporary CEP prototype using a silicone cap to close the vent

The cap was constructed entirely of silicone using a developed molding system showed in the Figure II-7.

Shortening the tube length and providing a mechanism for sealing the hole (vent) (see Figure II-12 and Figure II-16) on the device after the MEC calibration was performed was then found to be very effective. Improvements were made on the design until an accepted solution was deemed acceptable by the team members.

During the calibration procedure (MEC calibration) the lever must be locked in position (leak open). This lever opening is performed by the locker mechanism as per Figure II-13.

A rigid cap (Figure II-14) makes part of the design of the CEP device only and is intended to steer the sound-guiding tube along the earpiece upper body (Figure II-11).

The earpiece can support various types of eartip from double-flanged silicone eartips to high insulation ones, such as Comply^{TM} Isolation T-400 eartips (Hearing Components, Inc., St Paul, MN). The following pictures show details on the construction of the final CEP design and prototype:

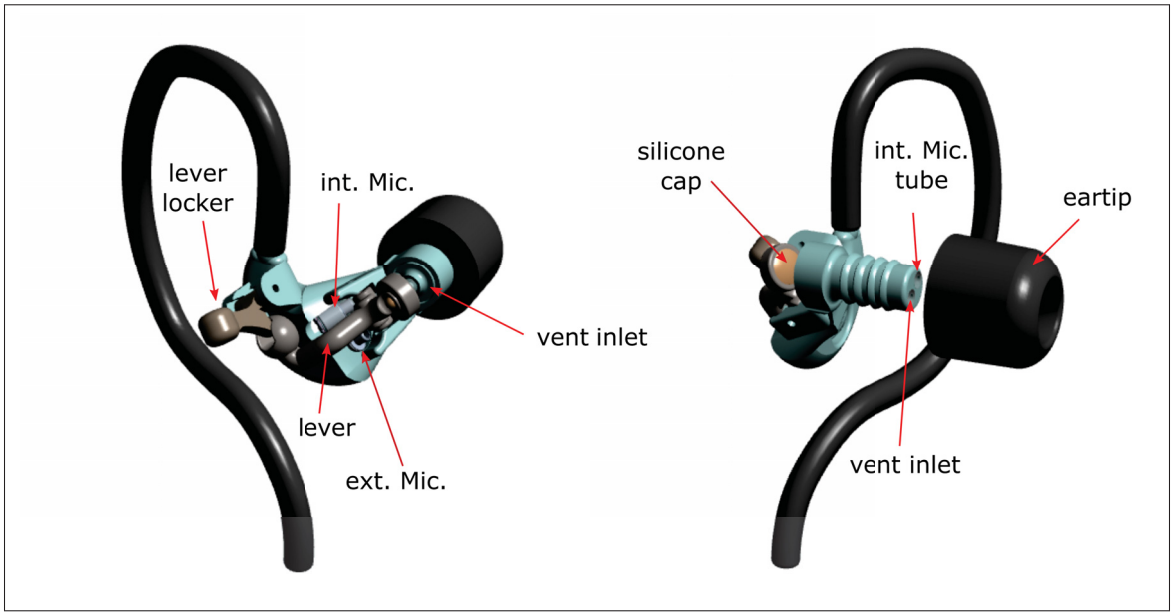

Figure 2.15 3D rendering model details of the closed-earpiece device

The final solution, as worn by a human participant, can be seen in Figure 2.16 and Figure 2.17.

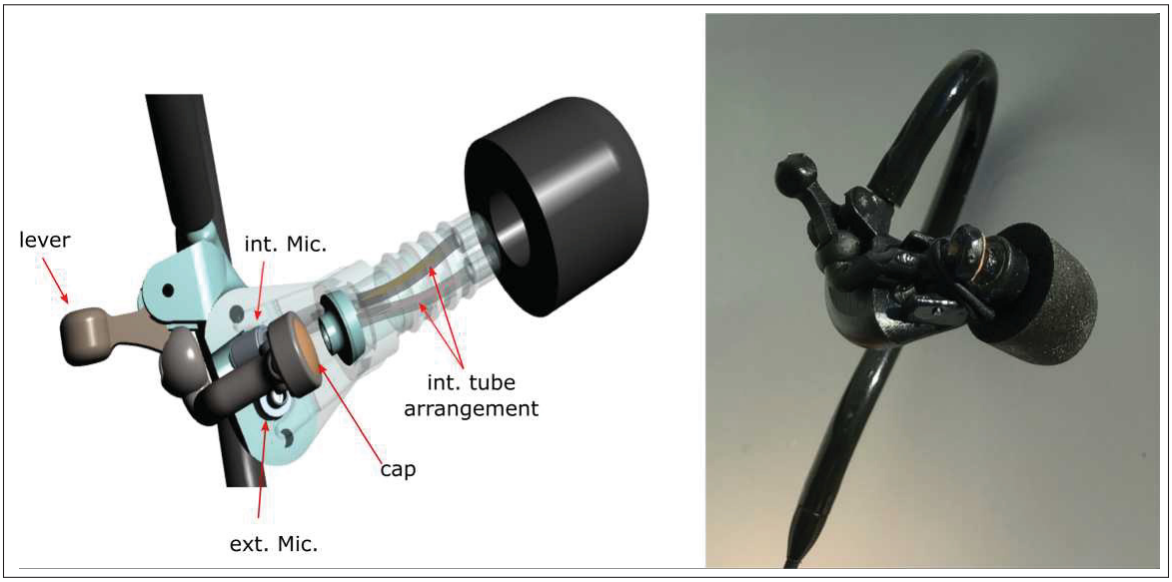

Figure 2.16 Construction details of the closed-earpiece prototype

a) Open Vent b) Closed Vent

Figure 2.17 Occluded device as worn by a subject

2.5.4.1 New proposed design

As pointed out by Bonnet et al. (Bonnet *et al.* (2018b)), there were some problems related to the positioning of the external microphone relative to the vent entrance. To overcome these problems, a new design was proposed by bringing the measuring intake for the external microphone closer to the vent inlet from about 3 to 4 mm, as shown in in Figure 2.18.

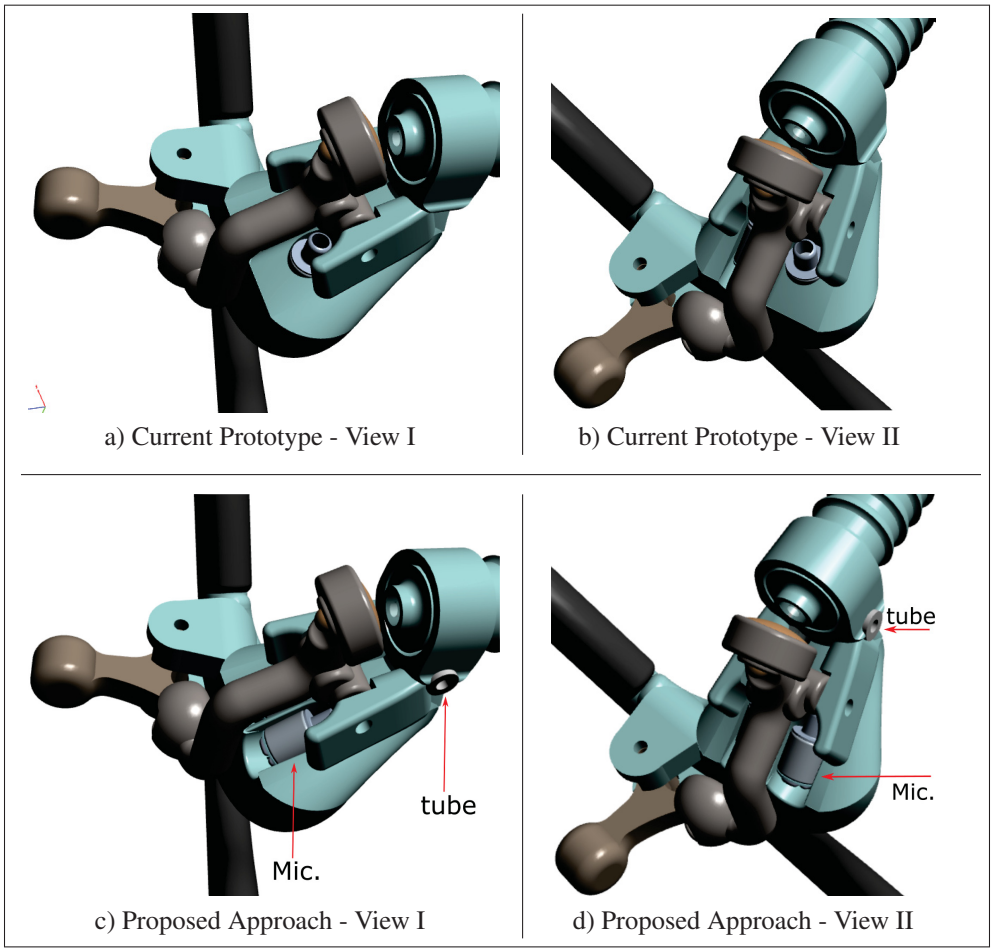

Figure 2.18 New design proposal

The red arrows pointed in Figure 2.18 (c) and 2.18 (d) indicate where the changes are to be made for a newer prototype design. Note that this is a rough design implementation suggestion only to show the concept. However, such concept was not built. Hence, the tube indicated in these figures is to be connected to the microphone, which is not shown in this representation.

2.5.5 Prototype assembling

Assembly preparation

Before starting the assembling of the CEP prototype (microphones, tubes, wires) some preparation must take place as depicted in Figure 2.19. It is intended to provide a very good and tight seal for the sound guiding tube connected to the microphone's entrance. This preparation procedure (described in the Tab. 2.1) also intends to avoid any damage to the tube's material.

a) Tube Inserted in the Needle

b) Warming up the Needle

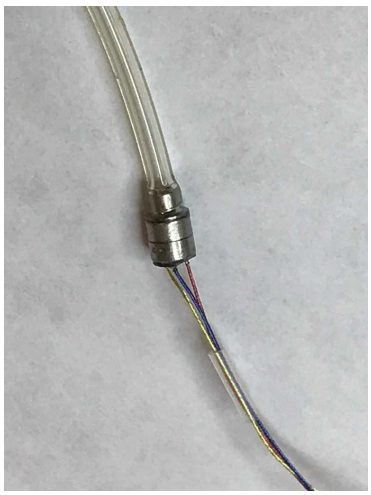

c) Inserting the Tube on the Mic.

Figure 2.19 Sound guiding tube preparation

Table 2.1 Assembling preparation steps (a) to (c)

Preparation	Description
Step (a)	Enlargement of the tube ending by an 1mm diameter needle.
Step (b)	Heating the tube at 100 Celsius degree with the iron solder for about 10 seconds.
Step (c)	Connection example of the sound guiding tube to the microphone.

The complete fabrication process (a 15 step procedure) is detailed below:

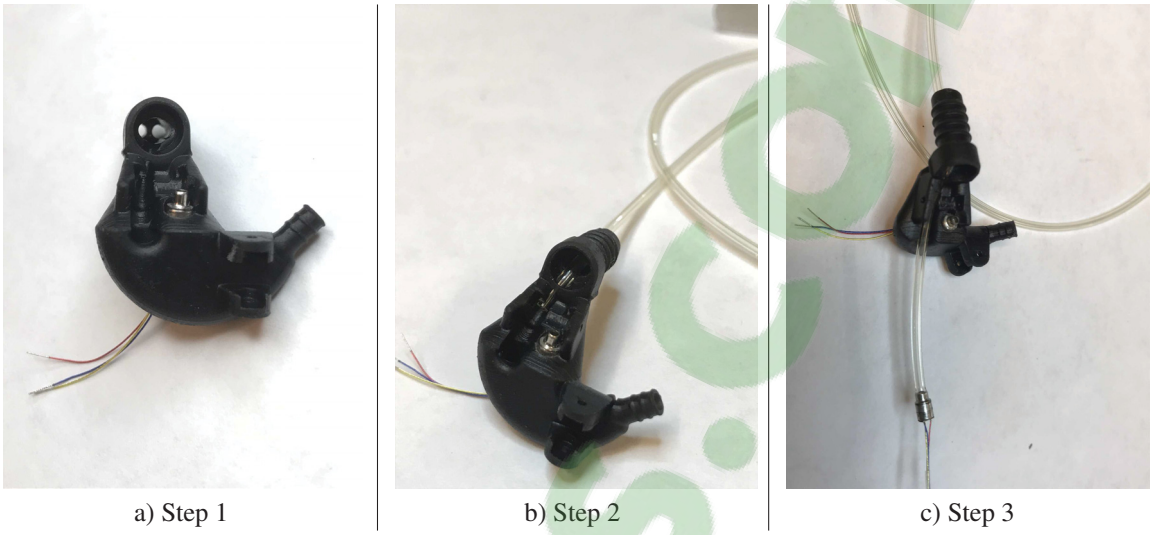

a) Step 1 b) Step 2 c) Step 3

Figure 2.20 Fabrication steps 1 to 3

Table 2.2 Assembling description for steps 1 to 3

Procedure	Description
Step 1	External microphone inserted in the earpiece.
Step 2	Insertion of the internal guiding tube into the earpiece upper body.
Step 3	Sound guiding tube inserted into IEM.

a) Step 4

b) Step 5

c) Step 6

Figure 2.21 Fabrication steps 4 to 6

Table 2.3 Assembling description for steps 4 to 6

Procedure	**Description**
Step 4	Fixation of the microphone in the earpiece upper body.
Step 5	Insertion of the vent guiding tube into the earpiece upper body and placement of the rigid cap (FigureII-14) into the tube.
Step 6	Epoxy (Figure II-17) depositing in the upper body eartip cavity.

a) Step 7 b) Step 8 c) Step 9

Figure 2.22 Fabrication steps 7 to 9

Table 2.4 Assembling description for steps 7 to 9

Procedure	Description
Step 7	Rigid cap hold in place until the epoxy's final cure. Extra tube cut right in the vent entrance.
Step 8	Details on the epoxy sealing. Nail polish must be applied to seal the connection microphone-guiding tube.
Step 9	Electrical cable passed through the earhook and earpiece main body.

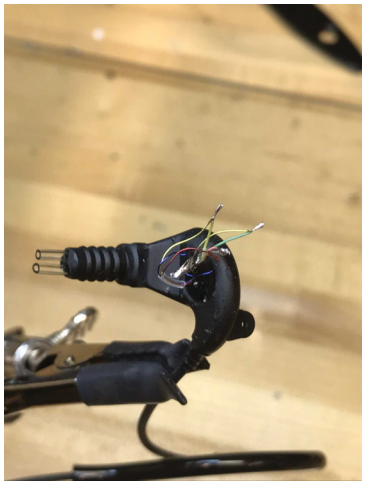

a) Step 10

b) Step 11

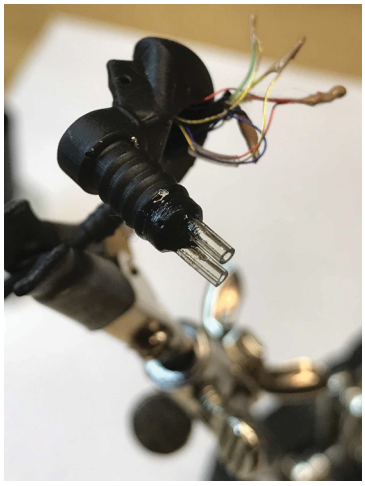

c) Step 12

Figure 2.23 Fabrication steps 10 to 12

Table 2.5 Assembling description for steps 10 to 12

Procedure	**Description**
Step 10	Wiring soldering connections to both IEM and OEM.
Step 11	Wiring connections to the mini DIN6 connector from Figure II-3.
Step 12	Nail polish must be applied to seal the connection uper body tip-guiding tubes. Exceeding tube ends must be removed and cut at the tip-end position.

a) Step 13 b) Step 14 c) Step 15

Figure 2.24 Fabrication steps 13 to 15

Table 2.6 Assembling description for steps 13 to 15

Procedure	Description
Step 13	Positioning of the rubber ring over the earpiece tip part.
Step 14	Nesting the lever Figure II-12 inside the CEP upper body. Steel pivot (from a thin needle) inserted to hold the lever in position.
Step 15	Nesting the lever locker (Figure II-13) inside the reserved position. Note that the lever cap must be filled with silicone (Figure II-18) before this step. Steel pivot (from a thin needle) must be inserted to hold the lever locker in position. The rubber ring (Figure II-15) is then wound round the lever.

2.5.6 Box and external connectors

The original sound card from Nadon was not build to be used as a standalone device. Therefore, some modifications were accomplished so that this device could work together with the ARP3 and the earpieces. A plastic box shown in Figure II-1 was printed out and it was used to accommodate the printed circuit board for a steady operation. Additionally, two mini-DIN 6-pin connectors were added to the box for electrical connection to the microphones on the earpieces. Figures II-2, II-3, II-4 and II-5 in Appendix II, present the necessary detailing for this construction.

2.5.7 Assembling all parts together

The ARP3 Hardware defined in Figure 2.1, a four channel sound card 2.3 and the battery pack 2.4 are to be used together for the in-ear measurements. A plastic box was used to accommodate the sound card hardware in a steady position during use. Besides its own USB connection, additional connectors had to be added in order to connect the microphones. It was achieved by adding two extra mini-DIN6 female connectors on the side. The connector pin-out is also presented in Figures II-2, II-3, II-4 and II-5.

In order to bundle all devices together while in operation, assembly holders were primarily developed. A 3D rendering view of these holders is depicted in Figure II-6.

The ready-to-use system measurement assembly is depicted below:

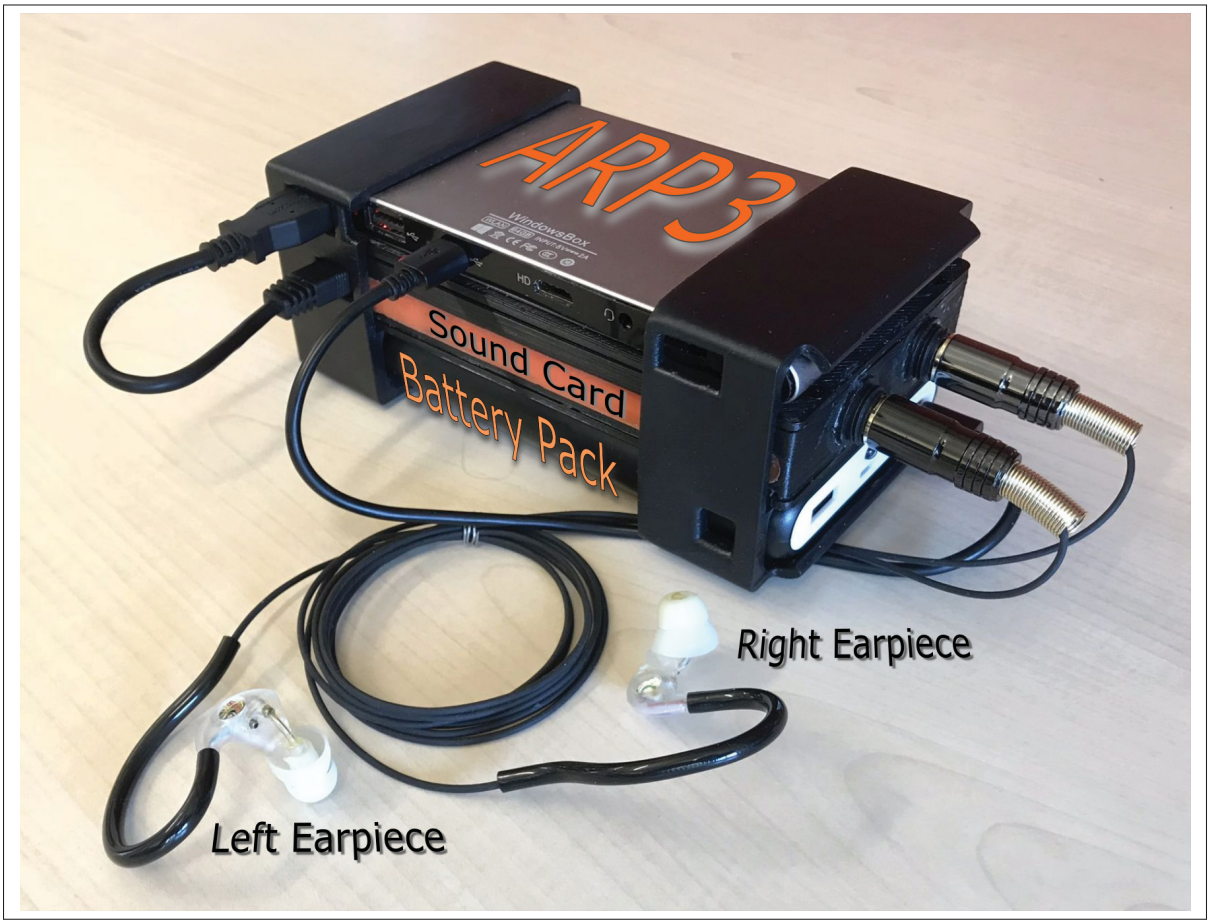

Figure 2.25 In-ear dosimetry system assembly (w/o loudspeaker)

CHAPTER 3

SOFTWARE DEVELOPMENT

Besides the hardware development exposed in the previous section, one important objective of this project was to be able to reproduce Bonnet et *al.* results using a real-time, high level programming language with low computational power requirements.

Many options could be used for this purpose. Among them, it is worth mentioning that C/C++ is largely used for the industry nowadays in many types of embedded applications and it is at first glance a very strong candidate. However, since the proposed development makes use of specific signal processing and acoustics functions, the use of C/C++ was not considered to be very convenient considering the extra energy and time necessary to develop the specific set of functions required in this work.

A brief summary of the features that were targeted follows below:

- High level and widely used programming language;
- Large community support;
- Available audio, math and acoustics libraries;
- Capable of making all needed calculations in very short time (less than 300 ms).

Except for the last item in the above list, which pretty much depends on the application and the implementation itself, all other requirements lead to the use of Python as the chosen software platform.

It worth emphasize that real-time data acquisition and analysis is an essential requirement for this project. With respect to the programming language, Python was chosen because it fulfils all the requirements listed above.

Indeed, Python is becoming a very popular programming language and has demonstrated a strong capacity to process real-time algorithms, thus providing reliability and speed for the implementation of the needed signal processing functions. The envisioned approach should also have some elements that could help reducing the efforts towards developing new pieces of codes, and consequently to cut down the necessary programming and implementation time. Moreover, it must be reliable and fast enough to perform in real time complex signal processing calculations.

Also, many free libraries are available in Python and are supposed to correspond, to a very high extent, to some developed in Matlab, such as Numpy (NumPy Developers (2019)), a fundamental package for scientific computing with Python. Furthermore, the required libraries for audio, math and acoustics are available at no cost. There are also a huge community behind it, which makes the language a reliable and ideal choice at this point.

The ARP3 hardware platform runs on Windows 10 OS and the software code was developed using Python version 3.7. The algorithms were based on the classic equations from ANSI S12.19 ANSI (1996), but were adapted to incorporate the occluded ear correction factors (Bonnet *et al.* (2018a,b)).

The core element responsible for the signal acquisition from the sound card is the Pyaudio library (Hubert Pham (2006)). It allows to process all four channels simultaneously, but the right driver must be selected in order for Pyaudio (Christoph Gohlke (2019)) to support Windows Audio Session API (WASAPI - Microsoft (2019)), a Microsoft's (Microsoft Corp., Redmond, Washington, WA) most modern method for talking with audio devices. Some libraries were also added to this project like NumPy (a fundamental package for scientific computing with Python), Python Acoustics (GitHub Developers (2019)) (various useful tools for acousticians), among others. The Python environment also provides resources to develop a graphical user interface (GUI), which was implemented in the calibration procedure using the PyQtGraph (University of North Carolina at Chapel Hill (2017)) package. As in the calibration process,

there was also a need for an application for acquiring and processing incoming time data from the earpieces.

This was achieved by designing a GUI that provides the user options to set some parameters for instance, the device type (open or occluded), A or C frequency weightings, exchange rate, threshold level for dose calculation, etc. Additionally, a wavefile recording option was also made available. A test strategy was planned to verify that the same results from those achieved as in the original work of Bonnet *et al.* (2019b, 2018a) could be obtained with the developed hardware and software.

The proposal here is to have a tool capable of performing real-time measurements while making the necessary data handling regarding the particular aspects of IEND, basically the calculation of the effective noise dose including and excluding WIDs one might be exposed and the identification and corrections for individual MEC functions.

All developed algorithms had to be validated in order to assure correct data processing by comparing with data obtained by Bonnet *et al.* (2018a,b). This resulted in the implementation of two additional supporting tools:

- Wavefile recording;
- Validation of the results processed by Bonnet's approach.

Although the development of those tools was not the main goal of this thesis, they had a very important role in the success of it, hence they are shortly presented in the section Supporting tools - section 3.5.

3.1 Python libraries

There are a few Python libraries that form the solid basis for this work and worth to be mentioned:

- **pyaudio:** cross-platform audio input/output stream library;
- **numpy:** scientific package, including linear algebra, Fourier transform, and random number generation capabilities;
- **scipy.signal:** similar to numpy, but more specifically for signal processing purposes;
- **pyqtgraph:** real-time plotting and graphical interface;
- **python-acoustics:** A Python library aimed at acousticians.

The core element responsible for capturing the signal from the sound card is the Pyaudio library. It allows to process all for 4-input audio channels simultaneously, assuming that the right driver is selected in order for the pyaudio to support Windows Audio Session API (WASAPI). This special version of pyaudio doesn't come with the original package and therefore must be installed separately by standard python procedures (e.g. pip install). The right python 3.7 version is the cp 3.7 64 bit (Christoph Gohlke (2019)).

3.2 Software programs

In order to reach the objectives of this project, a set of software units or programs were created as shown in Figure 3.1.

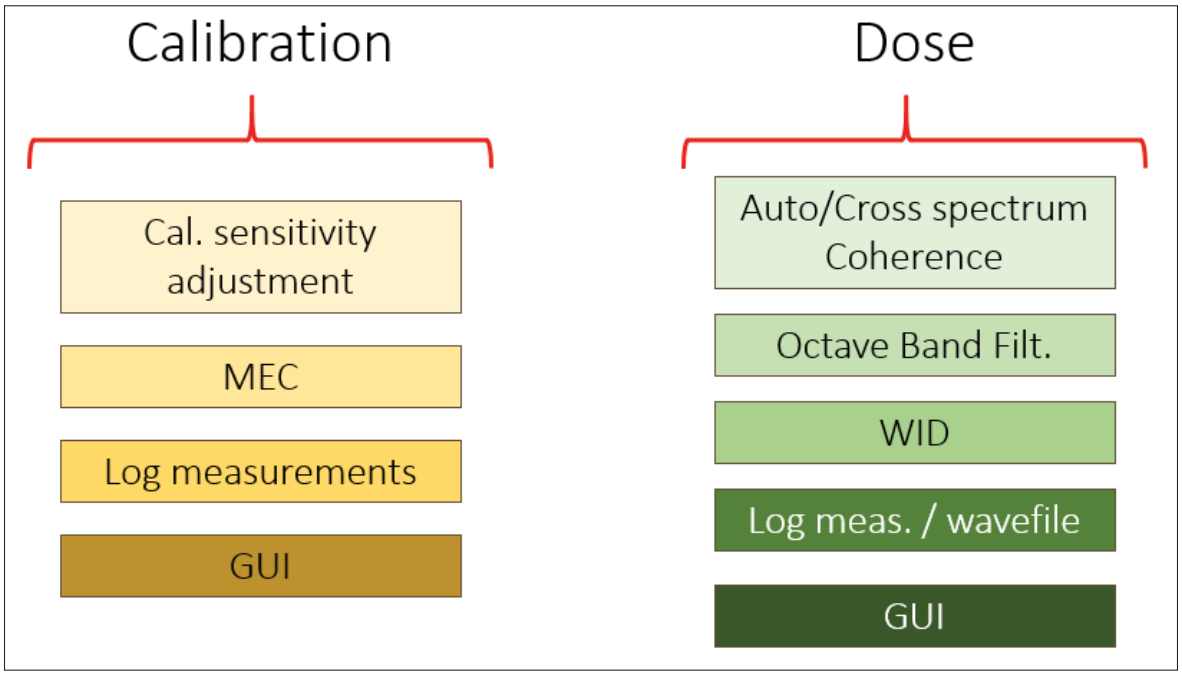

Figure 3.1 Software development overview

It consists primarily of two main programs:

- **Calibration**;
- **Dose calculation**.

Additionally, a third set of programs was develop to support and help in the development phases of two main programs. This set is called "supporting tools". Table 3.1 provides an overview about each program and their deliverable outcomes.

It is important to mention that the developed functions that constitute the above programs and those that are described in the following pages, can operate concomitantly to each other within a mechanism called "multithreading" available in Python. It was used to increase the performance of the system, for example in the concurrently operation with 4-input audio channels.

Table 3.1 Summary of software tools and their outcome

Program	**Description**	**Deliverable**
Calibration	Microphone Calibration and data storage	- White and Pink Noise Generation - Calibration factors - MEC function identification and corrections
Dose Calculation	Real-time dose calculation	- Instantaneous SPL - Dose - Wavefile and data log
Supporting Tools	Data comparison and validation with the source Matlab code from Bonnet	- Delta Analysis - SPL OEM and IEM - Coherence - Low/high level WID detection

The data acquisition block in Figure 3.1 is related to the sound reading or captured either from a microphone or from a wavefile and is further explained in the section 3.4.1. The set of "supporting tools" that was developed in order to support the final software implementation is detailed in section 3.5.

3.3 Calibration Program

The main functions that belong to the calibration program are listed below:

- **LpR-LpM**;
- **Peak Finder**;
- **Writing Calibration Data**;
- **Noise Generator**;
- **Read Tube Correction Spreadsheet**;
- **Microphones calibration**.

The calibration program block diagram is shown in Figure 3.2.

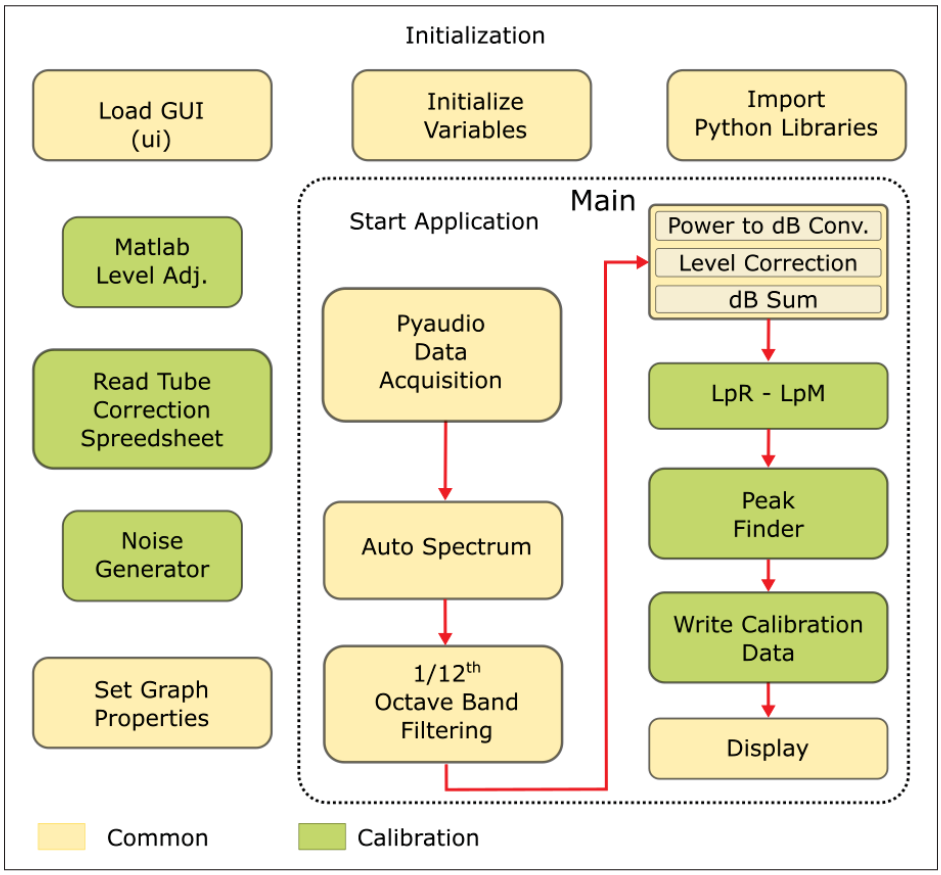

Figure 3.2 Calibration program block diagram

A detailed description of each specific function given above is provided in the following subsections as code snippets rather than algorithms in pseudocode. The main reason for that is to facilitate the continuation of any future development based on this work.

3.3.1 LpR-LpM

This specific function is presented and explained in subsection 1.4.1 and illustrated in the Figure 1.3. Table 3.2 shows a short piece of code containing this implementation.

Table 3.2 LpR-LpM

Function	Short Example
LpR-LpM	`Lp22_Lp00 = W22_Bands_dB - W00_Bands_dB#(LpR - LpM)`

3.3.2 Peak finder

This specific function aims to align the frequencies of the peaks (maximum) in the curves LpR-LpM above and the an averaged MEC template (provided by Bonnet from test subjects). The peak is expected to be at maximum between 4.5 and 7.5 kHz.

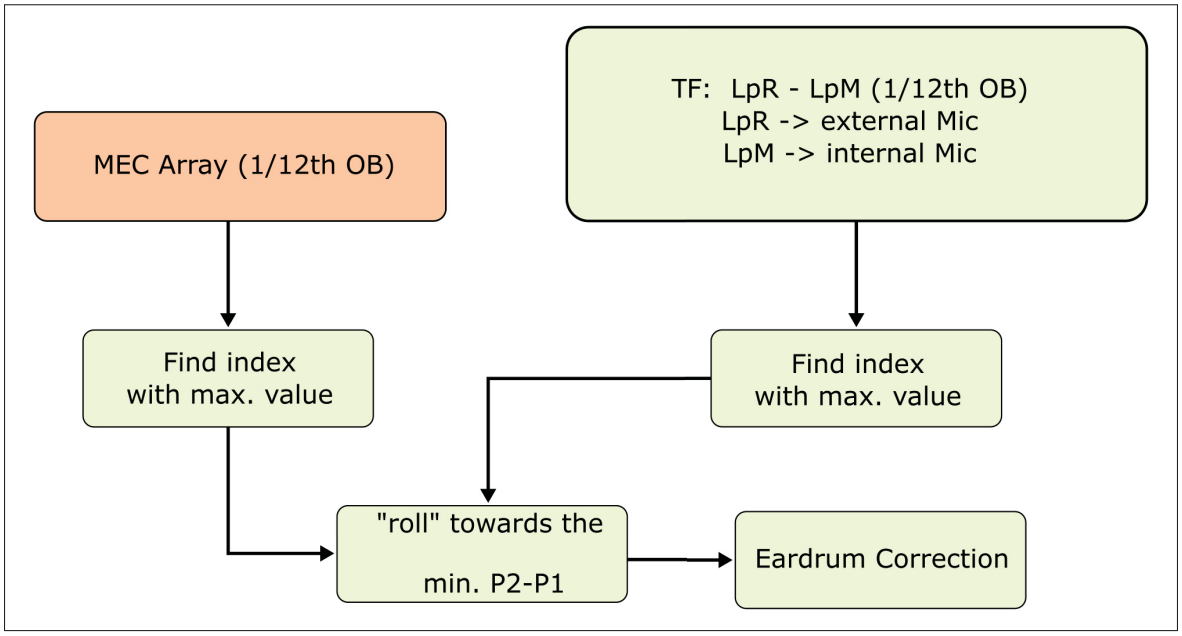

Figure 3.3 Peak finder algorithm for MEC identification and corrections

Table 3.3 Peak Finder

Function	Short Example

Peak Finder	`def Filter_MEC02(self, Lp22_Lp00 =None, FabiensED_moved_02 = None, max_frq02 = None ):`
	
	`max_posFB = np.argmax(self.FabiensED)`
	`max_pos02 = np.argmax(Lp22_Lp00[10:80])# position where to find the fpeak`
	`max_frq02 = Fabien_freq[max_pos02]# frequency where to find the fpeak`
	`max_val02 = np.max(Lp22_Lp00[10:80])`
	`self.move = max_pos02 - max_posFB # position of fpeak - max at Fabien's ED`
	`FabiensED_moved_02 = np.roll(self.FabiensED, self.move )`

Table 3.3 shows a short piece of code containing this implementation.

3.3.3 Writing calibration data

This function aims to write and save the calibration data in a specific file for later processing for the dose measurement program. A short code example of this implementation is presented in the following table:

Table 3.4 Saving the calibration factors

Function	Short Example

Calibration Factor	`if self.ui.rbtn_CEP.isChecked():`
	`  text_file = open("calibration_result/CAL_CEP_Cal_Factor_02.py", "w")`
	
	`if self.ui.rbtn_OED.isChecked():`
	`  text_file = open("calibration_result/CAL_OED_Cal_Factor_02.py", "w")`
	
	`text_file.write(time.strftime("#File generated on %Y-%m-%d @ %H:%M:%S"))`
	`text_file.write("\nimport numpy as np")`
	`text_file.write("\n#Cal_Factor_00 Value (Hz) (OB = %d) :" %ob)`
	`text_file.write("\nCal_Factor_00 = np.array(%s)" % str(Cal_Factor_00))`
	`text_file.write("\n#Cal_Factor_22 Value (Hz) (OB = %d) :" %ob)`
	`text_file.write("\nCal_Factor_22 = np.array(%s)" % str(Cal_Factor_22))`

3.3.4 Noise generator

The calibration program is able to generate either noise or white noise. Pink noise is essentially used for microphone calibration(Figure 3.17 and Figure 3.18) whereas white noise is specifically used for the MEC identification procedure (Figure 3.20). The Python module responsible for this implementation is the *winsound*. The winsound module (The Python Standard Library (2019)) provides access to the basic sound-playing machinery provided by the Windows platform.

Table 3.5 Noise generation function

Function	Short Example

Noise Generation	`def playWave(self):`
	
	`if self.ui.rbtn_MEC.isChecked():`
	`winsound.PlaySound("wav_source/white_noise_1min", winsound.SND_ASYNC | winsound.SND_ALIAS ) # start playing`
	
	`if self.ui.rbtn_Delta.isChecked():`
	`winsound.PlaySound("wav_source/pink_noise_1min", winsound.SND_ASYNC | winsound.SND_ALIAS ) # start playing`

3.3.5 Read tube correction spreadsheet

Due to the use of sound guiding tubes for the microphones on both OED and CEP devices, a special correction factor is to be applied to the microphone reading to take into account the effect of the sound guiding tubes. An Excel spreadsheet provided by Bonnet for this purpose was used. A dedicated Python function is able to read all data content in this table and extract the needed information. It is shown in the table 3.6.

Table 3.6 Tube correction spreadsheet reading function

Function	Short Example

Tube Correction	`def data_Tubes(self, position):`
	`  global single_list, full_list`
	
	`  workbook = xlrd.open_workbook('input_source_files/Earpieces_tube_responses_.xlsx')`
	`  worksheet = workbook.sheet_by_index(0) #open sheet by index`
	
	`  single_list = [] # or my_list = list()`
	`  full_list = []`
	`  for y in range(0,7):`
	`  for x in range(58,149): # line 59 to 149 – frequencies 52.56 to 9513 Hz`
	`  a = worksheet.cell(x,y).value`
	`  single_list.append(a)`
	`  full_list.append(single_list)`
	`  single_list = [] # reset this variable`
	
	`  return(full_list[position])`

3.3.6 Microphones calibration

A Matlab function was developed for the calibration of the microphones as depicted in the Figure 3.17 and Figure 3.18). It is important to note that both parts shown in the Table 3.7 and Table 3.8 have to be executed in order: part I first and then part II.

Table 3.7 Matlab function for microphones calibration - part I

Function	Short Example

Matlab - Part I	%% Calibrate the reference microphone (with calibrator) (do this only once)
	
	%before launch (CTRL+ENTER), place ref microphone in calibrator and swith calibrator on;
	%ref mic must have flat frequency response
	clc;clear;close all;
	
	s = daq.createSession('ni');
	s.Rate=44100;
	s.NumberOfScans=10*s.Rate;
	
	%analog inputs
	ch0=addAnalogInputChannel(s,'Dev2','ai0','Voltage'); %ref microphone
	ch0.Range=[-1 1];
	
	%start acquisition
	data=s.startForeground();
	
	%compute SPL (in 3rd oct, but could also be in 12th oct)
	OUT=SpectrumCalculation_v3_FB(data,0,0,3);
	
	%calculate calibration factor
	Calref=94-OUT.Ovl;
	%recompute SPL
	OUT=SpectrumCalculation_v3_FB(data,Calref,0,3);
	
	save('Calref','Calref');
	
	%display SPL
	semilogx(OUT.Octave.f,OUT.Octave.Lp)
	xlim([100 10000])

Table 3.8 Matlab function for microphones calibration - part II

Function	Short Example

Matlab - Part II	%% Measure the reference level at close distance from speaker with reference microphone (do this only once, right after calibrating the ref microphone)
	
	%before launch, place reference mic at a close distance d from speaker and
	%play pink pink noise at about (measured SPL does not need to be too loud, 60-70 dB)
	
	load('Calref.mat'); %load ref microphone's cal factor
	
	s = daq.createSession('ni');
	s.Rate=44100;
	s.NumberOfScans=10*s.Rate;
	
	%analog inputs
	ch0=addAnalogInputChannel(s,'Dev2','ai0','Voltage'); %ref microphone
	ch0.Range=[-1 1];
	
	%start acquisition
	data=s.startForeground();
	
	%compute SPL
	OUT=SpectrumCalculation_v3_FB(data,Calref,0,3);
	
	%calculate reference level at 125Hz
	Levelref=OUT.Octave.Lp(OUT.Octave.f==125,1);
	
	%recompute SPL
	OUT=SpectrumCalculation_v3_FB(data,Calref,0,3);
	
	%display SPL
	semilogx(OUT.Octave.f,OUT.Octave.Lp)
	xlim([100 10000])
	
	%display ref level
	disp(Levelref);
	
	%save ref level and acquisition data
	save('Levelref_data');

3.4 Dose calculation

The dose calculation program consists of a set of functions developed for the complete dose calculation. It consists in:

- **Data Acquisition**: either performed by pyaudio or using an available wavefile;
- **Auto-Spectrum and Cross-spectrum calculation**: Frequency domain analysis of the auto and cross-correlation time series;
- **Coherence function**: Defined by the Eq. 1.3;
- **1/12th Octave Band Filtering**: Converts the narrow-band spectrum to 1/12th-band spectrum;
- **Delta (Δ) function**: Defined by the Eq. 1.4;
- **WID detection**: Algorithm to detect noises induced by the wearer as defined in 1.4.1;
- **Dose**: Equivalent continuous sound level with and without WIDs;
- **Log File**: Log of specific data and parameters stored for further analysis;
- **Display**: Display of some defined results in a graphical user Interface (GUI).

Figure 3.4 shows those specific functions and how they are organized in the code. Note that both the validation and Dose codes are depicted in this figure. Yellow colored blocks are common functions shared by all codes.

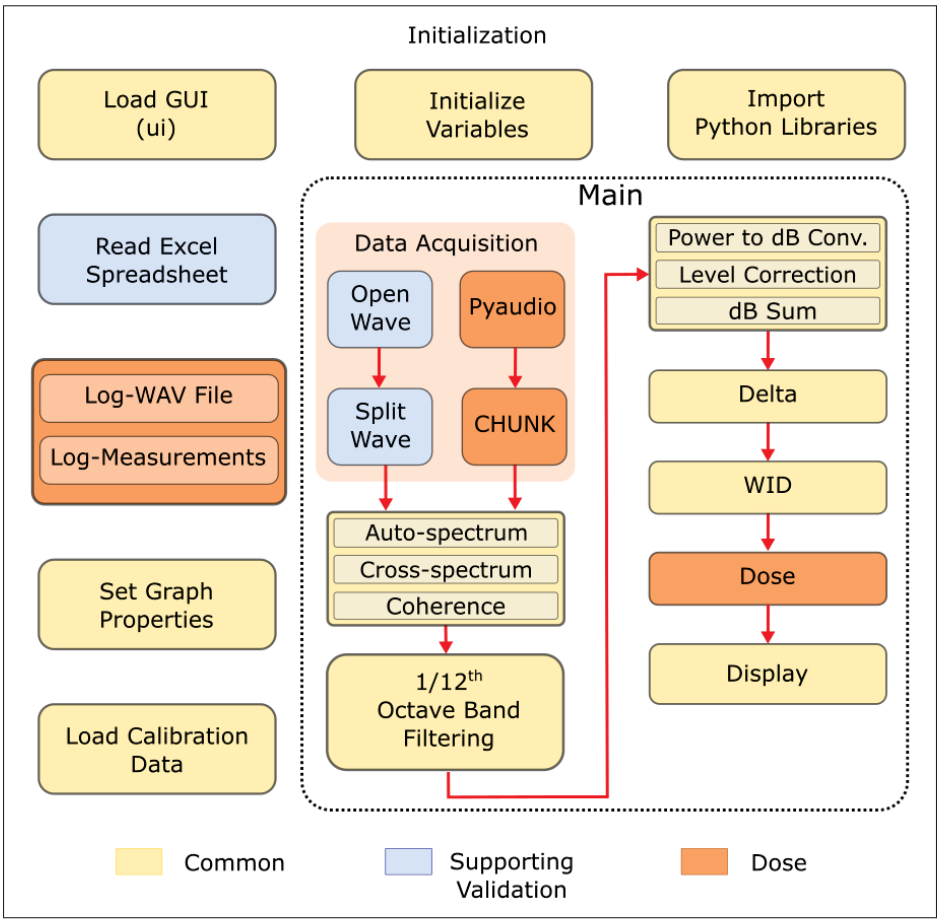

Figure 3.4 Block diagram of the main software functions

3.4.1 Data Acquisition

Data or sound acquisition is achieved using either pyaudio callback mode or a Python library called "wave". Short code implementation is provided as example in the Table 3.9, Table 3.10 and Table 3.11. No further details are given on those since all functions are self-explained.

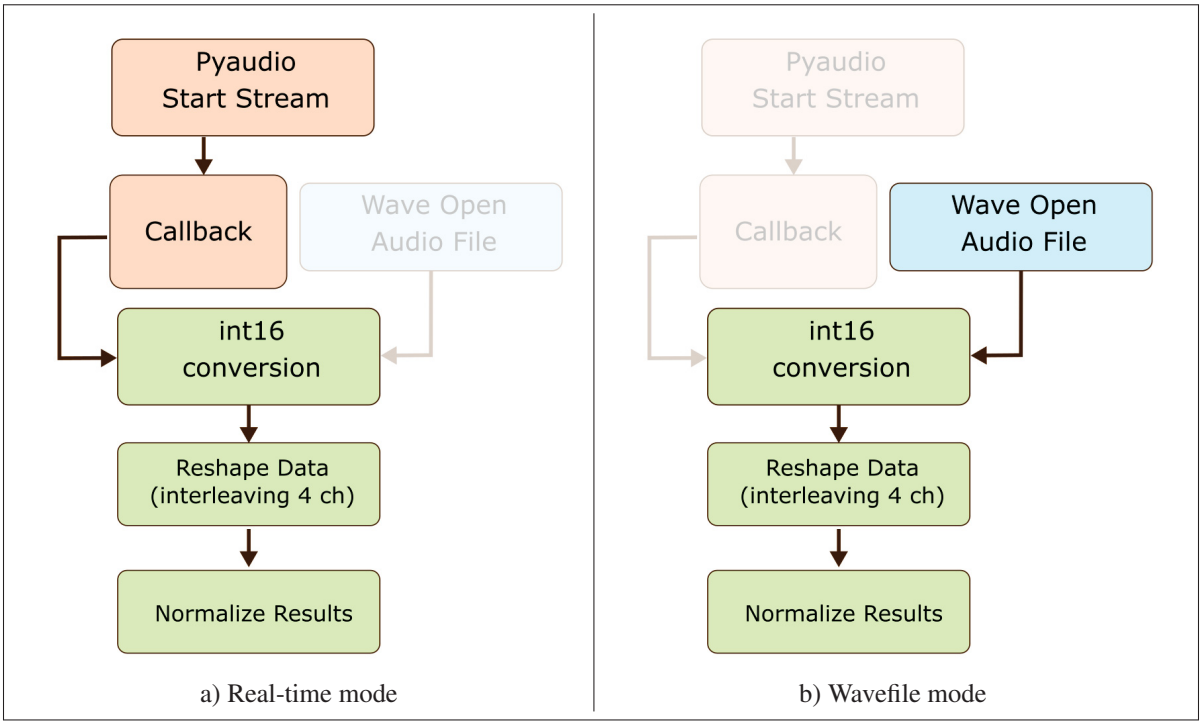

Figure 3.5 Data acquisition function block diagram

Table 3.9 Real time mode

Function	Short Example
Pyaudio Start Stream	`# Start audio input stream` `stream.start_stream()`

Callback	`def get_Samples_callback(self):`
	
	`self.p = pyaudio.PyAudio()`
	`# Setup audio input stream`
	`stream = self.p.open(`
	`format = FORMAT,`
	`channels = CHANNELS,`
	`rate = RATE,`
	`input = True,`
	`frames_per_buffer = CHUNK,`
	`stream_callback = self.callback)`

Table 3.10 Wave open - audio file

Function	Short Example

Wave Open - Audio File	`fp = wave.open('wav_source/16bit_44kHz.wav')`
	`FORMAT = np.int16`
	`CHANNELS = fp.getnchannels()`
	`RATE = fp.getframerate()`
	`CHUNK = int(RATE*0.3)`
	`spwdth = fp.getsampwidth()`
	`N = fp.getnframes()`
	`dstr = fp.readframes(N * CHANNELS)`
	`data = np.frombuffer(dstr, FORMAT)`

Table 3.11 Data conversion, reshape and normalization

Function	Short Example
int16 conversion	`audio_data = np.frombuffer(elem, dtype=np.int16)`
Reshape Data	`result = np.reshape(audio_data, (CHUNK, CHANNELS))`
Normalize Results	`Ch_Lp1 = (result[:,1])/32767 # IEM (left)` `Ch_Lp2 = (result[:,0])/32767 # OEM (right)`

3.4.2 Auto/Cross-spectrum and coherence functions

Auto/Cross-spectrum and Coherence block diagram is shown in the Figure 3.6 and short code examples are provided in the Table 3.12. Auto/Cross-spectrum estimate aims to estimate the power spectrum of two time signals with respect to themselves and to each other respectively The Welch method (Welch (1967)) was used to obtain the auto/cross-spectrum estimates. The coherence functions is explained in Eq. 1.3.

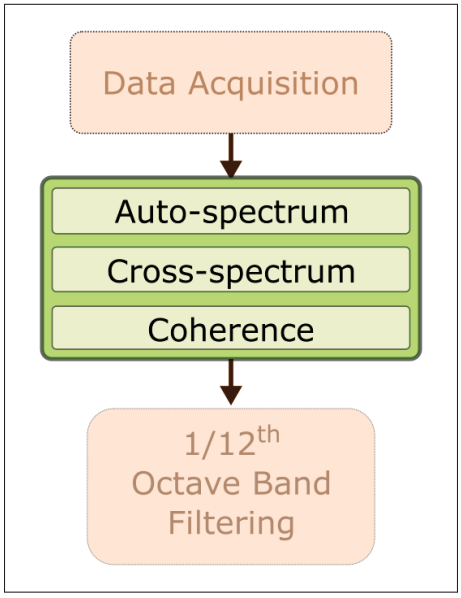

Figure 3.6 Auto / cross-spectrum and coherence functions

Table 3.12 Auto and cross-spectrum function examples

Function	Short Example
CSD or Cross-spectrum	`f12, P12 = signal.csd(Ch_Lp1_partial, Ch_Lp2_partial, fs=RATE, window='hann', nperseg= int(0.3 * RATE), noverlap= 0, nfft=int(0.3 * RATE), detrend=False, return_onesided=True, scaling='spectrum', axis=-1)`
Welch or Auto-spectrum	`W22 = (signal.welch(Ch_Lp2_partial, fs=RATE, window='hann', nperseg=int(0.3 * RATE), noverlap= 0, nfft=int(0.3 * RATE), detrend=False, return_onesided=True, scaling='spectrum', axis=-1)[1])`

Coherence*	`P12_Bands = Power_inBands(P12,i, f12)`
	`Cxy = (np.array(abs(np.array(P12_Bands))))**2 / W11_Bands /W22_Bands`
	`Cxy_bands= Cxy[(23-nf1):(59-nf1)] # range from 200Hz to 1500 Hz (23:59)`
	`Cxy_bands_all [i] = Cxy_bands`
	`Ch_Lp2_Nleq_coh[i] = acoustics.decibel.dbsum(Cxy_bands)`
	*Coherence is given by the Eq. 1.3.

3.4.3 Narrow band to 1/12th octave band spectrum conversion

Narrow band to 1/12th octave band spectrum conversion block is highlighted in the Figure 3.7. A short code example is also provided in the Table 3.13.

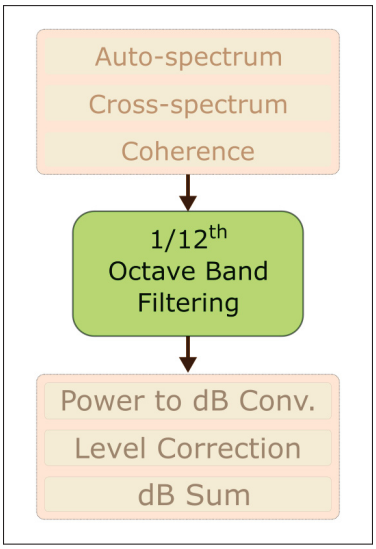

Figure 3.7 Fine band to octave band conversion function

Table 3.13 Fine band to octave band conversion function example

Function	Short Example

Band Conversion	`def Power_inBands(self, Pxy, i, f12):`
	
	`  global Reference_freq, f1`
	`  sum_all = [[]]*len(Reference_freq)`
	
	`  for ii in range(0, len(Reference_freq)):`
	`  a = np.asarray(np.where((f12>= f1[ii]) & (f12 < f1[ii+1])))[0,:] # gives a range where those values are found , removes one dimension of the vector`
	`  b = Pxy[a] # takes the index a from the Cxy array`
	`  sum_all[ii] = np.sum(b)# summ all elements`
	`  power = sum_all # complex number if cross-spectrum`
	
	`  return(power)`

3.4.4 Power to dB - level correction - dB sum functions

Power to dB calculation, Level Correction and dB Sum functions are highlighted in the Figure 3.8.

Power to decibel calculation function converts power spectral values for each frequency band, given by the function given on subsection 3.4.3, in decibels.

Level correction takes into account adjustment and calibration values coming from the calibration procedure, predefined tube length corrections and frequency weighting (A or C) compensation values.

The dB sum function finally consists in summing the power in all frequency bands in order to provide the overall energy of the signal. A short code example for each function is presented in the Table 3.14.

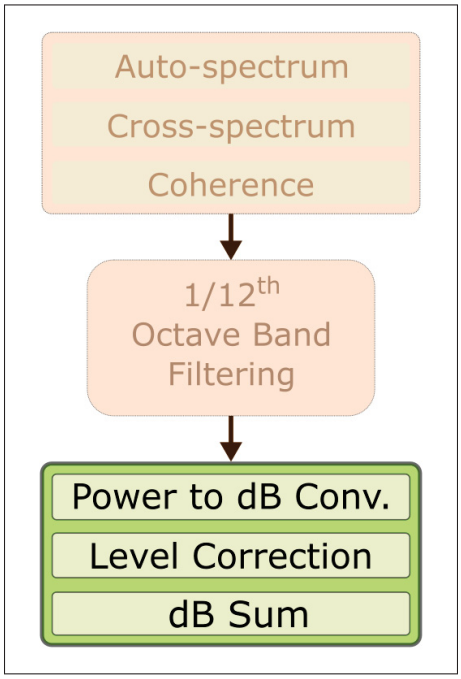

Figure 3.8 Power to dB - Level correction - dB sum functions

Table 3.14 Power to dB - Level correction - dB sum functions

Function	Short Example
Power to dB	`W22_Bands_dB = 10.0*np.log10(np.array(W22_Bands)/ ref**2.0)`
Level Correction	`W11_Bands_dB = W11_Bands_dB + LCorr_OEM`
dB Sum	`Ch_Lp1_Nleq[i] = acoustics.decibel.dbsum( W11_Bands_dB) # OEM`

3.4.5 Delta

Delta function is highlighted in the Figure 3.9 and is given by the Eq. 1.4. A short code example is presented in the Table 3.15.

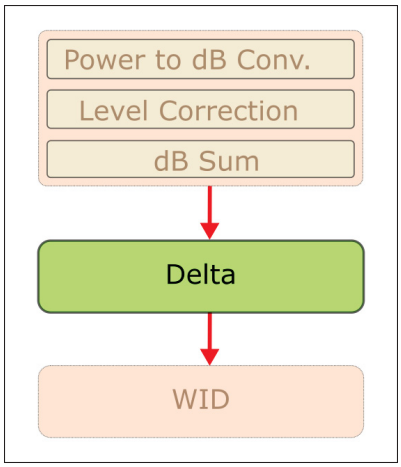

Figure 3.9 Delta function diagram

Table 3.15 Delta function

Function	Short Example
Delta	`Delta[i] = -10*np.log10((np.mean(Cxy_bands)))`

3.4.6 WID detection function

The WID detection function is highlighted in the Figure 3.10 and detailed in the diagram presented in Figure 3.11. This function is responsible for identifying WIDs during operation with the worn earpieces, using the Delta (Δ) and Coherence functions already discussed here. WID detection example code is shown in the Table 3.16.

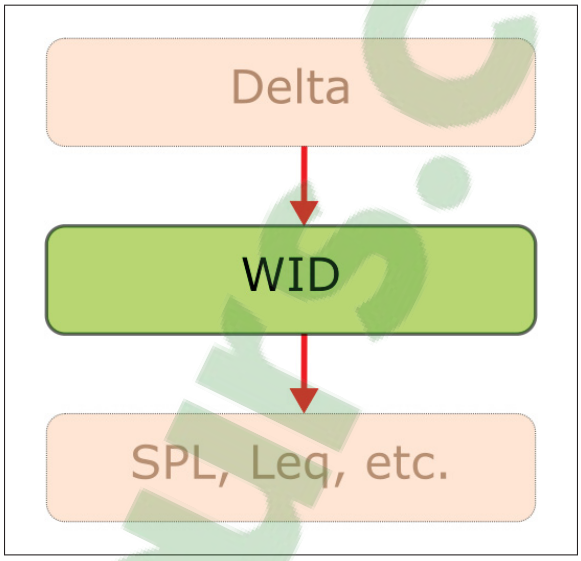

Figure 3.10 WID detection function

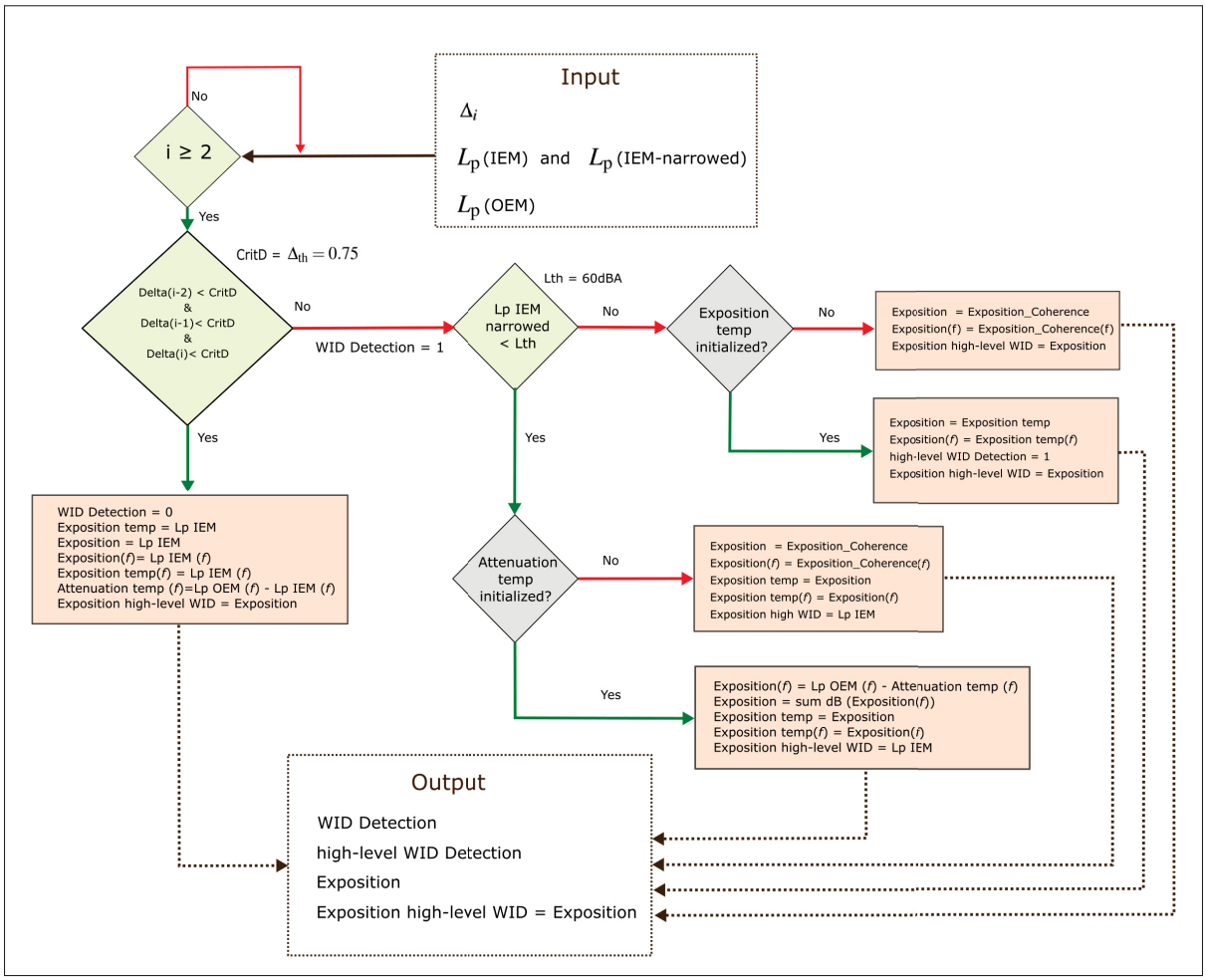

Figure 3.11 WID detection algorithm diagram

Table 3.16 WID function

WID Function Example

```
def WID_Calc(Delta, idx, W11_Bands_dB, W22_Bands_dB, Ch_Lp2_Ovl2nar):
    W11_Bands_dB_WID[idx] = W11_Bands_dB
    W22_Bands_dB_WID[idx] = W22_Bands_dB
    W11_Bands_dB_WID_nar[idx] = W11_Bands_dB[(23-nf1):(59-nf1)]
    W22_Bands_dB_WID_nar[idx] = W22_Bands_dB[(23-nf1):(59-nf1)]
    if idx > 2:
       SPL1[idx-1] = W11_Bands_dB_WID[idx-1]
       SPL2[idx-1] = W22_Bands_dB_WID[idx-1]
       Ch_Lp2_Ovl2[idx-1] = acoustics.decibel.dbsum(SPL2[idx-1]
       if Delta[idx-2]<CritD and Delta[idx-1]<CritD and Delta[idx]<CritD:
            det[idx-1]=0
            Ch_Lp2_Ovltmp = Ch_Lp2_Ovl2[idx-1]
            Ch_Lp2_Ovlexp[idx-1] = Ch_Lp2_Ovl2[idx-1]
            Ch_Lp2_Nleq_No_WID[idx-1]
            SPLexp[idx-1] = SPL2[idx-1]
            SPLtmp = SPL2[idx-1]
            Atttmp = np.array(SPL1[idx-1]) - np.array(SPL2[idx-1])
            Ch_Lp2_Ovlexp2[idx-1] = Ch_Lp2_Ovlexp[idx-1]
       else:
            det[idx-1]=1
            if Ch_Lp2_Ovl2nar[idx-1]<Lth:
                 if np.isnan(Atttmp).any() == False:
                    SPLexp[idx-1] = np.array(SPL1[idx-1])-np.array(Atttmp)
                    Ch_Lp2_Ovlexp[idx-1] = acoustics.decibel.dbsum(SPLexp[
   idx-1])
                    Ch_Lp2_Ovltmp = Ch_Lp2_Ovlexp[idx-1]
                    SPLtmp = SPLexp[idx-1]
                    Ch_Lp2_Ovlexp2[idx-1] = Ch_Lp2_Ovl2[idx-1]
                 else:
                    Ch_Lp2_Ovlexp[idx-1] = OvlCoh[idx-1]
                    SPLexp[idx-1] = SPLcoh[idx-1]
                    Ch_Lp2_Ovltmp = Ch_Lp2_Ovlexp[idx-1]
                    SPLtmp = SPLexp[idx-1]
                    Ch_Lp2_Ovlexp2[idx-1] = Ch_Lp2_Ovl2[idx-1]
            else:
                 if np.isnan(Ch_Lp2_Ovltmp) == False:
                    Ch_Lp2_Ovlexp[idx-1] = Ch_Lp2_Ovltmp
                    SPLexp[idx-1] = SPLtmp
                    det2[idx-1] = 1
                    Ch_Lp2_Ovlexp2[idx-1] = Ch_Lp2_Ovlexp[idx-1]
                 else:
                    Ch_Lp2_Ovlexp[idx-1] = OvlCoh[idx-1]
                    SPLexp[idx-1] = SPLcoh[idx-1]
                    Ch_Lp2_Ovlexp2[idx-1] = Ch_Lp2_Ovlexp[idx-1]

    return
```

3.4.6.1 Spoken sentences and WIDs

The WID detection procedure is explained in the subsection 1.4.1. The following table provides the specific WIDs that were used in the some validation tests described later in chapter 4.

Table 3.17 WID events description

WID Type	Transcription / Description
Speech (Portuguese)	*Ei você aí, tudo bem? Você consegue me ouvir? Pode vir para cá?*
Noise	coughing
Noise	throat clearing
Noise	whistling
Noise	swallowing
Noise	tapping the earpiece

3.4.7 Dose

The dose calculation function is highlighted in the Figure 3.12. One calculates the equivalent sound pressure level $L_{Aeq,T}$ as can be found in Eq. 1.1. Another way of writing this equation is shown below:

$$L_{Aeq,T} = \frac{b}{log_2} \log_{10} \left(\frac{1}{T} \sum_{i=1}^{m} T_i 10^{\frac{log_2}{b} L_{Aeq,i}} \right), \tag{3.1}$$

where:

T is the total measurement time;

T_i is the time duration defined by the CHUNK size. This time-frame is 300 ms;

$L_{Aeq,i}$ is sound pressure level equivalent [dBA] within the time-frame of 300 ms;

b is the exchange rate value currently in use: 3 dB or 5 dB according to the L_c values defined for each region (see Tables I-1 and I-2).

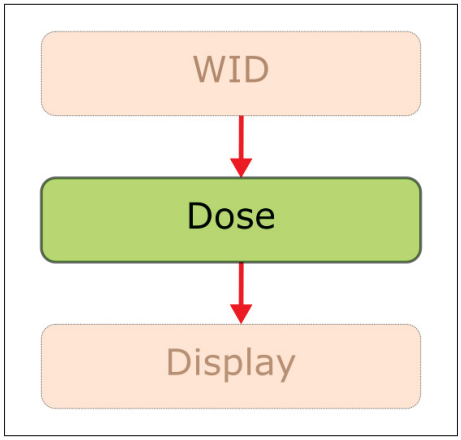

Figure 3.12 Dose function

Table 3.18 Dose function

Dose Calculation Example

```
sum_Aeq0_et = sum_Aeq0_et + 10**(Const * Ch_Lp0_Nleq)
Ch_Lp0_Nleq_disp_acc_et =  (1/Const)*np.log10((1*0.3/T_elp)*sum_Aeq0_et)
Dose_Aeq0_disp_et = (100*T_elp /(T_elp)) * 10**((Ch_Lp0_Nleq_disp_acc_et-
    self.CL)*Const)
```

3.4.8 Display

The display function focuses on displaying, via a graphical user interface (GUI), the results of the calculations for the acquired signals. This function is highlighted in the Figure 3.13 and a short code example is provided in the Table 3.19.

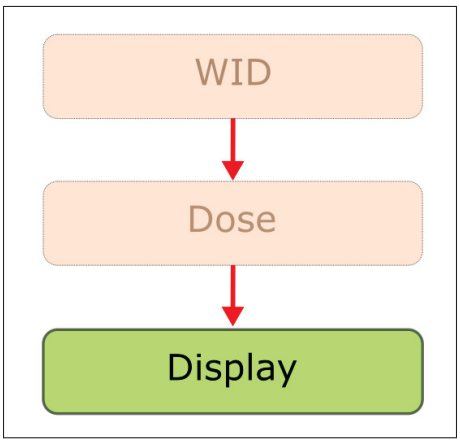

Figure 3.13 Display function

Table 3.19 Display function

Display Function Example

```
def Display_Dose_02(self, T_elp,..., max_RNW):
    if i02 % 3 == 0:  #  update display only every 1s
        #Display accumulated Leq
        self.ui.lbl_SPL_right.setText(str(round(Ch_Lp0_Nleq_disp_acc_et
    ,1)))
        self.ui.lbl_Dose_right.setText(str(round(
    Ch_Lp0_Nleq_No_WID_disp_acc_et,1)))
        self.ui.lbl_SPL_right_level_8h.setText(str(round(
    Ch_Lp0_Nleq_disp_acc,1)))
        self.ui.lbl_SPL_right_level_No_WID8h.setText(str(round(
    Ch_Lp0_Nleq_No_WID_disp_acc,1)))
        self.ui.pg_SPL_right.setValue(int(Dose_Aeq0_disp))
        self.ui.pg_Dose_right.setValue(int(Dose_Aeq0_No_WID_disp))
        self.ui.lbl_SPL_right_level_inst.setText(str(Ch_Lp0_Nleq_disp))

        if (Ch_Lp0_Nleq_disp) > (max_R):# display the max. values
            max_R = Ch_Lp0_Nleq_disp
            self.ui.lbl_SPL_right_level_inst_2.setText(str(round(max_R,1)
    ))
            self.ui.lbl_SPL_right_level_No_WID.setText(str(
    Ch_Lp0_Nleq_No_WID_disp))

        if (Ch_Lp0_Nleq_No_WID_disp) > (max_RNW):# display the max.
    values without WIDs
            max_RNW = Ch_Lp0_Nleq_disp
            self.ui.lbl_SPL_right_level_No_WID_2.setText(str(round(
    max_RNW,1)))
```

3.4.9 Log of data and parameters

The Log function is available for post processing analysis and verification. Data calculation results and parameters of interest can be saved to a textfile or an Excel spreadsheet, and wavefiles can be generated..

Table 3.20 Log functions

Function	Short Example

Log - Measurements	`def Writing_Results_02 (self,nstack) :`
	`  with open("log_files/Results_02.csv","a") as f:`
	`  wr = csv.writer(f)`
	`  global header_in02`
	`  if header_in02 == 0:`
	`  wr.writerow(['Date', 'Time', 'Elapsed Time ', 'Lp0 Inst.', 'Lp0 Inst. No WID', 'Lp0 Aeq,8', 'Lp0 Aeq,8 - No WID', 'Dose', 'Dose No WID', 'VAD_02[i-1]', ' Delta02M2', 'Delta02M1', 'Delta02M0' ])`
	`  header_in02 = 1`
	`  wr.writerows(nstack)`

Log - Wavefile	`def Rec_Wav(self,arg):`
	`  global index`
	`  print("recording...")`
	`  index_str = str(index)`
	`  file_name = 'log_wavefile/log_wavefile_'`
	`  extension = '.wav'`
	`  if self.ui.chkB_Wav.isChecked():`
	`  file_name=file_name + index_str + extension`
	`  waveFile = wave.open(file_name, 'wb')`
	`  waveFile.setnchannels(CHANNELS)`
	`  waveFile.setsampwidth(self.p.get_sample_size(FORMAT))`
	`  waveFile.setframerate(RATE)`
	`  waveFile.writeframes(b''.join(wave_app))`
	`  waveFile.close()`
	`  wave_app.clear()`
	`  i02 = 0`
	`  i13 = 0`
	`  i= 0`
	`  index += 1`

3.5 Supporting tools

"Supporting tools" is a set of functions that were employed to support the development and the debugging of the main codes. It uses data collected and processed via Matlab functions, developed by Bonnet. Those tools helped to identify potential implementation mistakes when comparing the Matlab and Python implementations with the original Matlab code and algorithms.

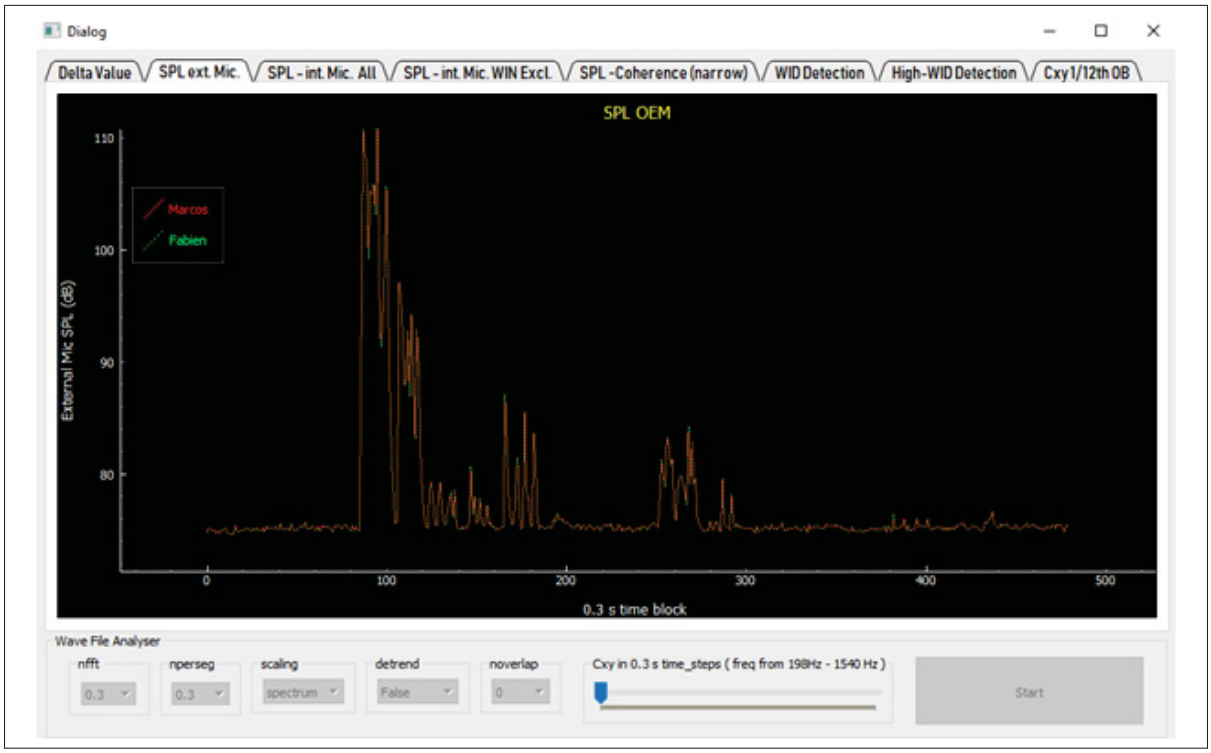

Figure 3.14 Supporting tool results example: SPL OEM

In addition to the common functions already described in section 3.4, the main functions developed in the "supporting tools" set are:

- **Open Wave / Split Wave** - as described in 3.4.1 and depicted in the Figure 4.4;
- **Read Excel Spreadsheet** - Read some results and information generated by Bonnet for comparing the Matlab and Python implementations of the algorithms;

- **Audio Recording** - wavefile recording program used for initial tests.

Examples of results obtained with the supporting tools are illustrated in the Figure 3.14 and in Figure 3.15 where results obtained with Bonnet's Matlab implementations (noted Fabien) and Python implementations (noted Marcos) are shown.

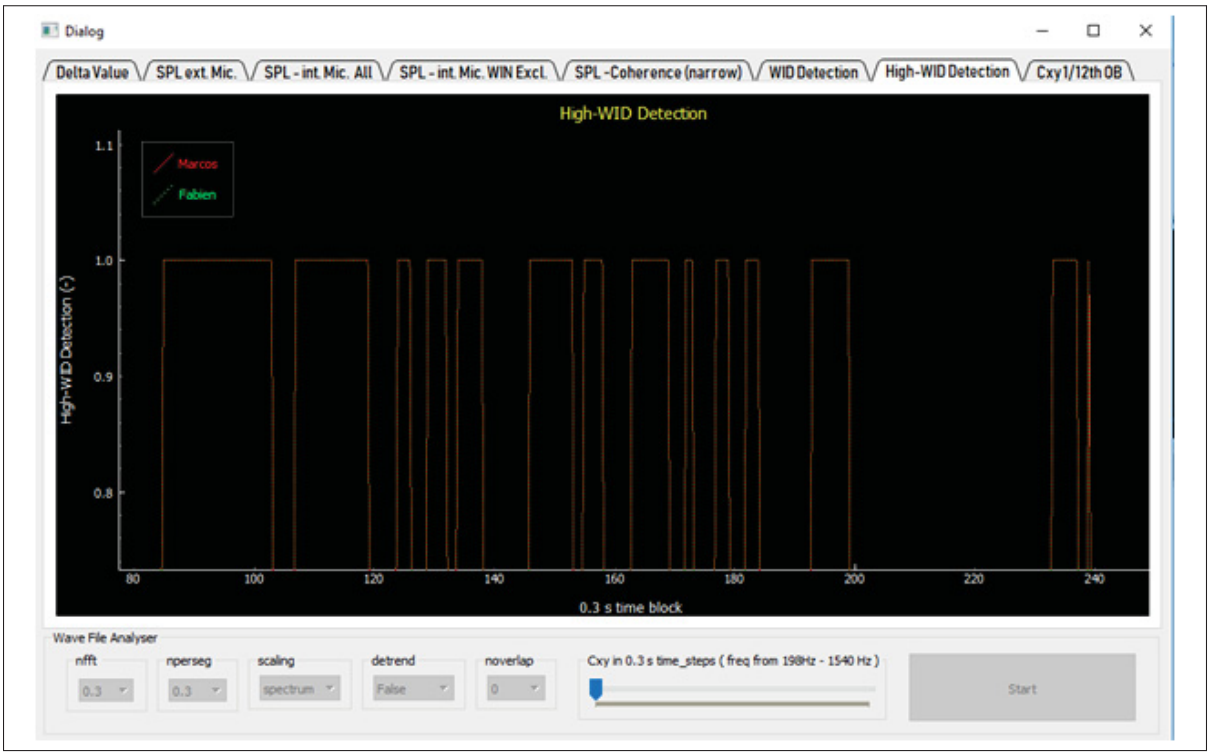

Figure 3.15 Supporting tool results example: High-WID Detection

3.5.1 Spreadsheet reading

Table 3.21 Spreadsheet reading function

Function	Short Example

Spreadsheet Reading	`from input_source_files.latest import For_MN_Cxy`
	`from input_source_files.latest import For_MN`
	`n_Col_MN = int(len(result)/CHUNK)`
	`MN_SPL = np.array(For_MN.data_Fabien(9, n_Col_MN, tab)).ravel()`
	`MN_WID_det = np.array(For_MN.data_Fabien(10, n_Col_MN, tab)).ravel()`
	`MN_highWID_det = np.array(For_MN.data_Fabien(11, n_Col_MN, tab)).ravel()`

A short code example for the spreadsheet function is given in the Table 3.21. Spreadsheet reading function basically reads data acquired and processed by Bonnet using his own methodology and algorithms. The data was stored in an Excel spreadsheet using a specified format. It consists in a simple GUI allowing to define the recording of time samples for a specified duration.

3.5.2 Audio recording

The audio recording program was first developed to support initial tests from Bonnet. Screenshots from this program is shown in the Figure 3.16. This program allows the audio recording for up to 4-hour with maximum wavefile size of 15 minutes.

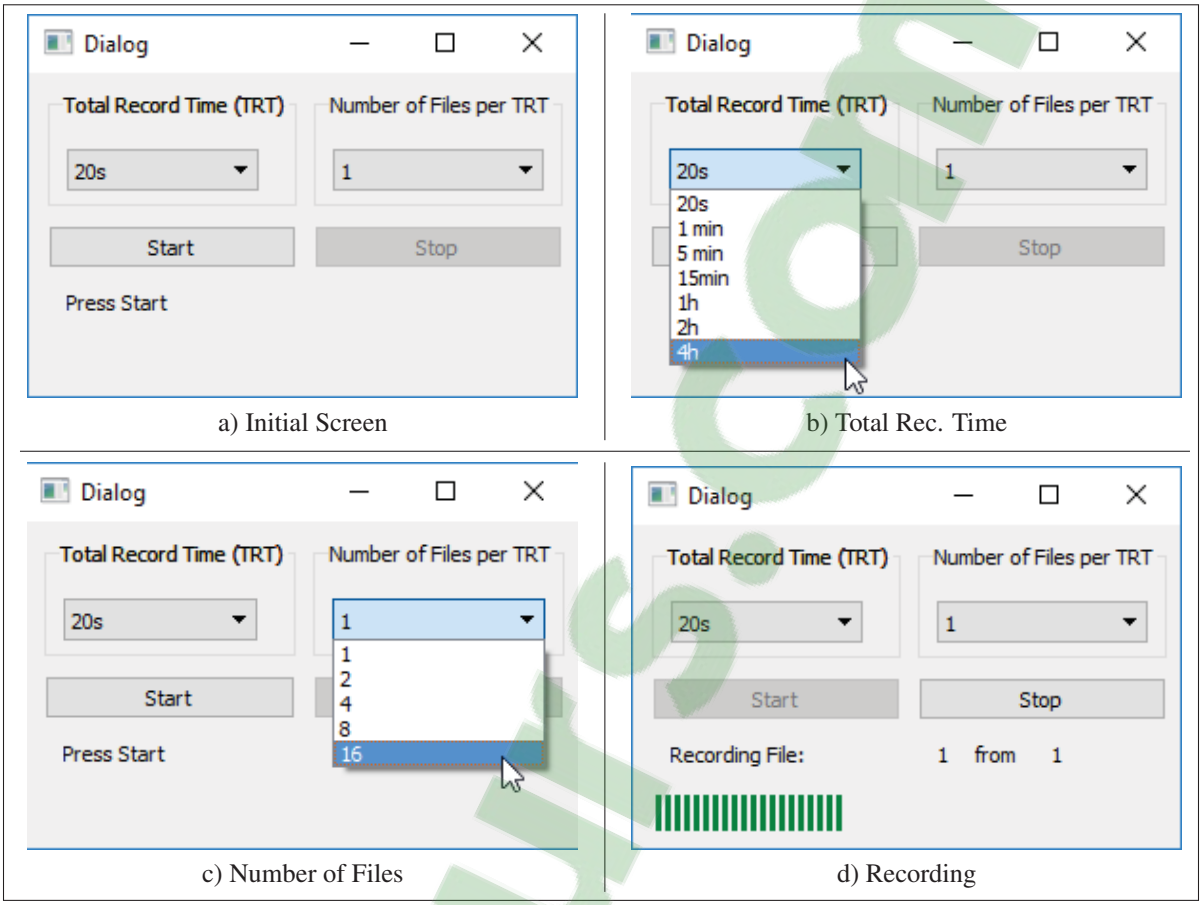

Figure 3.16 Wavefile recording - initial program

3.5.3 Calibration

The calibration procedure comprises three distinct steps, as depicted in Figure 3.17, Figure 3.18 and 3.20. The first two steps (A and B) pertain to the microphones calibration. First, sound data from a reference microphone G.R.A.S. (GRAS Sound Vibration A/S, Skovlytoften, Denmark) model 40HF connected to a sound calibrator BK (Brüel Kjær Sound and Vibration Measurement A/S, Nærum, Denmark) Type 4231, shown in step A, is acquired.

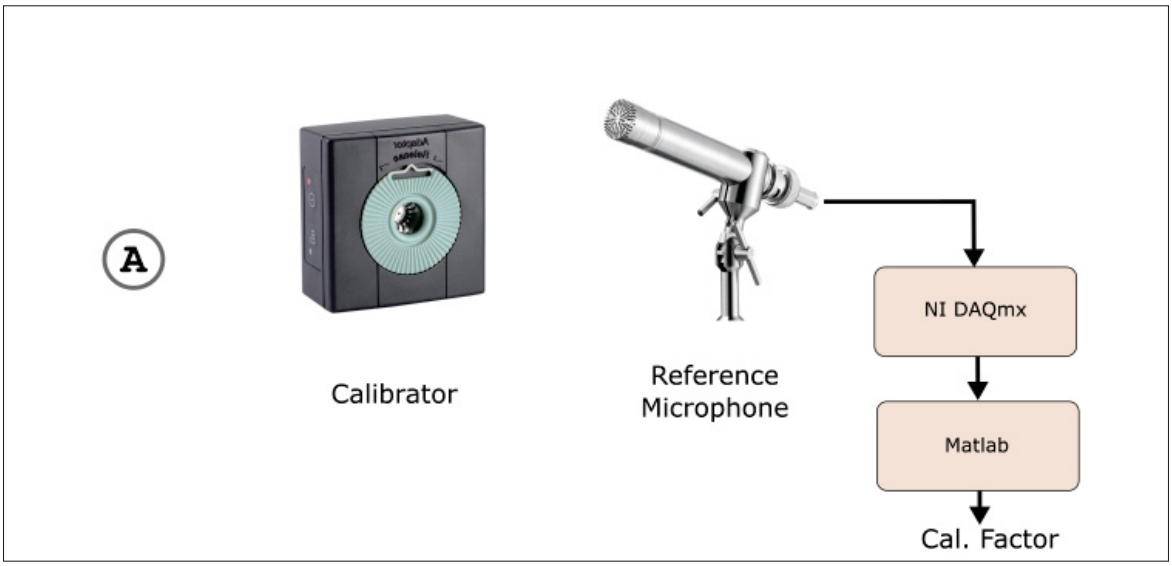

Figure 3.17 Calibration diagram - Step A

In this phase, the data acquisition is performed using a National Instruments (National Instruments Corp., Austin, TX, USA) DAQmx equipment and an appropriate Matlab code.

In step B, the prototypes and the reference microphone are all placed together at the same position facing an amplified loudspeaker - PreSonus (PreSonus Audio Electronics, Inc., Baton Rouge, LA, USA) Model ERIS E3.5 - generating white noise. Signal measurements are then performed and calibration factors for the miniature microphones are then obtained using comparisons with the reference microphone measurements.

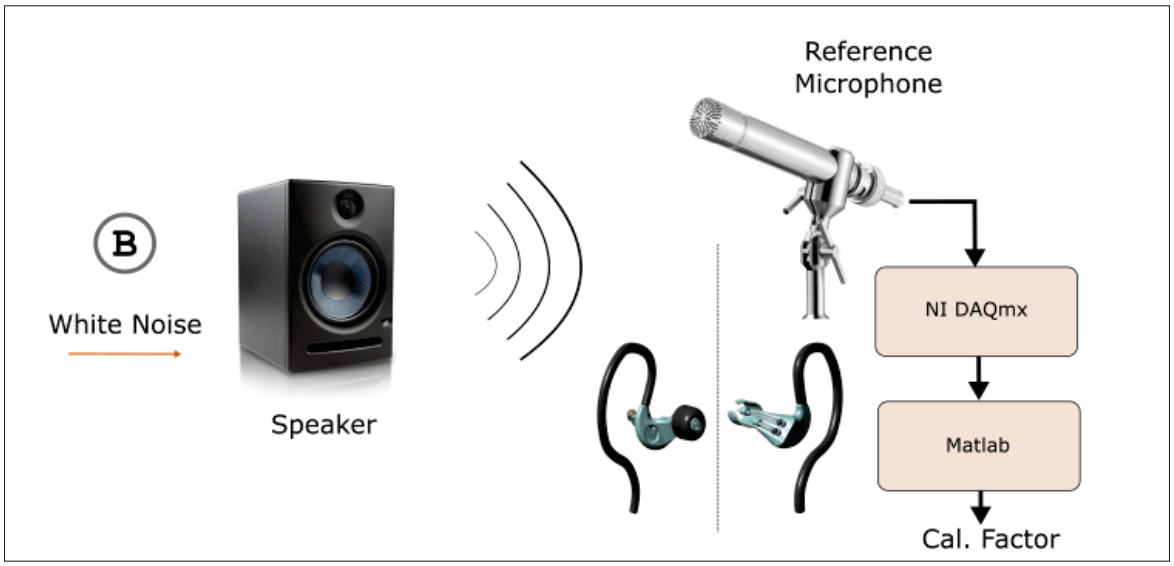

Figure 3.18 Calibration diagram - Step B

The result from the above steps provides a number which is then fed back into the calibration program for the calibration factor calculations as can be seen in the figure 3.19.

The last calibration step (Figure 3.20) is used to obtain the individual correction factors via the MEC function identification. The subject is asked to remain seated and insert the prototypes in his/her own ears. White noise is then generated and measurements are performed. As explained by Bonnet *et al.* (2019a), in the case the CEP device, the subject is required to turn around 180 degrees for about 15 s during the MEC identification. Example of subjects performing the entire calibration procedures is shown in the Figure 3.21.

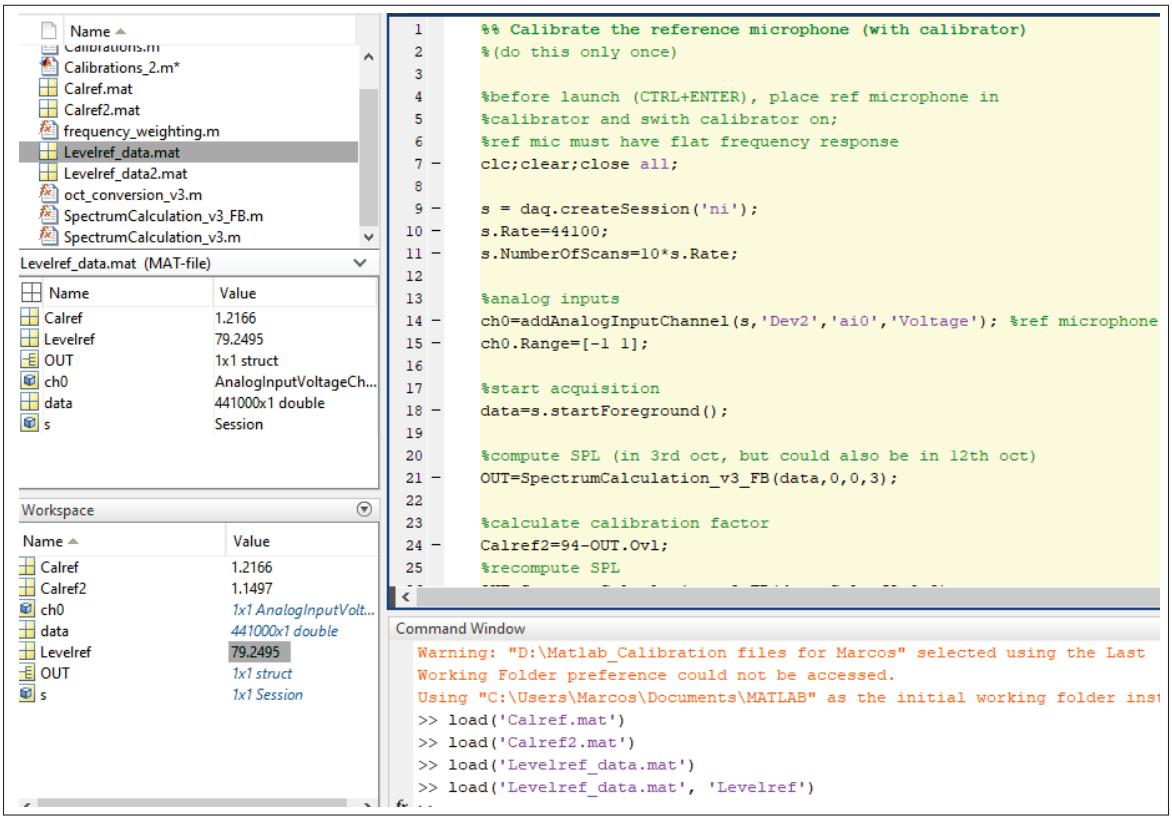

Figure 3.19 Example of microphones calibration results in Matlab

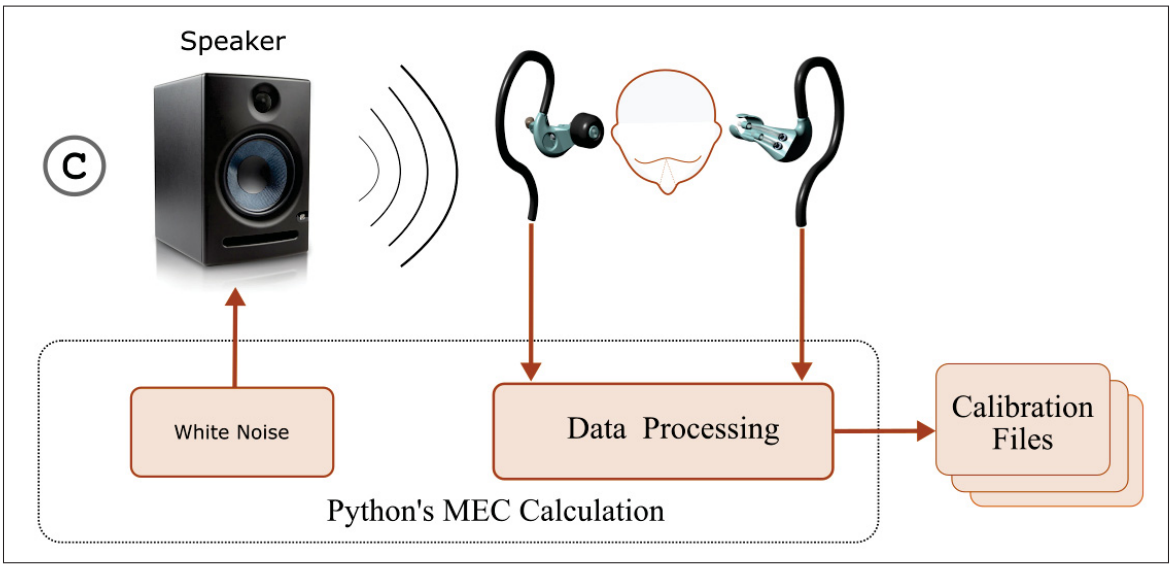

Figure 3.20 Calibration diagram - Step C

Examples of MEC identification are shown in Figure 3.25. The procedure described in Figure 3.20 has to be carried out in a room set up with the right tools and necessary instructions. Instructions on this procedure are depicted in the Figure IV-2 and Figure IV-3. Figure 3.21 shows subjects during the calibration procedure. The test environment can also be seen in the Figure 3.22.

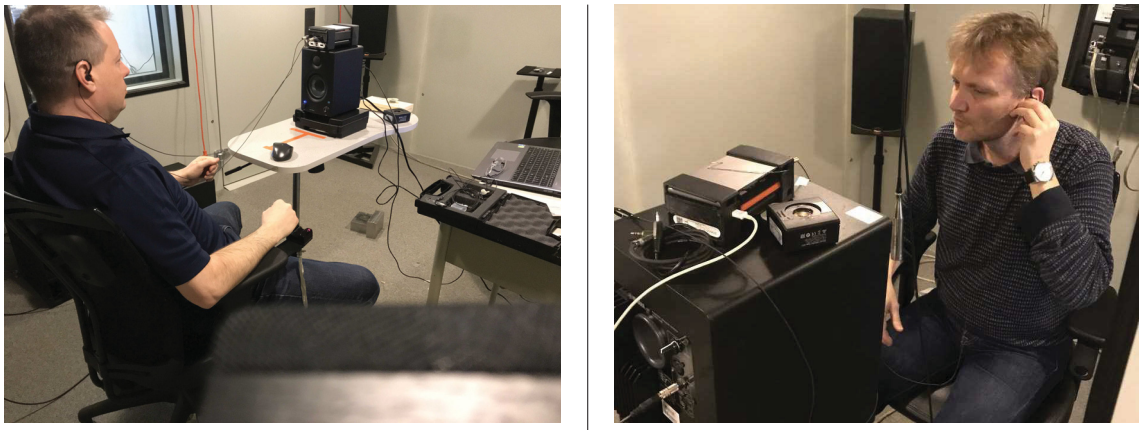

a) Subject 1 Performing the Calibration

b) Subject 2 Performing the Calibration

Figure 3.21 Examples of subjects during the calibration tests

a) Environment and Tools - View I

b) Environment and Tools - View II

Figure 3.22 Environment and tools used during the calibration tests

An illustration of the interface used for the calibration procedures is presented in Figure 3.23. If one excludes the steps shown on figure 3.17 and on figure 3.18, which have to be done by

a trained personal, the step shown on figure 3.20 can be done by the subject him/herself. In this process, it is assumed that any individual should be able to perform his/her own calibration without any exterior help, as it will be the case when potentially wearing the device in the workplace. Additionally, it is recommended to conduct ear examinations before using the device, especially an otoscopic screenings to ensure that no ear abnormalities are present.

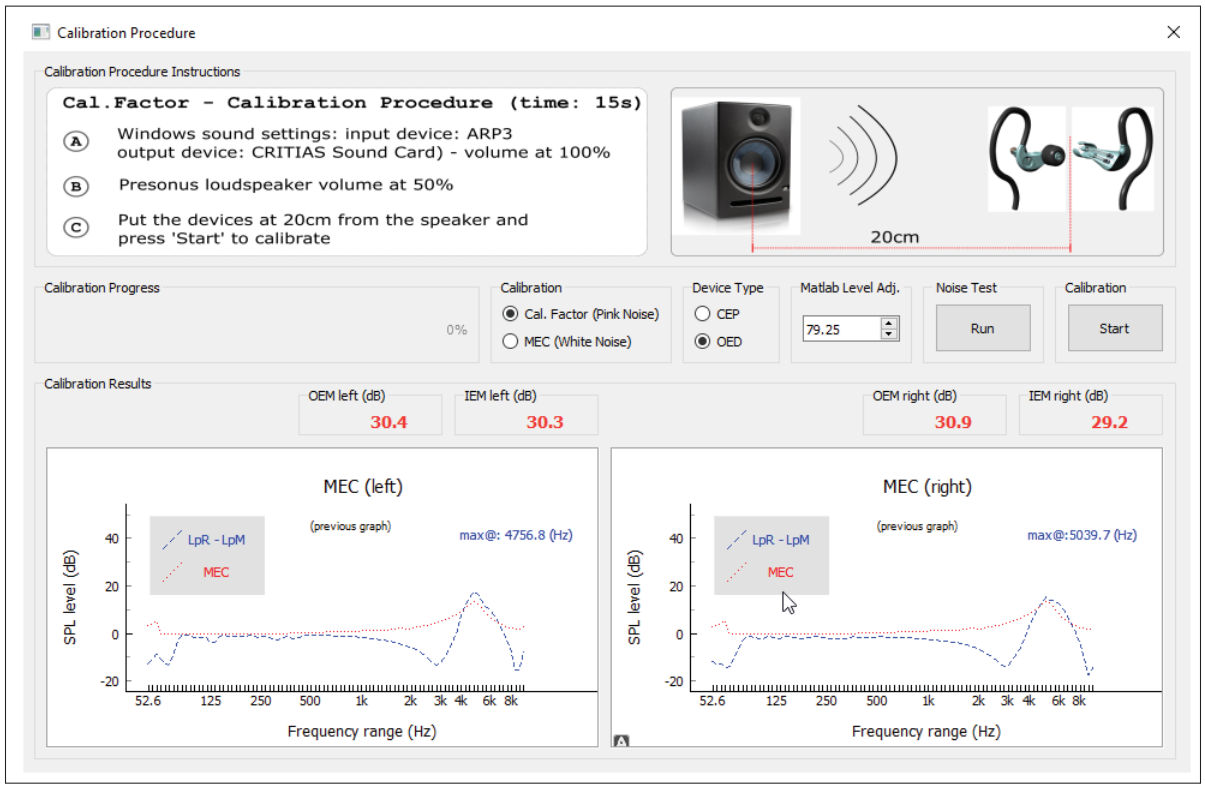

Figure 3.23 Screenshot of the interface for the calibration procedures

Examples of calibration values obtained at the end of the calibration procedures for a given subject wearing the OED are shown in Figure 3.24 and examples of MEC curves are shown in Figure 3.25.

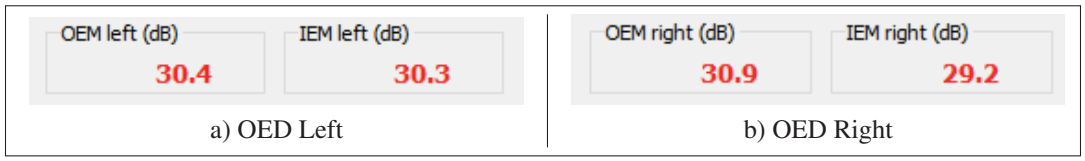

a) OED Left b) OED Right

Figure 3.24 Examples of microphone calibration factor values for the OED

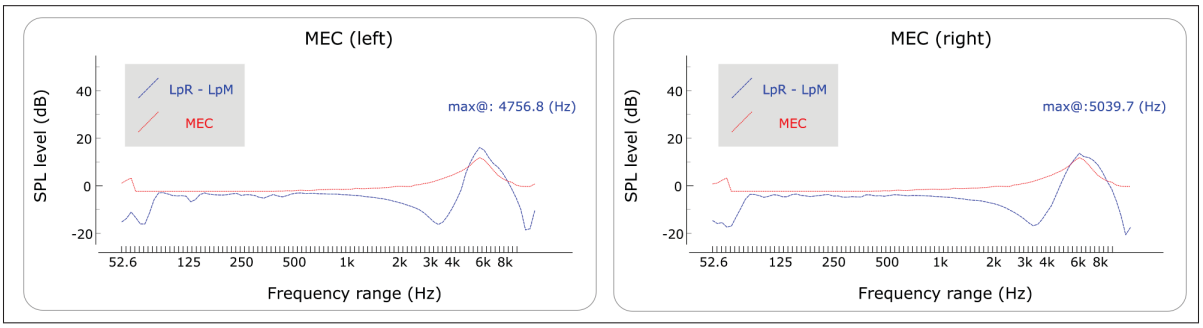

Figure 3.25 Examples of MEC curves obtained on a given subject wearing the OED

Similarly, examples of calibration values obtained at the end of the calibration procedures for a given subject wearing the CEP are shown in Figure 3.26 and examples of MEC curves are shown in Figure 3.27.

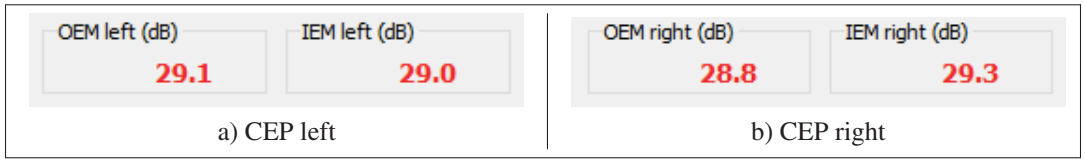

a) CEP left b) CEP right

Figure 3.26 Examples of microphone calibration factor values for the CEP

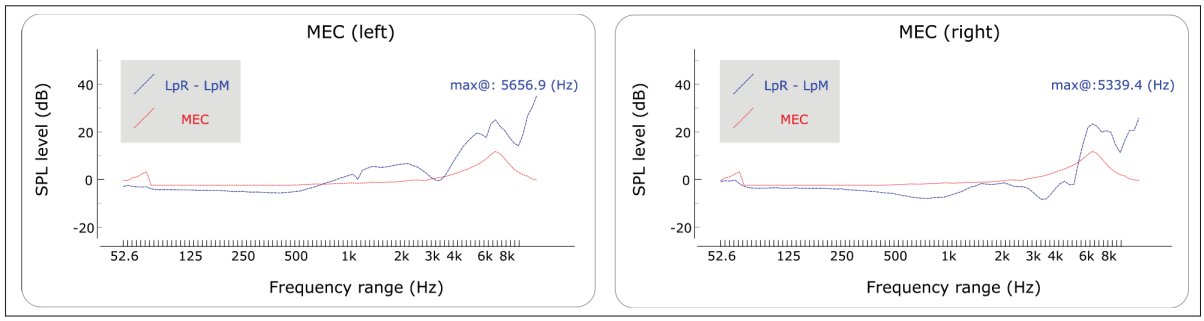

Figure 3.27 Examples of MEC curves obtained on a given subject wearing the CEP

CHAPTER 4

VALIDATION TESTS

Once all the correction factors were obtained from the calibration procedure in section 3.5.3, a validation of the entire system (prototypes, platform, assembly and software) was validated in a laboratory environment.

A subject was instrumented with the CEP in the right ear and was asked to generate some WIDs in background noise. Two validation procedures were exercised in this work:

- **Validation I** - from existing data collected in an open field environment;
- **Validation II** - from data collected in a controlled environment:in a semi-anechoic room and in a reverberent room.

Time signals were recorded on the ARP3 platform and saved as wavefiles. These files were processed with both the Python implementation and Bonnet's Matlab implementation for comparisons. Output results included data such as Outer-ear SPL, In-ear SPL (WID included), In-ear SPL (ALL WID excluded), etc.

Data for the validation I comes from the work of Bonnet et *al.* and is illustrated in Figure 4.4 and Table 4.1.

This set of data was acquired from tests performed by Bonnet from a test made in an indoor noisy shopping mall where the wearer remained seated, with the recording platform resting on a table aside. Recording time was around 15 min long and was made possible by using a Python based recording program shown in the Figure 3.16.

For the validation II, the following test scenarios indicated in Figure 4.1 were carried out in the semi-anechoic room and reverberent room.

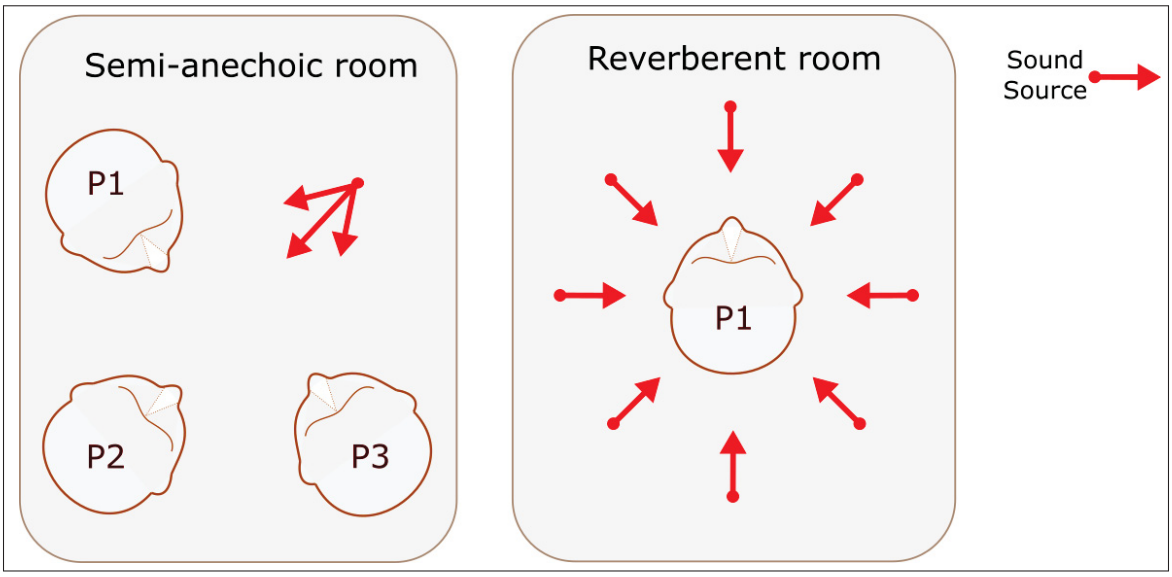

Figure 4.1 Illustration of the subject's positioning in the semi-anechoic room (left) and reverberent room (right) during the acoustical tests

The tests in the semi-anechoic room were performed with only one loudspeaker whereas in the reverberent room four loudspeakers were employed for white noise generation. In both cases, the SPL generated was around 87 dB(A) and the subject was asked to utter a short sentence and make various noises , such as coughing, sneezing, tapping the earpiece, etc. (see Table 3.17), very similar to the tests in the original work of Bonnet *et al.* (2019a); École de technologie supérieure (2018); Bonnet *et al.* (2018a). The positions P1, P2 and P3 shown in Figure 4.1 refer to the head position relative to the loudspeaker(s) during the tests. The CEP device was worn in the right ear side.

The tests for validation II were conducted in the ICAR(Infrastructure commune en acoustique pour la recherche ÉTS-IRSST) reverberent room and the semi-anechoich room both located at ÉTS Montreal. Figure 4.2 and Figure 4.3 shows the two rooms used for the validation II tests.

Figure 4.2 Semi-anechoic room used for tests with the earpieces

Figure 4.3 Example of the reverberent room used for tests with the same earpieces

Two validation scenarios are detailed in the following subsections.

4.1 Validation I

Data collected during the validation phase with subjects from the work of Bonnet *et al.* (2019b) were used in validation I. The core timedata was stored in a wavefile and the results from Bonnet's implementation was stored in an Excel spreadsheet. This wavefile was used as the

input for the Python's implementation and the results were compared to Bonnet's results. These comparisons primarily served during the development of the code as a debugging tool.

Figure and Table 4.1 show some parameters and fields that were used during the validation process.

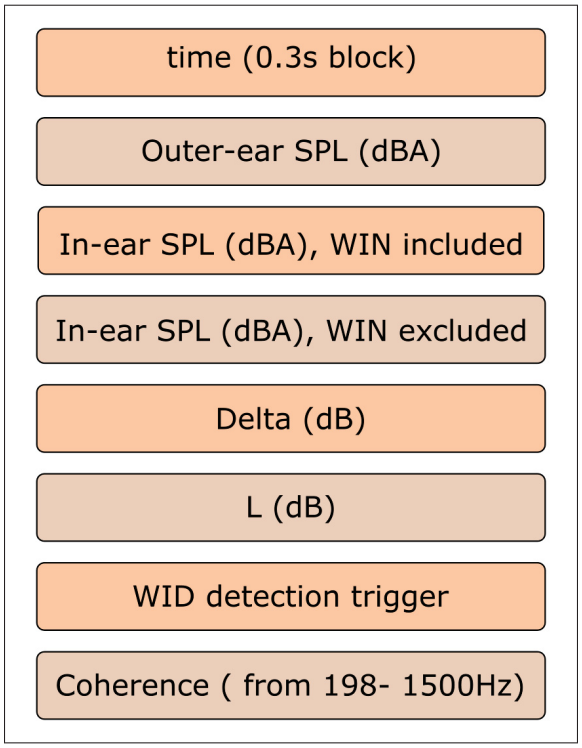

Figure 4.4 Validation table content

Table 4.1 Additional parameters

Additional Parameters	**Value**
Cal factor OEM (dB)	30.6
Cal factor IEM (dB)	32.2
f_{min} (Hz)	198
f_{max} (Hz)	1500
L_{th} (dB)	60
$Delta_{\text{ th}}$ (dB)	0.75
Tube correction IEM (dB)	see Figure 4.5

The tube correction curve is intended to "correct" the microphone original frequency response to take into account the effect of the small tube that. An example of such curve is given in Figure 4.5.

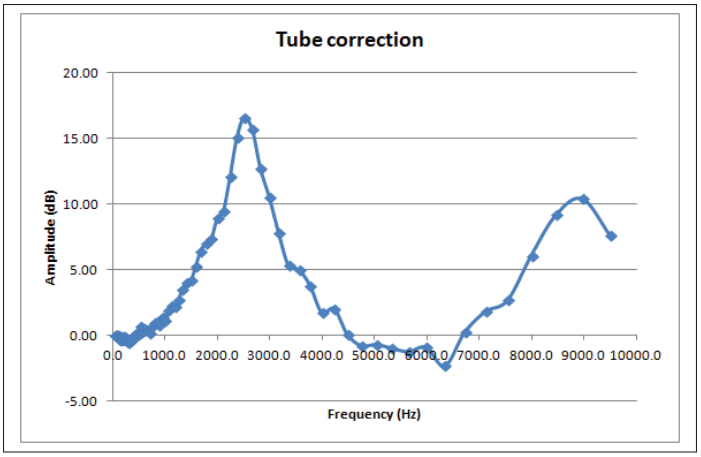

Figure 4.5 Tube correction example curve

4.2 Validation II

The second validation process underwent by collecting data in-situ during the tests conducted in anechoic chamber and reverberation room. The core timedata was also saved on a wavefile that was then analysed by Matlab original algorithms and by the Python's implementation for comparisons.

4.3 Dose application program

A screenshot of the output interface for the dose is given in the following picture:

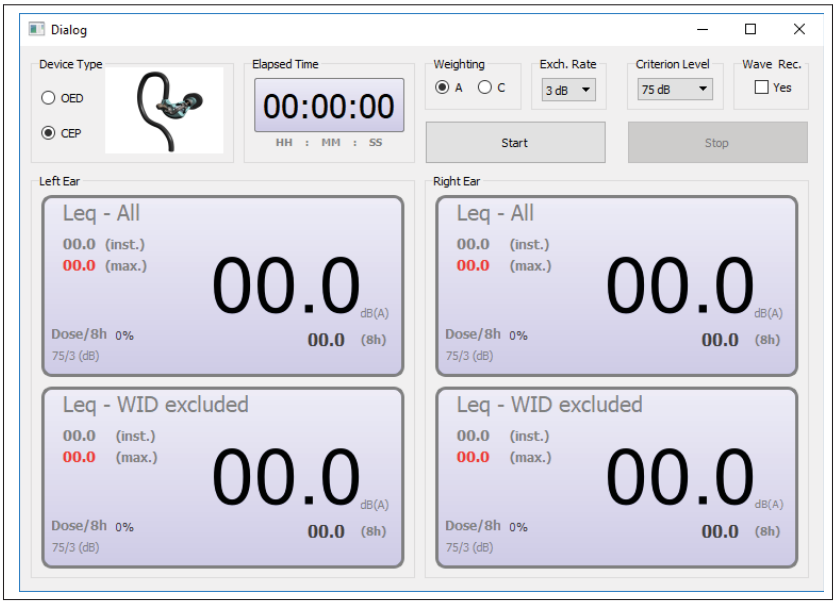

Figure 4.6 Illustration of the dose calculation interface

Some parameters can be set in the main window:

- Device type (occluded or open)
- A/C weighting filtering
- Exchange rate and Criterion level for dose purposes
- Wavefile recording option

The displayed data are:

- Elapsed time;
- Leq (includind and exluding WIDs);
- Elapsed time dose and per 8h;
- Maximum and current sound pressure level.

Figure 4.7 Dose detailed outcome

Remote access feature was also implemented on this work as explained in the Appendix VI section.

4.4 Validation results

The two validations tasks presented above showed that the same values were obtained when comparing the Python's implementation with the Matlab one. Examples of results obtained with the two implementations are shown in the next sections. Important to notice that all those results are identical to the implementation in Matlab and thus they don't need further explanations.

4.4.1 Results from validation I

This section presents comparisons obtained in the validation I task. For all results presented, Spreedsheet/Wavefile 1 and Spreedsheet/Wavefile 2 are data provided by Bonnet. The results from Bonnet implementation in Matlab are noted "Reference Data" whereas the results from the Python implementation are noted "Real-Time Algorithm".

4.4.1.1 Delta values

The Delta variable is explained in details in section 1.4.1 by the Equation 1.3.

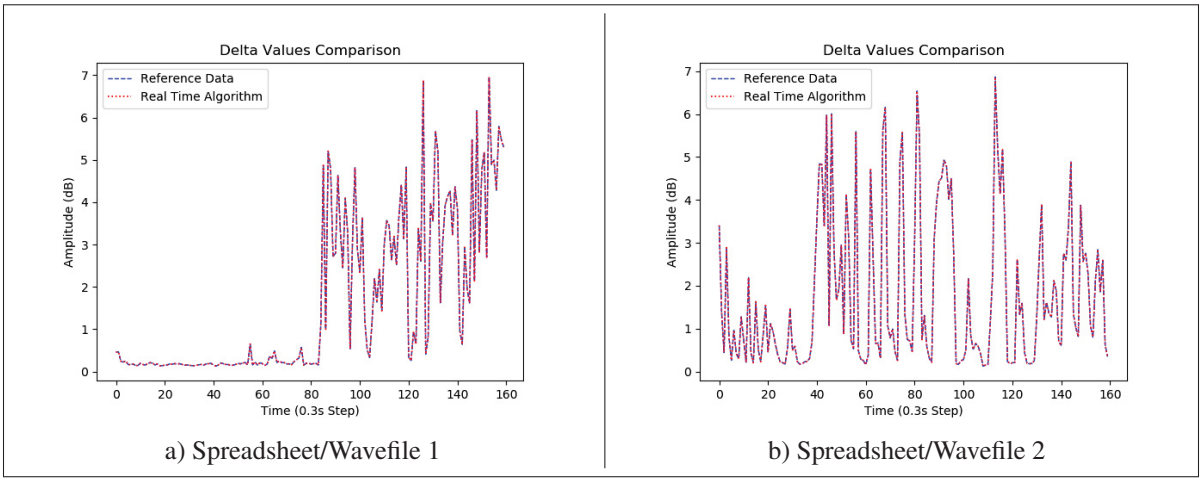

a) Spreadsheet/Wavefile 1 b) Spreadsheet/Wavefile 2

Figure 4.8 Delta values in dB as a function of time for validation-I

4.4.1.2 WID detection

The following test results show the WID detection decision ("1" indicates that WID has been detected) as a function of time for four subject positions as represented in Figure 4.1. It shows that the results coming from the tests and processed with the Python implementation matched exactly the data processed with Bonnet's Matlab implementation.

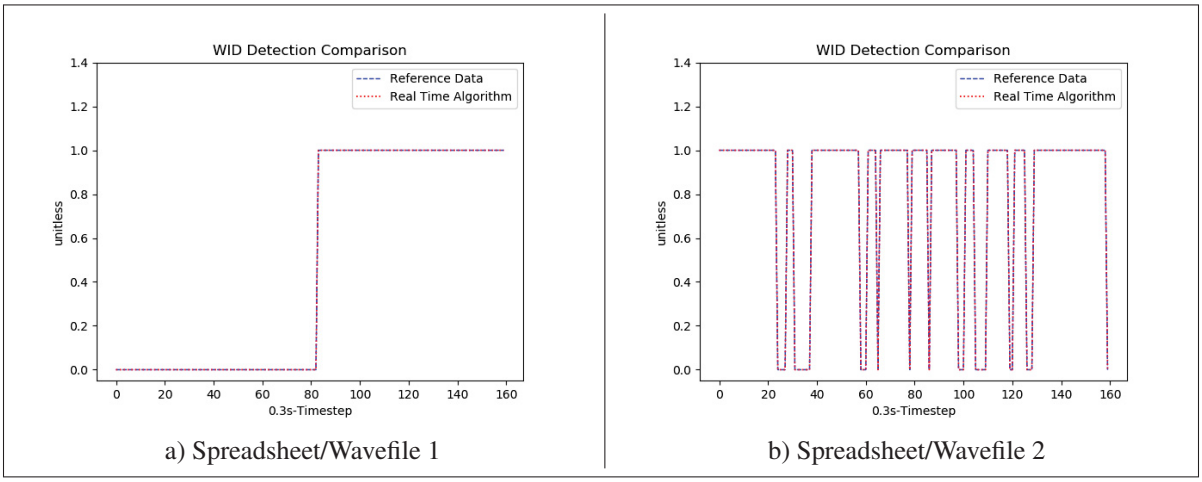

a) Spreadsheet/Wavefile 1 b) Spreadsheet/Wavefile 2

Figure 4.9 WID detection values for validation-I

4.4.1.3 High WID detection

The following results show the high-WID detection decision ("1" indicates that WID has been detected) as a function of time for four subject positions as represented in Figure 4.1. High-WID detection refers to the WIDs detected when the ambient noise is higher than a threshold value (e.g. 60 dB). It shows that the results coming from the tests and processed with the Python implementation matched exactly the data processed with Bonnet's Matlab implementation.

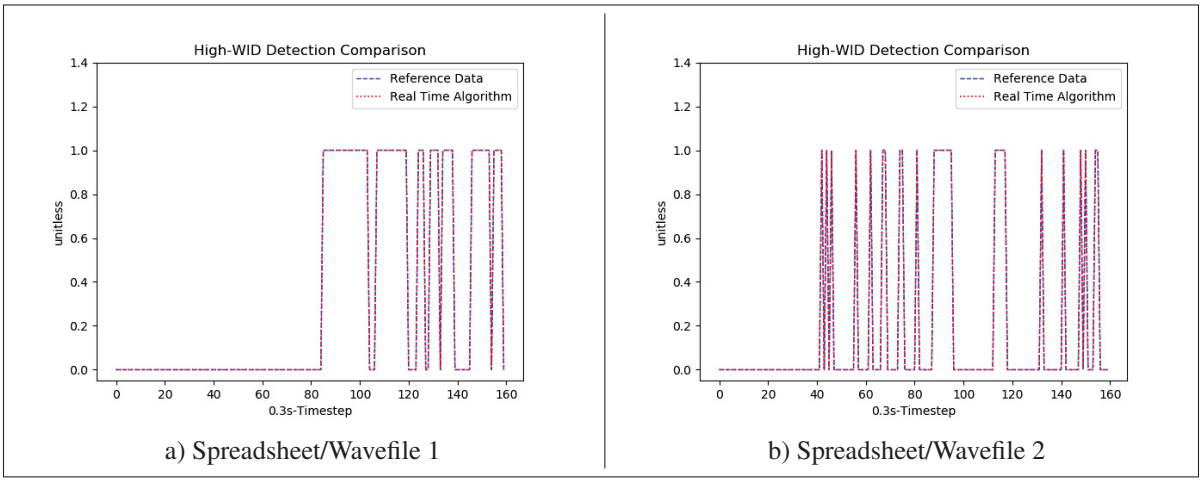

a) Spreadsheet/Wavefile 1 b) Spreadsheet/Wavefile 2

Figure 4.10 High-WID detection values for validation-I

4.4.1.4 OEM

Figure 4.11 shows the SPL measured by the external microphone (OEM). It shows that the results coming from the tests and processed with the Python implementation matched exactly the data processed with Bonnet's Matlab implementation.

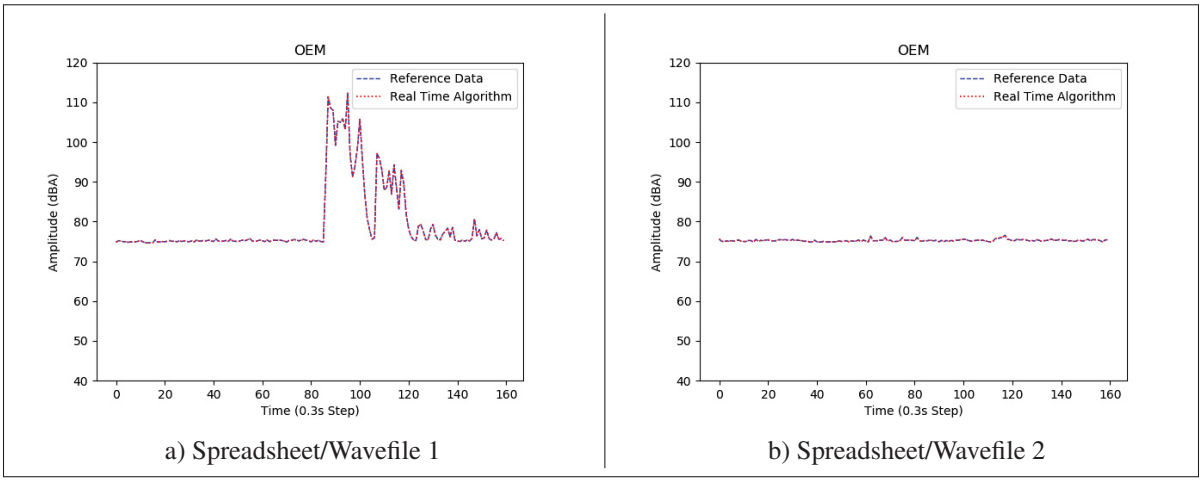

a) Spreadsheet/Wavefile 1 b) Spreadsheet/Wavefile 2

Figure 4.11 SPL in dBA at the OEM as a function of time for validation-I

4.4.1.5 IEM including WID

Figure 4.12 shows the SPL measured by the internal microphone (IEM) including the self-induced noises from the user. It shows that the results coming from the tests and processed with the Python implementation matched exactly the data processed with Bonnet's Matlab implementation.

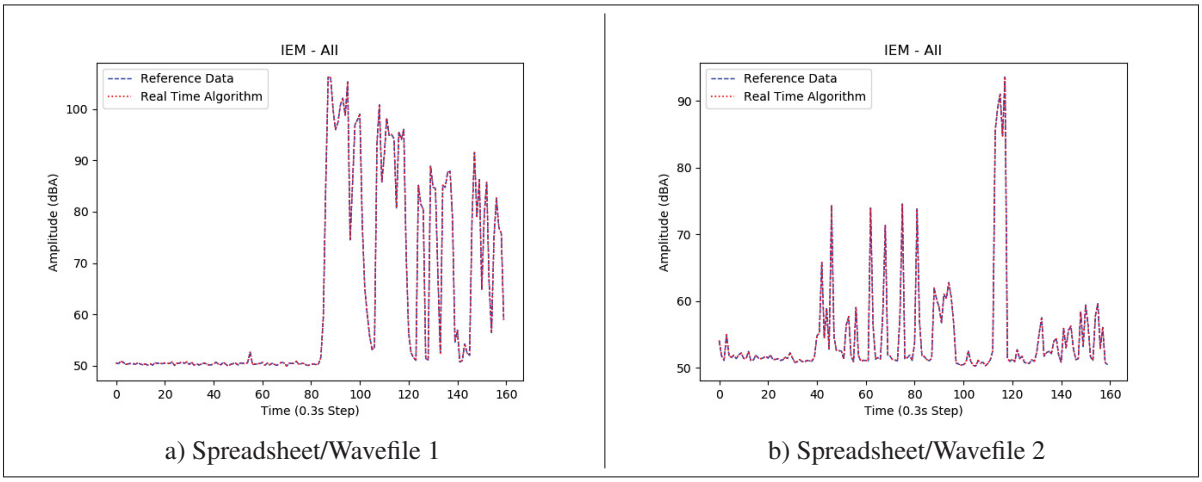

a) Spreadsheet/Wavefile 1 b) Spreadsheet/Wavefile 2

Figure 4.12 SPL in dBA at the IEM as a function of time/ WID included for validation-I

4.4.1.6 IEM excluding WID

Figure 4.13 shows the SPL measured by the internal microphone (IEM) excluding the self-induced noises from the user. It shows that the results coming from the tests and processed with the Python implementation matched exactly the data processed with Bonnet's Matlab implementation.

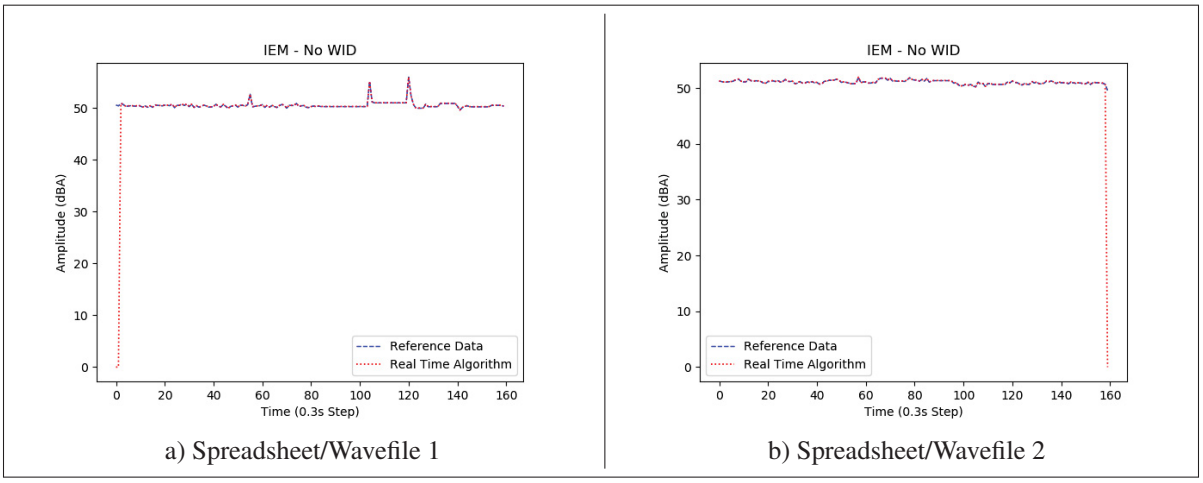

a) Spreadsheet/Wavefile 1 b) Spreadsheet/Wavefile 2

Figure 4.13 SPL in dBA at the IEM as a function of time/ WID excluded for validation-I

4.4.1.7 IEM excluding high WID

Figure 4.14 shows the SPL measured by the internal microphone (IEM) excluding the self-induced noises from the user when the ambiant noise is higher than a threshold value (high-WID).It shows that the results coming from the tests and processed with the Python implementation matched exactly the data processed with Bonnet's Matlab implementation.

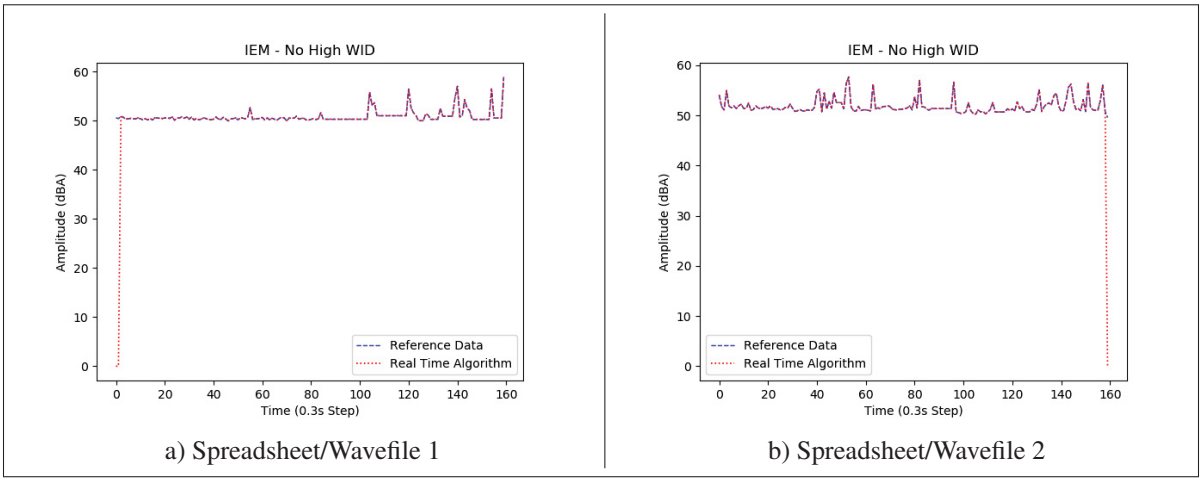

a) Spreadsheet/Wavefile 1 b) Spreadsheet/Wavefile 2

Figure 4.14 SPL given in dBA at the IEM as a function of time with high-WID excluded for validation-I

4.4.1.8 Coherence

The coherence function is defined by the Equation 1.4. Figure 4.15 shows the coherence as a function of frequency for two time frames. It shows that the results coming from the tests and processed with the Python implementation matched exactly the data processed with Bonnet's Matlab implementation.

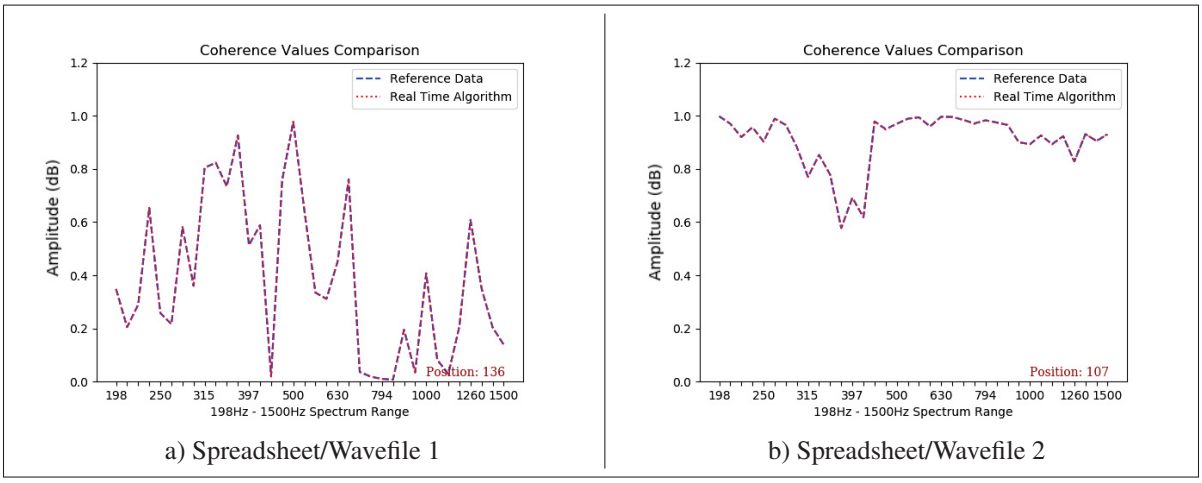

a) Spreadsheet/Wavefile 1 b) Spreadsheet/Wavefile 2

Figure 4.15 Coherence as a function of frequency for two time frames for validation-I

4.4.2 Results from the validation II

This section presents some results obtained in the Validation II task. This task was divided in 4 sections, P1, P2, P3 in the anechoic chamber and P1 in the reverberant room as described in Figure 4.1. The results are presented in a similar way as for Validation I.

4.4.2.1 Delta values

Same definition as in subsection 4.4.1.1.

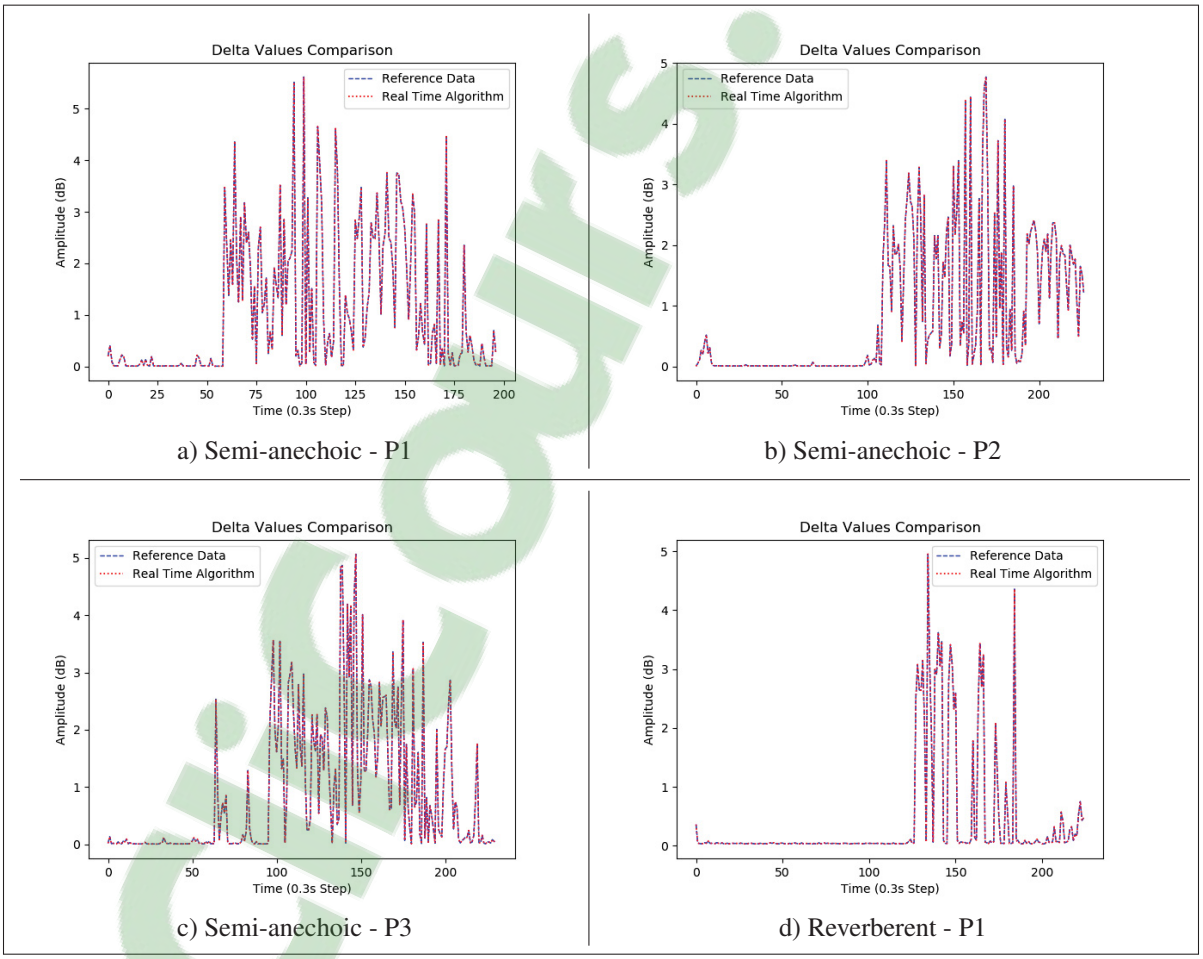

Figure 4.16 Delta values as a function of time for different test scenarios

4.4.2.2 WID Detection

Same definition as in subsection 4.4.1.2.

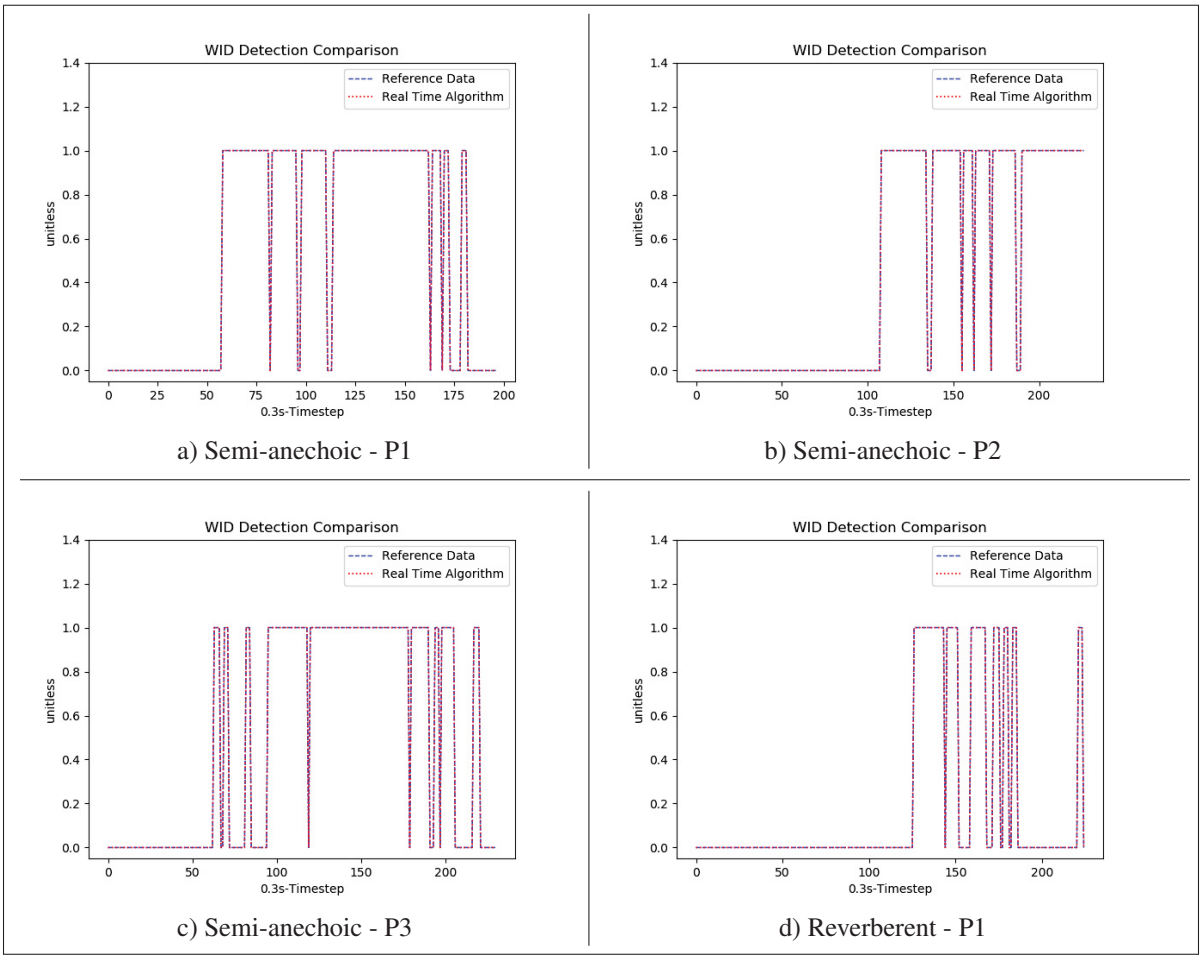

Figure 4.17 WID detection comparison for different test scenarios

4.4.2.3 OEM

Same definition as in subsection 4.4.1.4.

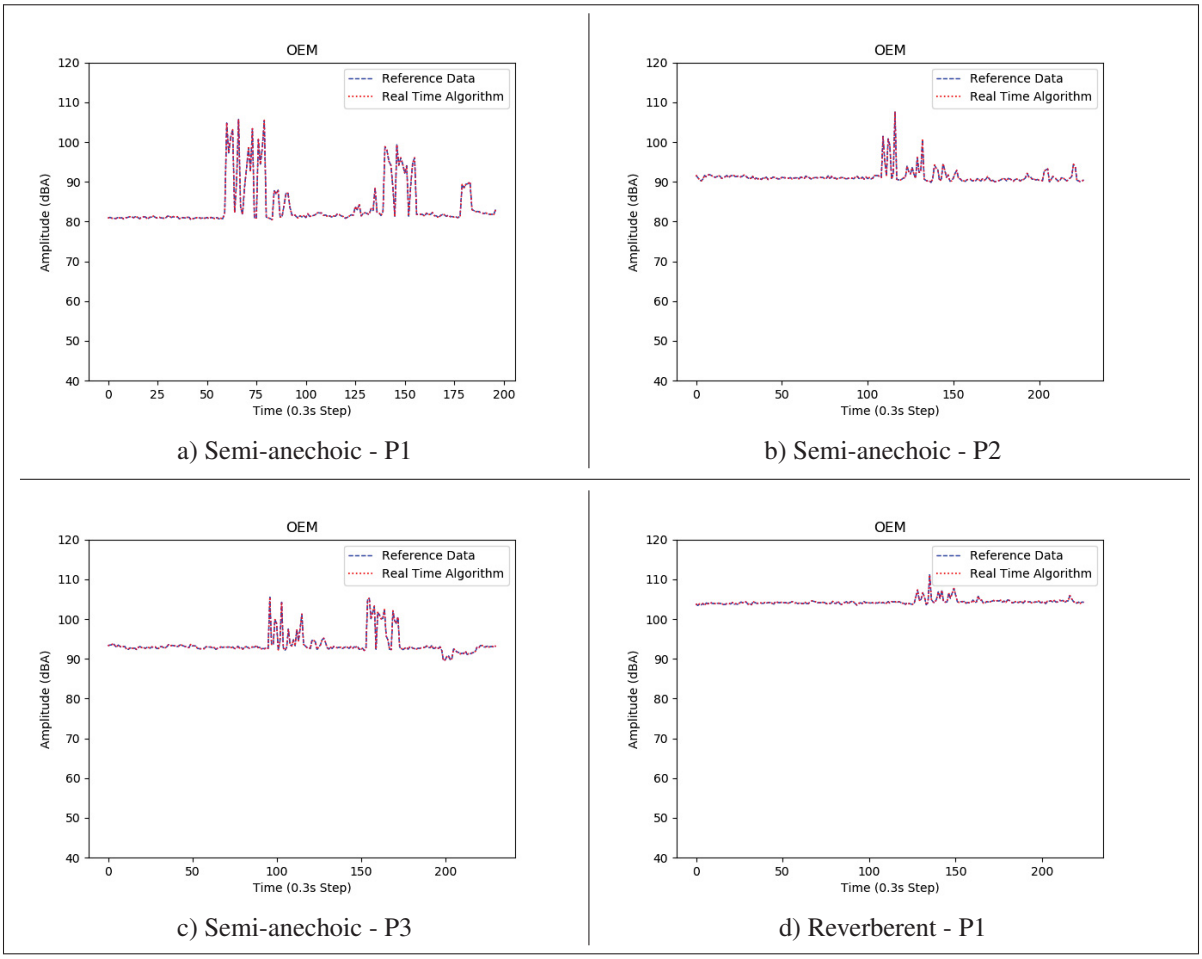

Figure 4.18 SPL measured by the external mic (OEM) as a function of time for different test scenarios

4.4.2.4 IEM Including WID

Same definition as in subsection 4.4.1.6.

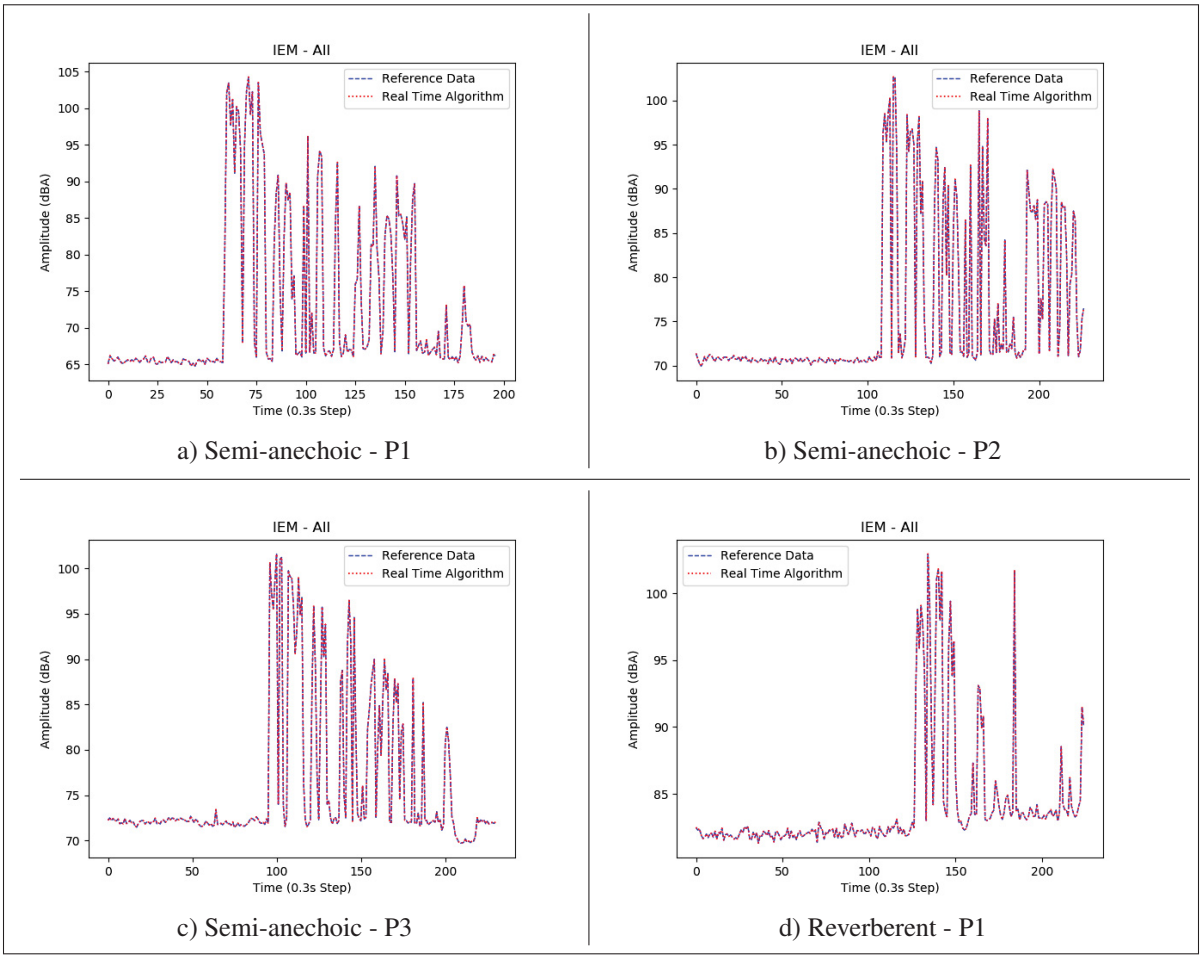

Figure 4.19 SPL measured by the internal mic (IEM) including the WID for different test scenarios

4.4.2.5 IEM Excluding WID

Same definition as in subsection 4.4.1.6.

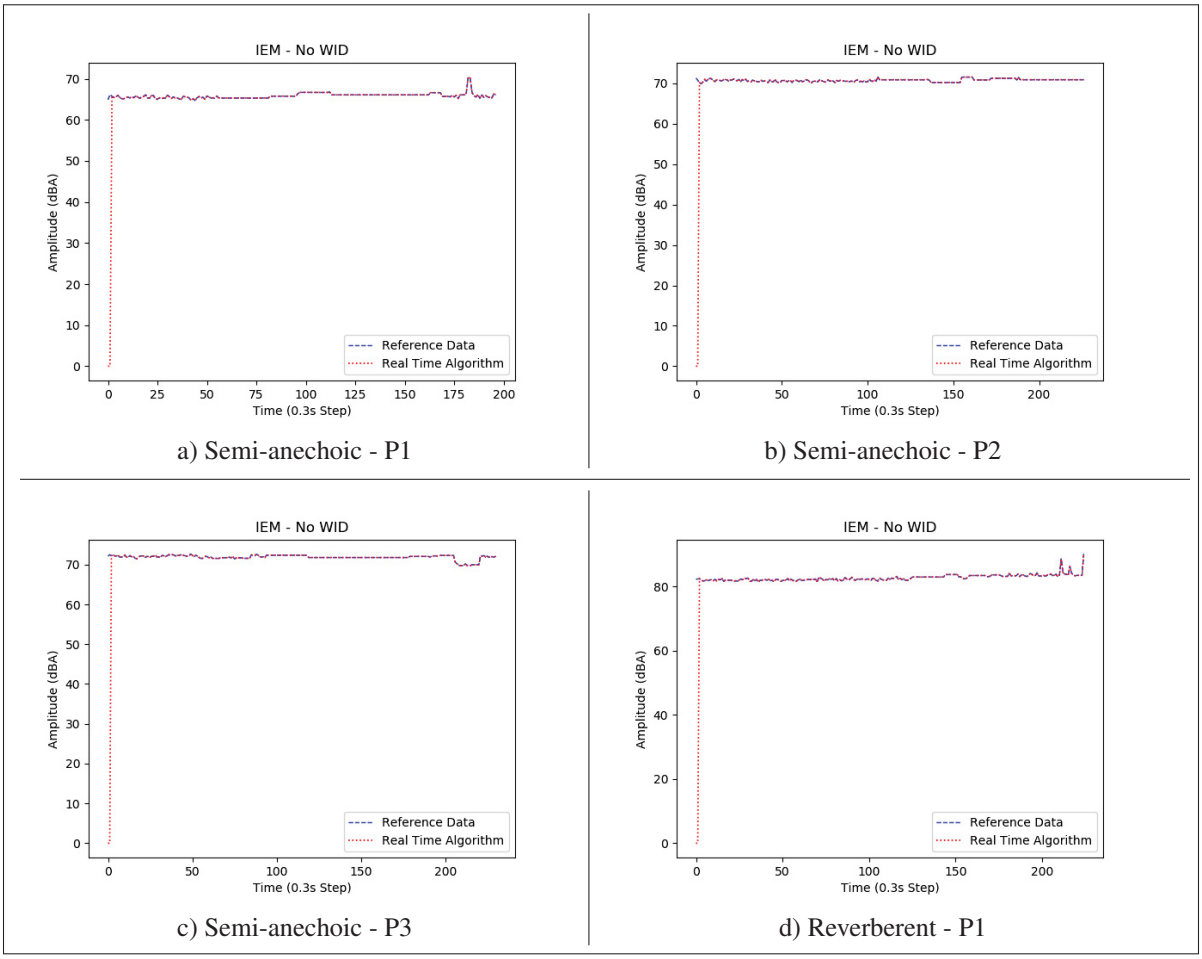

Figure 4.20 SPL measured by the internal mic (IEM) excluding the WID for different test scenarios

4.4.2.6 Coherence function

Same definition as in subsection 4.4.1.8.

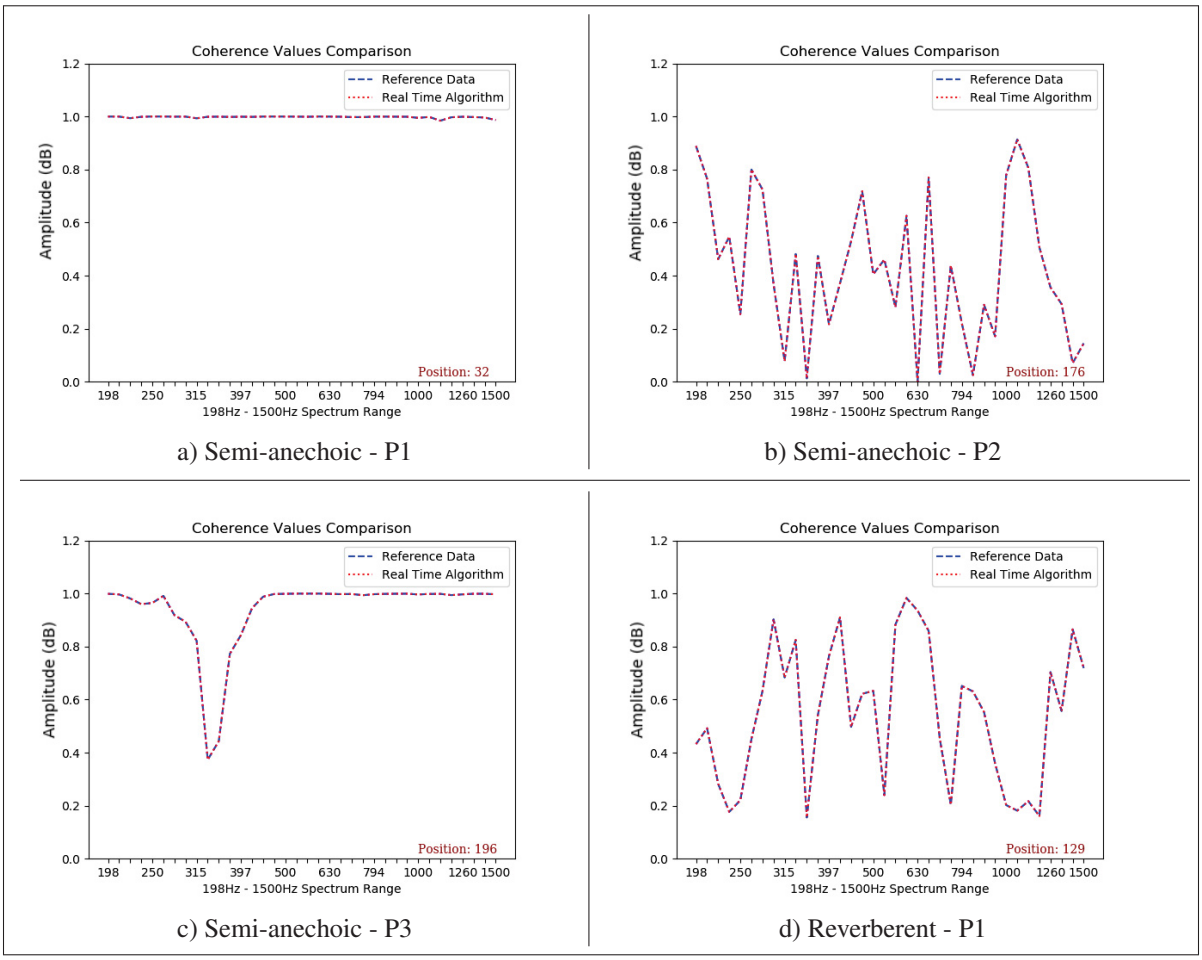

a) Semi-anechoic - P1

b) Semi-anechoic - P2

c) Semi-anechoic - P3

d) Reverberent - P1

Figure 4.21 Coherence values as a function of frequency at different time frame for different test scenarios

CONCLUSION AND RECOMMENDATIONS

The goal of the work presented in this master's thesis was to develop a new and innovative approach to measure the ambient noise exposure in the workplace in an effort to reduce noise induced hearing-loss. Through a new approach proposed in the doctoral work of Bonnet and with the help of the measurement system designed during this master's thesis, in-ear noise exposure assessments can now be performed in a much more reliable way for the benefit of hearing conservation programs.

Results obtained

As pointed out in the Introduction, the goals and sub-goals of this master's thesis were fully achieved, both for the measurement hardware and software, as well as for the experimental validation of the resulting system.

Regarding the hardware development, the design, development and construction of two dosimetric earpiece prototypes were accomplished successfully. These two earpieces make it possible to perform measurements in the earcanal, thus making it possible to assess the level of in-ear noise exposure for different noise scenarios.

As seen throughout Section 2.5 - Prototypes, both prototyping approaches went through stages of consideration and evolution until the entire proposed measurement system (hardware and software) could deliver the same results as those found by Bonnet *et al*. Figures 2.9 and 2.13 illustrate the work's evolution and its complexity, show that the prototypes underwent numerous changes and improvements interactively and that all this was accomplished during this master's thesis. Important points were considered for the usability of the final devices, namely fit and comfort. The correct design parameters regarding microphone positioning in the earcanal and consequently inside the earpiece body were exhaustively developed until the perfect solution was found. Many challenges were overcome in the mechanical design and implementation

phases relating to the robustness, stability and durability of the prototypes, as attested by the fact that these prototypes have "survived" dozens of tests in many different cases and conditions and that they can still be used for further evaluation tests. The mechanical design efforts to achieve reliable functional prototypes culminated in a provisional US patent application covering both the measurement method and the developed earpieces for in-ear dosimetry.

Regarding software development and implementation, a portable real-time measurement system implementing all the algorithms required for the use of the earpieces, equipped with two miniaturized microphones, was eventually delivered.

This system adopted the Python programming language to implement fast and well-grounded functions to reproduce with extreme coherence the findings achieved by Bonnet *et al.* Indeed, Python was chosen for its great capacity to process algorithms in real-time while being sufficiently fast and reliable to perform all the required calculations. In addition to this, it provided tools to develop specific graphical user interfaces (GUI), which was extremely useful for data acquisition in both the calibration procedure and dose measurements.

Acoustical calibration procedures and tools were developed and implemented to ensure reliable noise-dose measurements. The first was a tool to calibrate the earpieces with the reference microphone. This was crucial for reliability as without it no further measurements would be acceptable. The second step of the calibration procedure used the individual in-ear corrections, MEC, which enables users to set their own individual corrections regarding the eardrum reference values, then link the sound pressure levels measured with the two miniaturized microphones with respect to the eardrum, to the "free-field equivalent" levels prescribed in current Occupational Health and Safety (OHS) legislation.

For dose measurements, the implementation and fine-tuning of the algorithm developed by Bonnet *et al.* for the identification of WIDs as well as the implementation of noise dose calcu-

lation routines, considering or not this identification function, were accomplished successfully as well. These measurements used the same GUI as the calibration procedure which not only provided quick readings of the incident noise levels in occluded and non-occluded conditions (using both the OED and CEP prototypes) but also provided monitoring of the dose values for a specific time period. In addition, this tool can provide useful information for noise assessment procedures in the workplace such as instantaneous display of SPL values and dose levels for both ears at the same time. Furthermore, all data collected can be saved in a log file for post-processing purposes and further analysis.

Experimental validation of this work was carried out by integrating the software and hardware elements and then analysing the results of this integration. Validation can be seen as a specific item in the overlapping area of the Venn diagram depicted in Figure 0.1. During measurements with the initial design, it was unfortunately difficult to identify a stable and reliable MEC. This unexpected result led to modifications in the prototypes by first adding a sealing mechanism with a silicone cap (Figure 2.14), which did not particularly behave as expected and thereafter, a vent mechanism (Figure 2.16) was added that has resolved all issues thus far.

Two validation cases were then carried out to verify the performance and accuracy of the implemented functions. The first case (Validation I) used specific data collected by Bonnet *et al*. in an open field environment context. This approach played an important role in the whole validation process, since all the tools needed for the noise exposure assessment were, at the time, only partially implemented and therefore not yet tested.

The second case (Validation II) consisted in testing the two scenarios in controlled laboratory conditions using a semi-anechoic room and a reverberant room. Obviously, these tests did not represent real-life conditions given the controlled parameters such as a perfect room setup and steady sound pressure levels. However, they did help to prove that both the methodology and implementation were at first, headed in the right direction, and ultimately, successful.

Limitations

The limitations of the present work are few but should be mentioned as well. First, the prototypes were only tested on a few subjects, just enough to satisfy the basic requirements of wearability, that is, comfort and fit. The final prototype was not intended to satisfy the requirements associated with a large sample of people nor those of a commercial product.

A second minor limitation is that the prototypes were not designed to be used in extreme work conditions or for heavy duty industrial use, such as an external environment with strong winds or dirty and humid places. These operation conditions would require further research and consideration.

A third minor limitation has to do with the current bundle made up of the ARP3 + Sound Card + Battery pack devices, which could be improved for better portability. Based on all this, it is clear that further research is still needed to overcome these limitations.

Future work

This master's thesis work led to the development of a complete system - hardware and software - capable of performing real-time measurements and calculating acoustic corrections needed for in-ear noise dose measurement in the workplace. Further research in now required to understand how such systems could be deployed in the field and used as part of hearing conservation programs, to better prevent the risk of noise-induced hearing loss for individual workers. Of particular interest is the fact that the system is able to take measurements in real-time, enabling continuous monitoring of the worker's exposure during a work shift. This unique and very new capability offers interesting possibilities to health and safety professionals who will now have access in real-time to the effective noise exposure levels of their workforce and who will have to ensure that these levels are in compliance with occupational health and safety regulations:

how to handle the case of a worker who has reached his allowed daily dose while in the middle of his work shift is one of the many questions that will arise from this new hearing conservation tool.

APPENDIX I

EXPOSURE LIMITS AND CURVES

1. Legislation

Table-A I-1 Maximum allowed exposure acc. to Canadian jurisdiction or provinces Adapted from CCOHS (2019)

Province \Territory	**Maximum exposure level in dB(A) allowed for 8 hour**	**Exchange rated dB(A)**
Quebec	90	5
Canada (Federal)	87	3
British Columbia	85	3
Alberta	85	3
Saskatchewan	85	3
Manitoba	85	3
Ontario	85	3
News Brunswick	85	3
Nova Scotia	85	5
Prince Edward Island	85	3
Island	85	3
Newfoundland	85	5
Northwest Territories	85	5
Territories Yukon	85	3

Table-A I-2 Maximum exposure level and exchange rated values by province \territory
Adapted from Réseau de santé publique en santé au travail (2019)

Province \Territory	**Maximum exposure level in dB(A) allowed for 8 hour**	**Exchange rated dB(A)**
Quebec	90	5
U.S.A. (OSHA)	90	5
ACGIH *	85	3
Allemagne, 1990	85	3
Argentine	85	3
Australie, 1993	85	3
Brésil	85	5
CEE (Communauté Économique Européenne)	85 (87 sous protecteur)	3
Chili	85	5
Chine	70−90	3
Danemark	90	3
Espagne, 1989	85	3
Finlande	85	3
France, 1990	85	3
Grande-Bretagne, 1989	85	3
Hongrie	85	3
Inde, 1989	90	–
Italie	85	5
Nouvelle-Zélande, 1981	85	3
Norvège, 1982	85	3
Pays-Bas, 1987	80	3
Suède, 1992	85	3
Uruguay	90	3

*ACGIH : American Conference of Governmental Industrial Hygienists

2. Curves for dB(A) and dB(C)

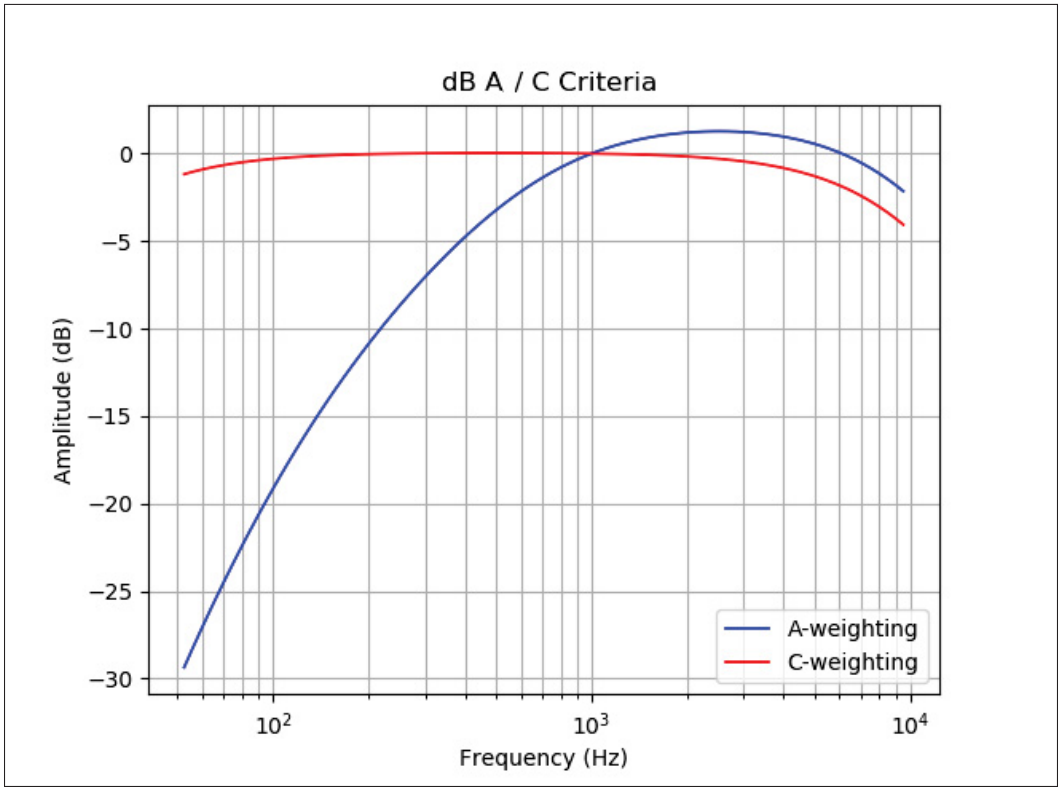

Figure-A I-1 A/C Weighting Curves

APPENDIX II

PROTOTYPING AND FABRICATION

1. Mechanical parts

1.1 Sound card box

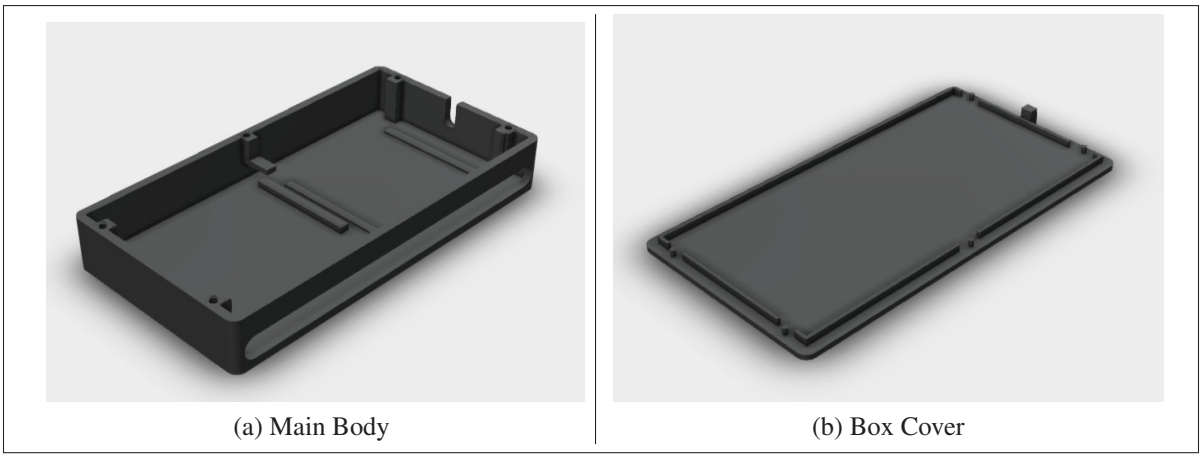

(a) Main Body (b) Box Cover

Figure-A II-1 Plastic box for accommodating the sound card
(CAD files courtesy of Guilhem Viallet - CRITIAS)

1.2 Mini DIN6 connector

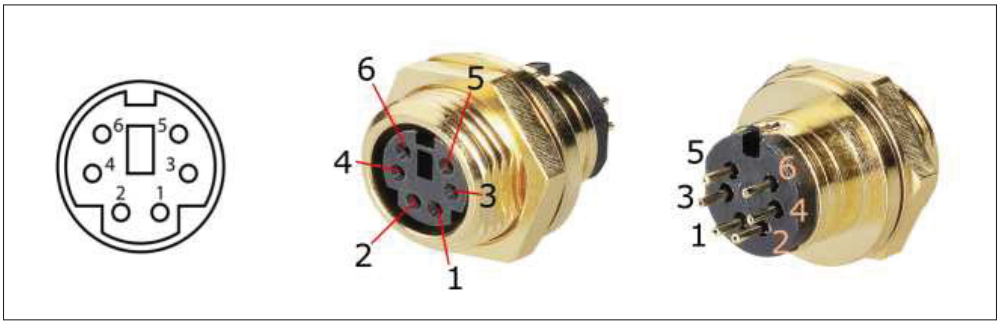

Figure-A II-2 Mini DIN 6-pin female connector and pin-out
Taken from BKL Electronic (2019)

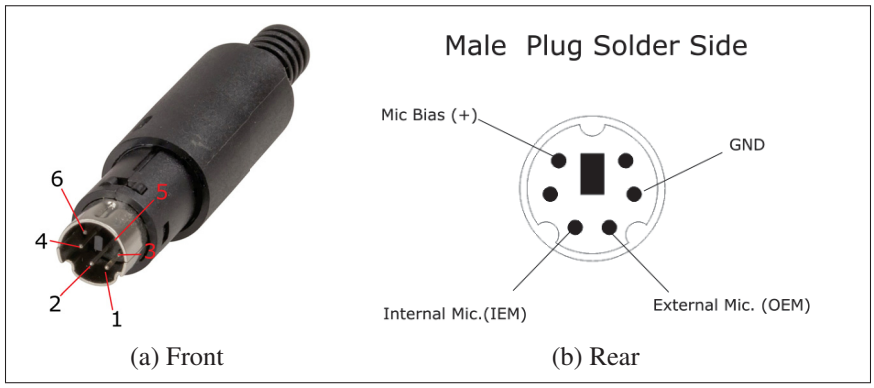

Figure-A II-3 Mini DIN 6-pin male connector and pin-out

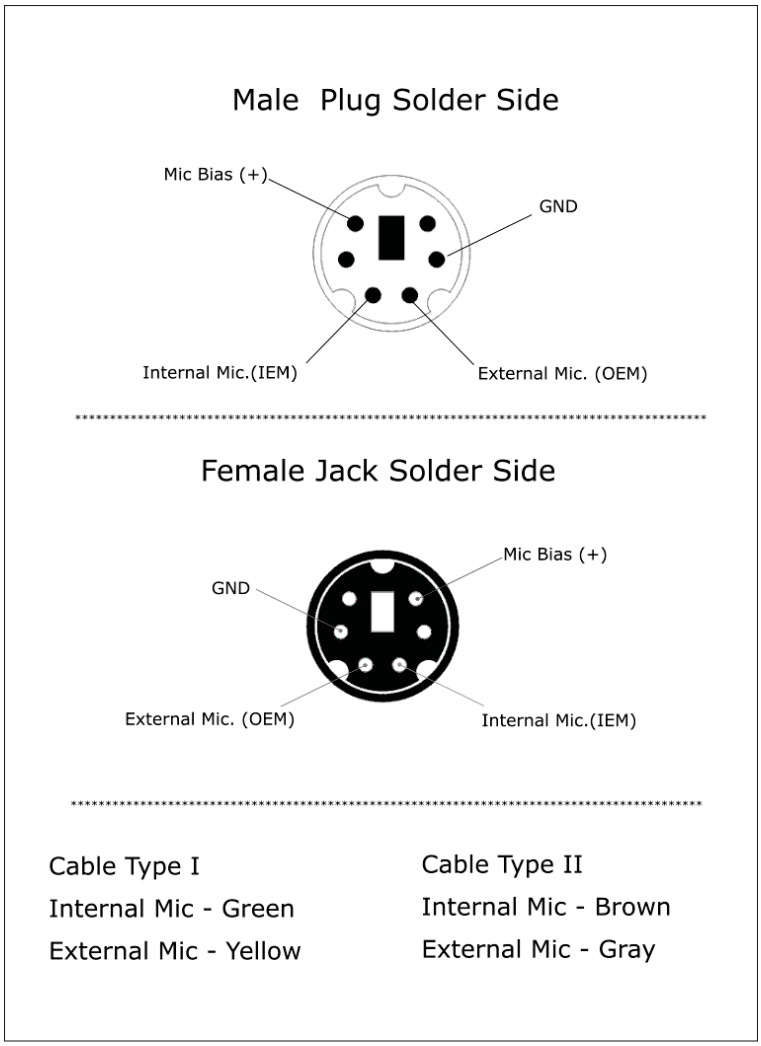

Figure-A II-4 Mini DIN 6-pin Male / Female connectors and cabling details

1.3 Cabling

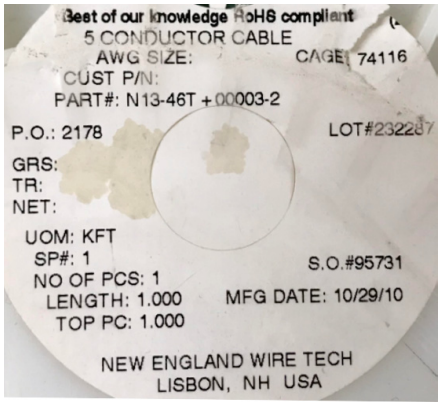

(a) Type-I Cable

(b) Type-II Cable

Figure-A II-5 Examples of cables used in the prototypes

1.4 Assembly holders

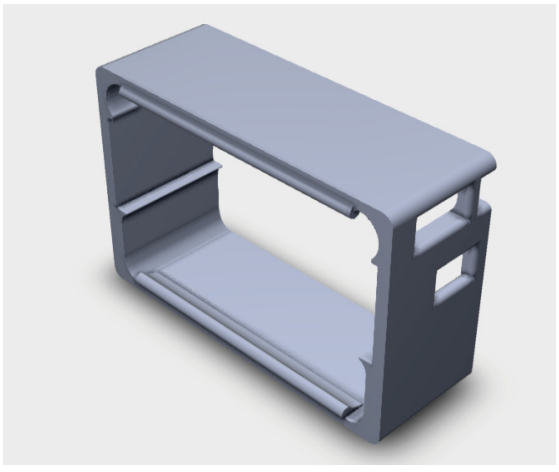

(a) Right Side Holder

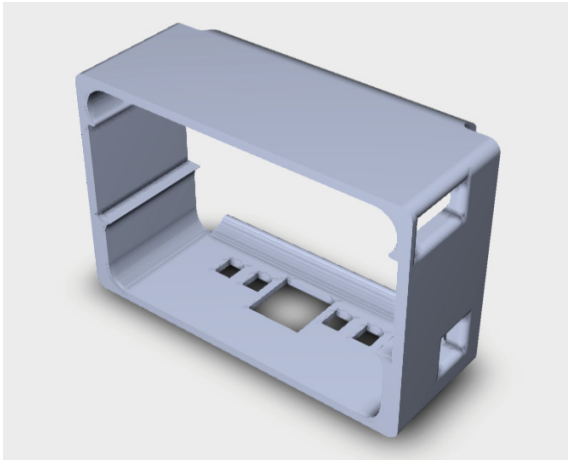

(b) Left Side Holder

Figure-A II-6 Assembly holders for bundling all system parts

1.5 Silicone cap molding

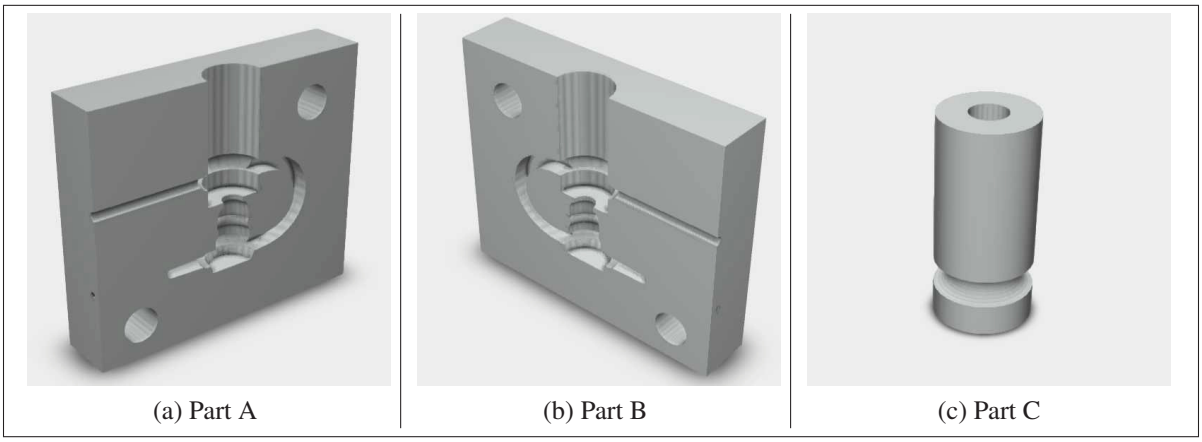

(a) Part A (b) Part B (c) Part C

Figure-A II-7 Molding parts for the fabrication of the silicone cap

1.6 OED

1.6.1 Ear hook

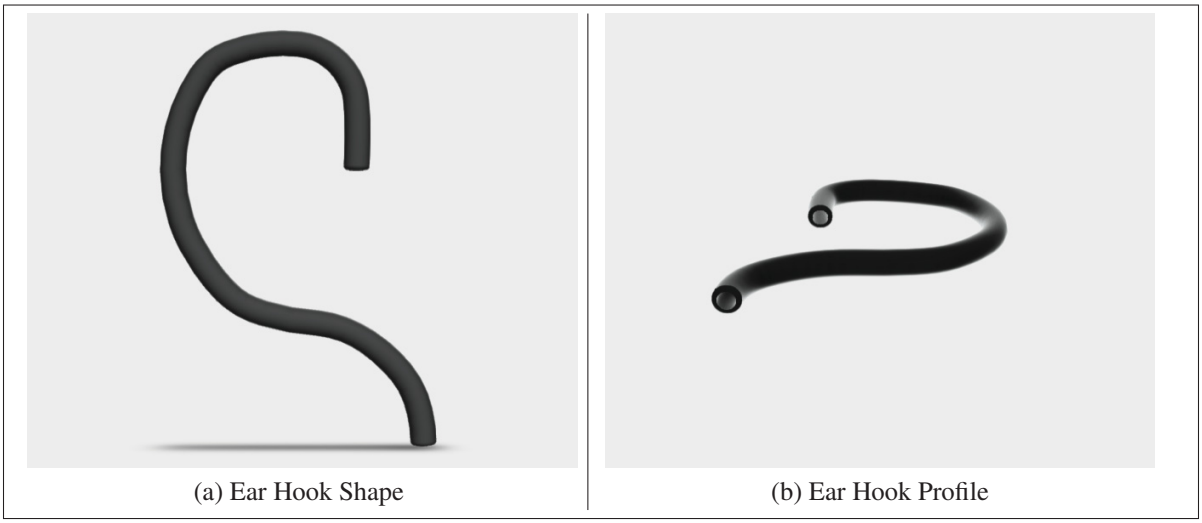

(a) Ear Hook Shape (b) Ear Hook Profile

Figure-A II-8 Ear hook 3D rendering views

1.6.2 Main body

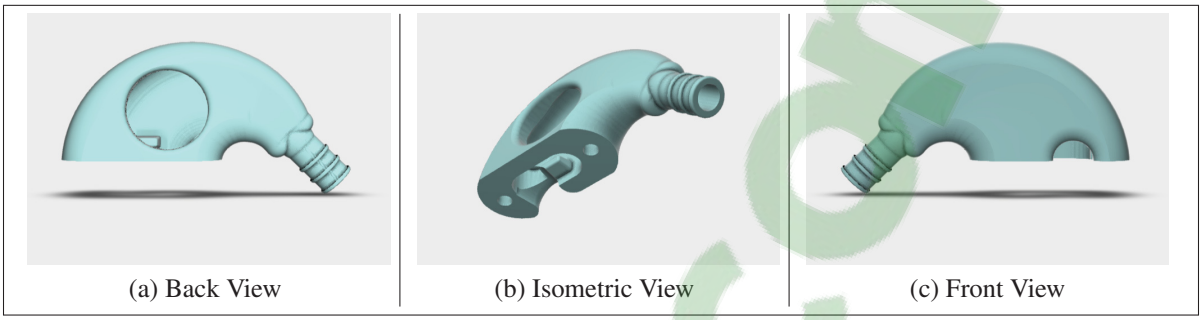

(a) Back View (b) Isometric View (c) Front View

Figure-A II-9 OED and CEP main body 3D rendering views

1.6.3 Upper body

(a) Front View (b) Isometric View

(c) Side View (d) Top View

Figure-A II-10 OED upper body 3D rendering views

1.7 CEP

1.7.1 Upper body

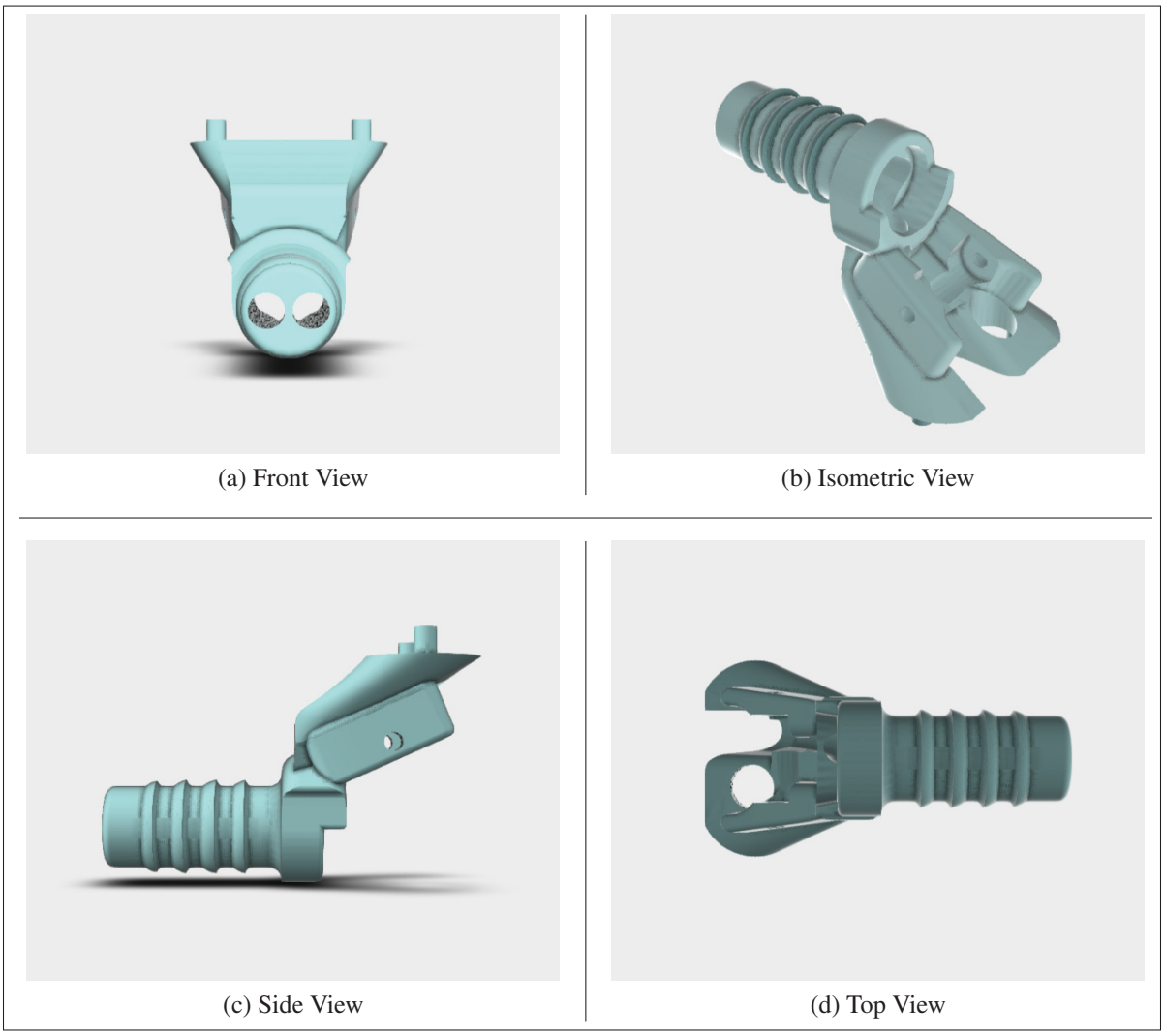

(a) Front View

(b) Isometric View

(c) Side View

(d) Top View

Figure-A II-11 CEP upper body 3D rendering views

1.7.2 Lever

(a) Front View

(b) Isometric View

(c) Side View

(d) Top View

Figure-A II-12 Lever 3D rendering views

1.7.3 Lever locker

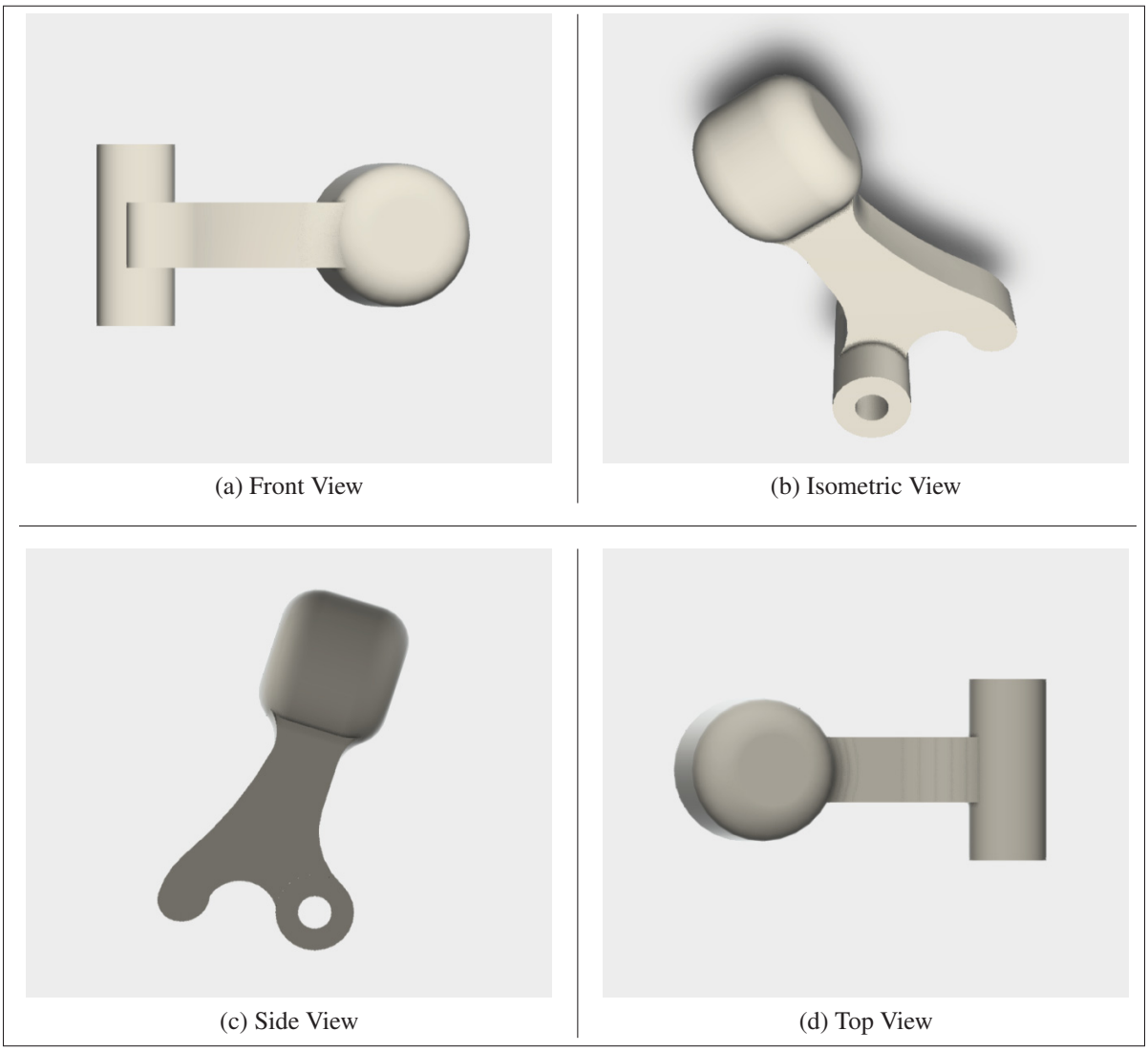

(a) Front View

(b) Isometric View

(c) Side View

(d) Top View

Figure-A II-13 Lever locker 3D rendering views

1.7.4 Rigid cap

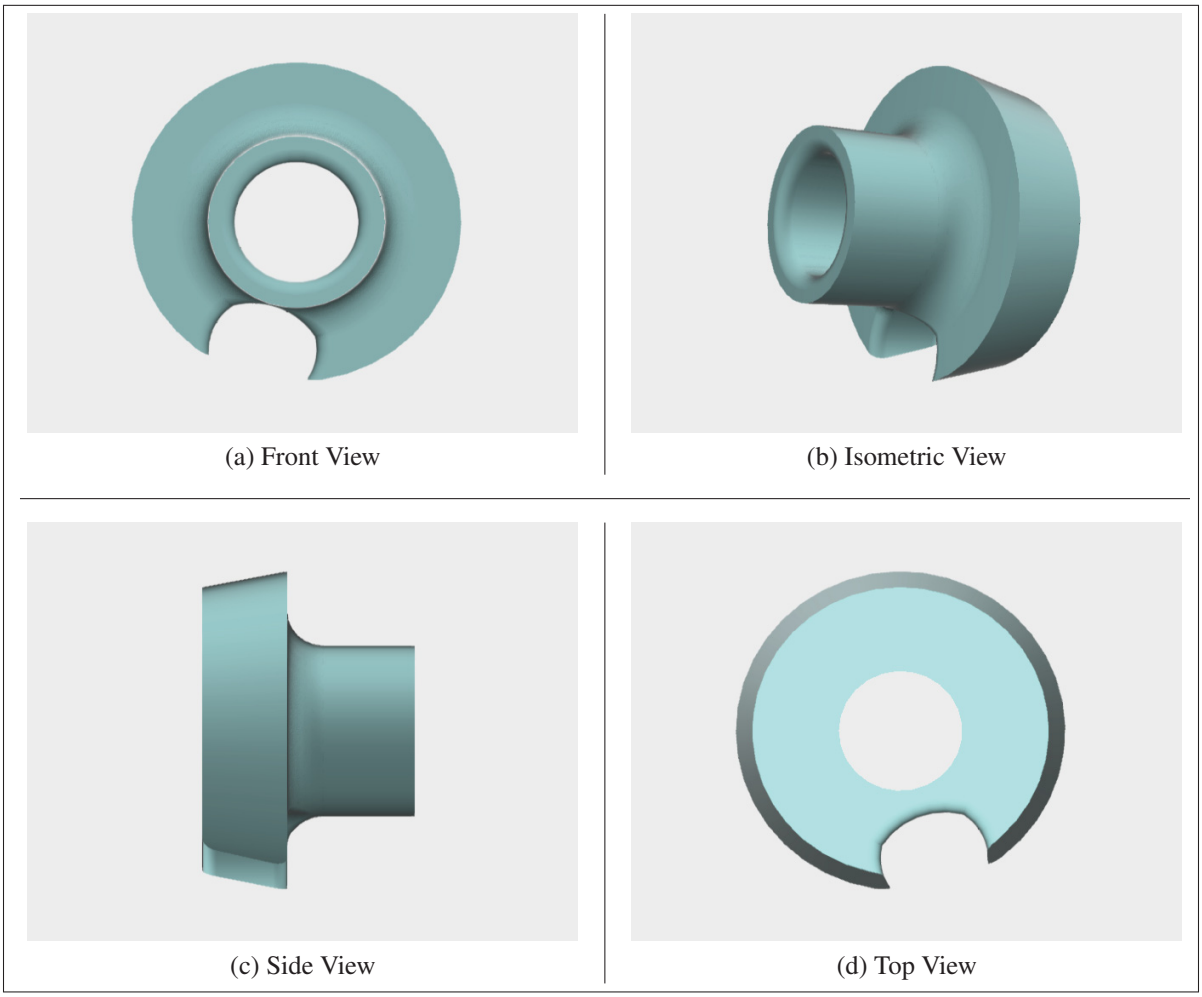

(a) Front View

(b) Isometric View

(c) Side View

(d) Top View

Figure-A II-14 Rigid cap 3D rendering views

1.8 Fabrication

1.8.1 Rubber ring (O'ring)

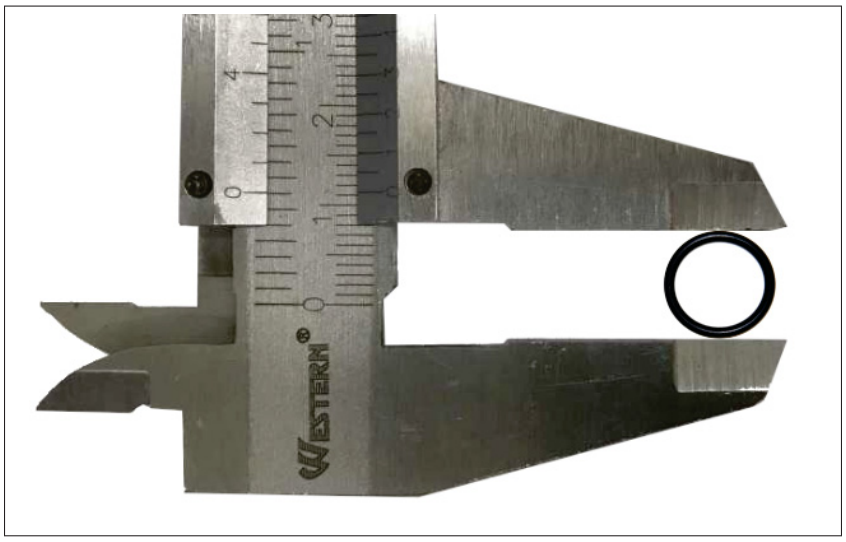

Figure-A II-15 O'ring size

1.8.2 Cap with silicone

Figure-A II-16 Lever filled with silicone

1.8.3 Epoxy

Figure-A II-17 Example of epoxy type

1.8.4 Medical grade silicone

Figure-A II-18 Example of silicone type

APPENDIX III

MINI-DIN6-F ASSEMBLY INSTRUCTIONS

1. Main Work

Figure-A III-1 Main Work: USB opening - Silicone filling - Connectors holes (left) and final assembling with the two holders (right)

2. Mechanical Setup

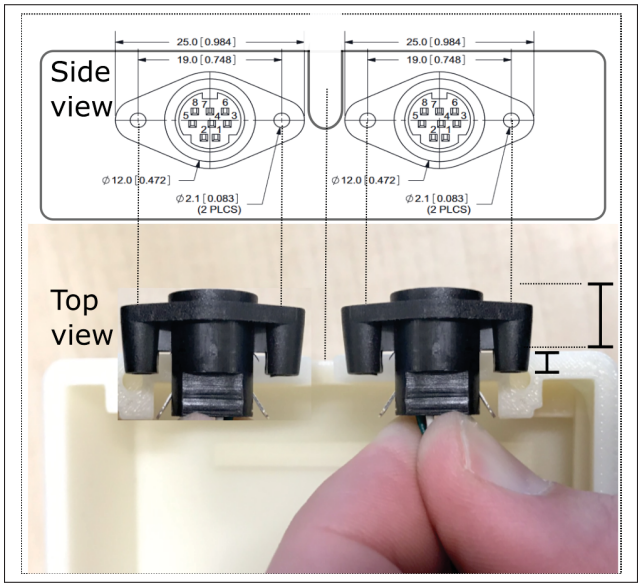

Figure-A III-2 Positioning the mini-DIN6-F on the plastic box

3. PCB Pinout and Connections

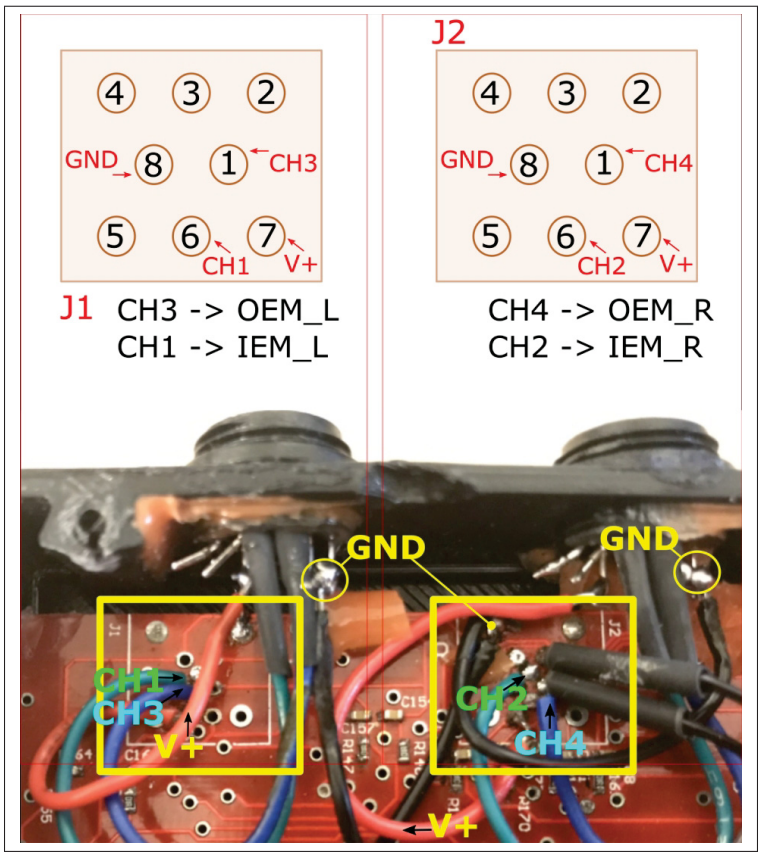

Figure-A III-3 PCB pinout and connections

4. Mini-DIN6-F Pinout (Front View)

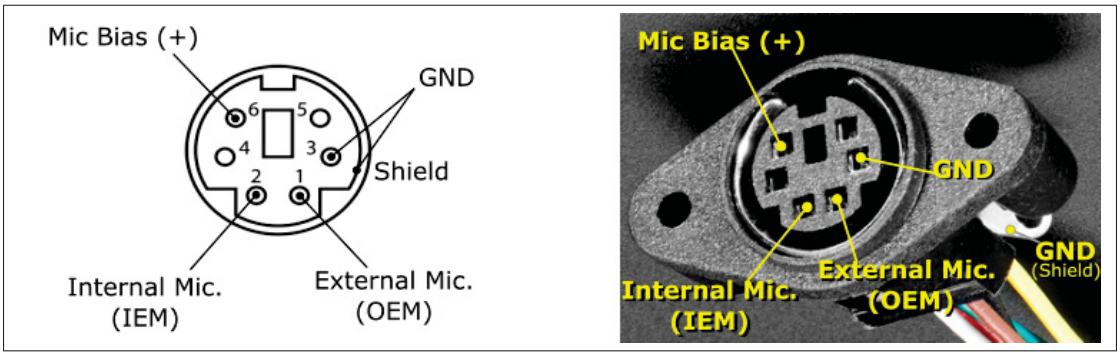

Figure-A III-4 Mini-DIN6-F pinout (front view)

APPENDIX IV

CALIBRATION

1. Calibration room preparation

(a) Mic. Height Pos.

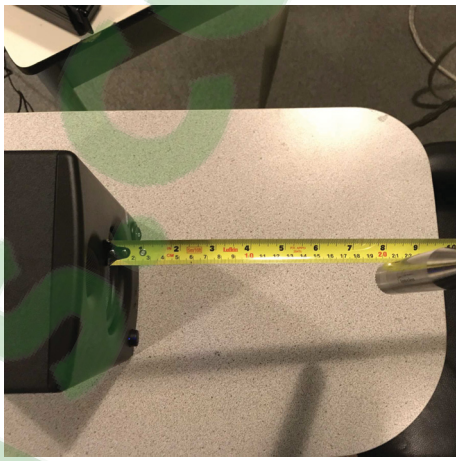

(b) Mic. Lenght Pos.

Figure-A IV-1 Microphones reference positioning

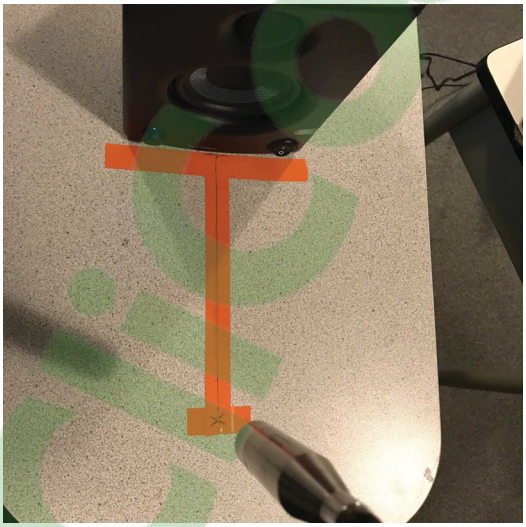

(a) View I

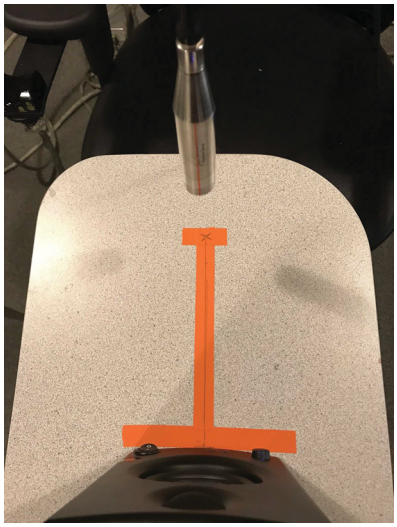

(b) View II

Figure-A IV-2 Positioning strips

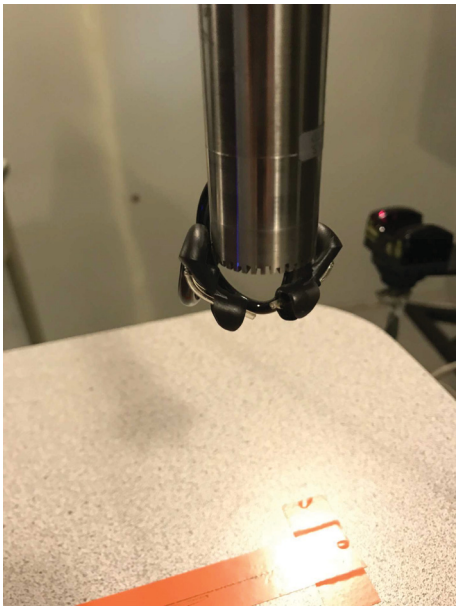

(a) OED

(b) CEP

Figure-A IV-3 Earpieces positioning

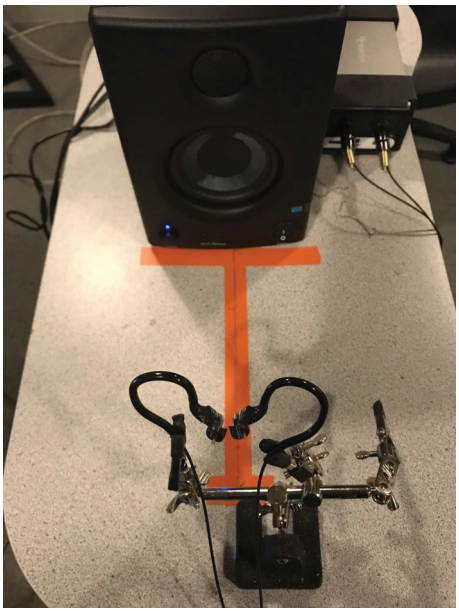

(a) OED

(b) CEP

Figure-A IV-4 Alternative earpieces positioning

APPENDIX V

SOUND CARD

1. Hardware workaround

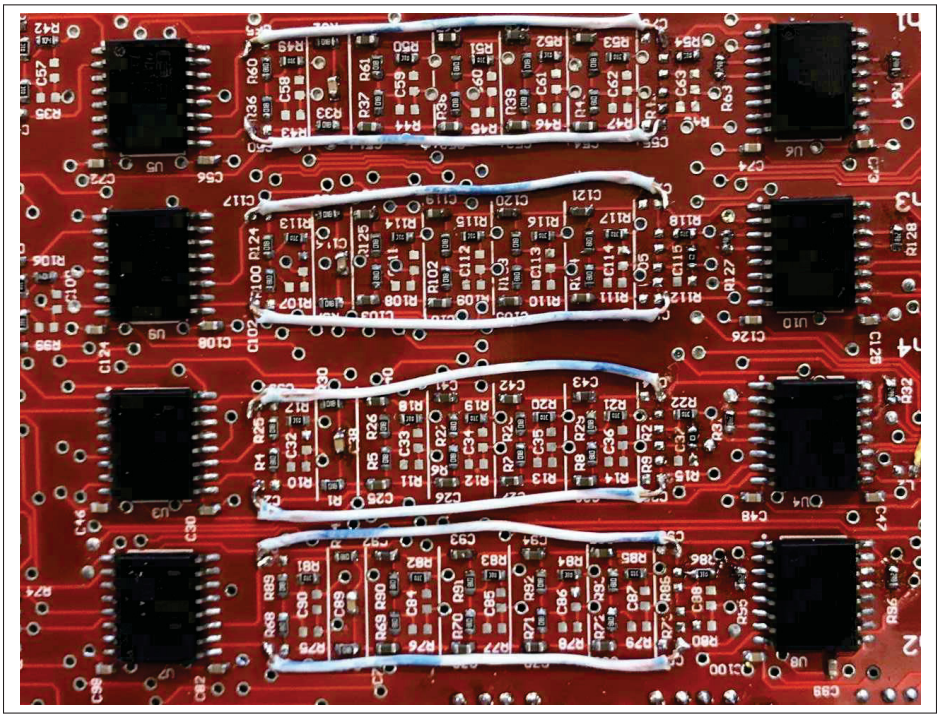

Figure-A V-1 Necessary sound card filter modification

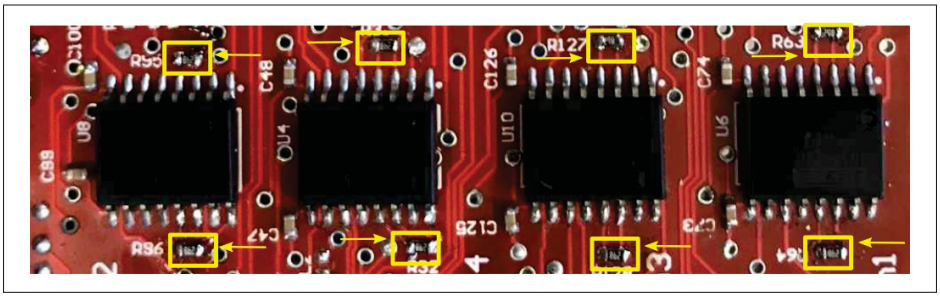

Figure-A V-2 Gain adjustment (all yellow marked resistors must be removed)

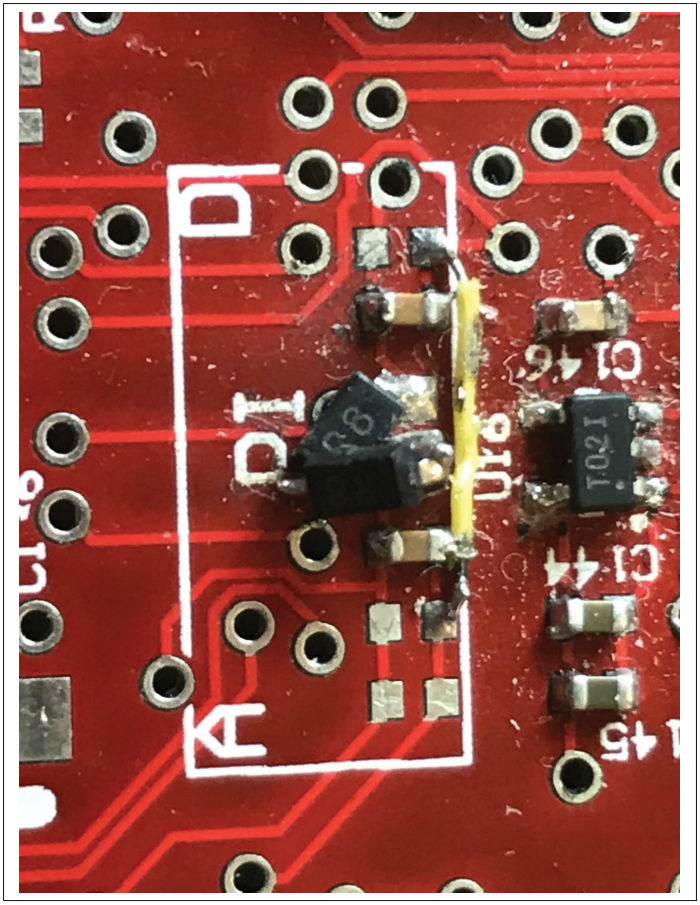

Figure-A V-3 Schottky diode in series in the current hardware

APPENDIX VI

REMOTE ACCESS

1. Remote access

Remote access to the noise exposure values and other results during the operation of the system is an important feature. Since the ARP3 unit does not have its own screen for this purpose, a remote desktop program - VNC Viewer (Real VNC (2019)) - that can be installed on a cellphone as depicted the Figure VI-2, was used to monitor the results remotely. The following steps summarize how to configure the ARP3 and the cell phone for remote operation.

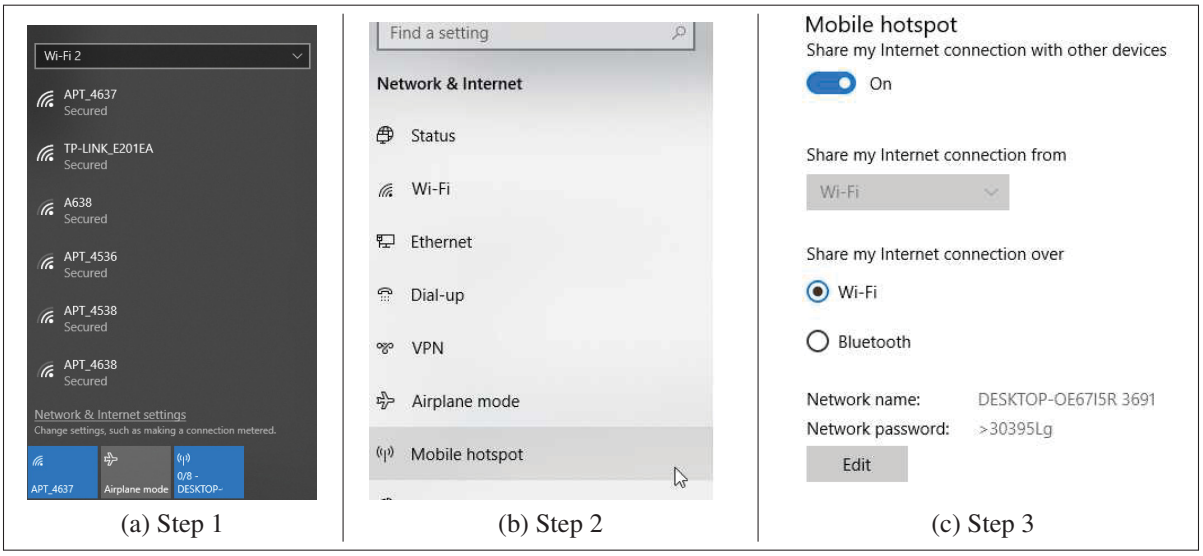

(a) Step 1 (b) Step 2 (c) Step 3

Figure-A VI-1 Remote configuration on ARP3

Table-A VI-1 Remote configuration on ARP3

Procedure	Description
Step 1	"Mobile hotspot" enabled on Windows.
Step 2	Choose "Mobile hotspot" configuration.
Step 3	Enable "Share my Internet connection with other devices" and then choose "Wi-Fi" option.

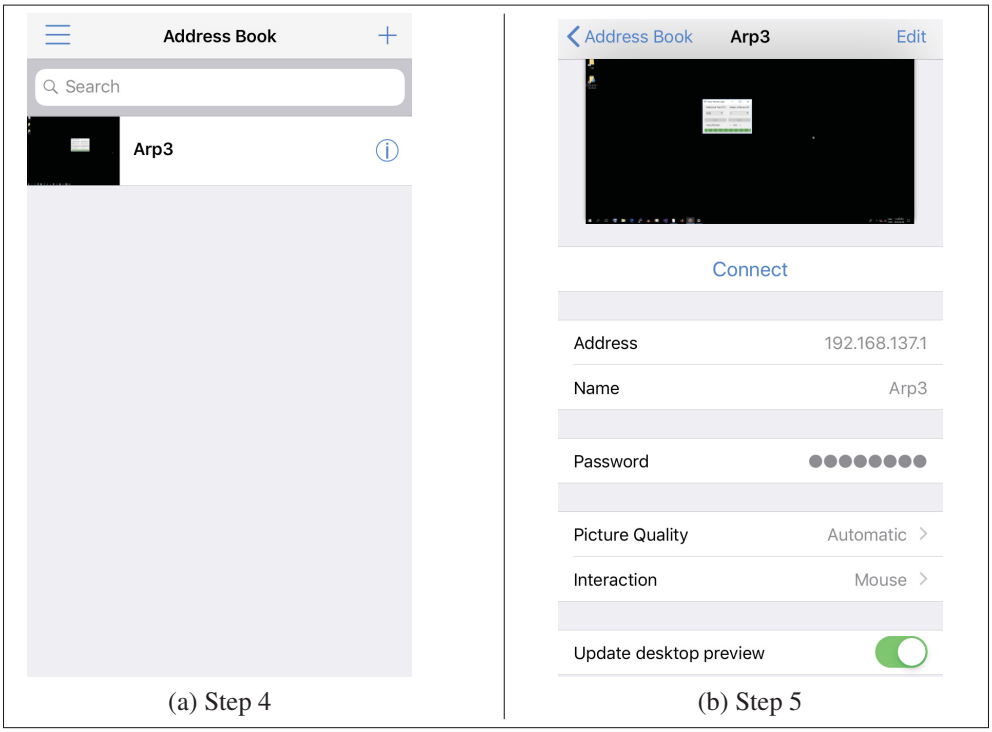

(a) Step 4 (b) Step 5

Figure-A VI-2 Remote configuration on cellphone

On the ARP3 side, only a specific configuration in the wireless (Figure VI-1) network is necessary in order both devices (ARP3 and cellphone) can be connected together and thus data can be visualized in the cellphone screen.

The procedure to turn the computer (Windows OS) into a mobile hotspot is as follows:

Table-A VI-2 Remote configuration on cellphone

Procedure	Description
Step 4	Firstly connect your mobile phone with the Wi-Fi network provided in the Step 3. Open the VNC Viewer application.
Step 5	Click on symbol "+" on the upper right corner and then provide the desired connection name and respective password.

- Navigate to Settings > Network and internet > Mobile hotspot;
- Under the “share my internet connection from”, select either Wifi or Ethernet, though more often than not, you’ll have a wifi connection;
- Turn on “Share my internet connection with other devices”.

BIBLIOGRAPHY

ANSI. (1996). *Measurement Of Occupational Noise Exposure*. ANSI/ASA S12.19. Washington DC, USA: American National Standards Institute.

Ballachanda, B. (Ed.). (2013). *The Human Ear Canal* (ed. 2nd). Plural Publishing.

Benacchio, S., Doutres, O., Le Troter, A., Varoquaux, A., Wagnac, E., Callot, V. & Sgard, F. (2018). Estimation of the ear canal displacement field due to in-ear device insertion using a registration method on a human-like artificial ear. *Hearing Research*, 365, 16–27. doi: 10.1016/j.heares.2018.05.019.

Berger, E. H. (2003). *The Noise Manual*. American Industrial Hygiene Association.

Bessette, R. & Michael, K. (2012). Measure and Intervene: An In-Ear Dosimetry Method That Can Change an OSHA Violation - and Internal Attitudes. *Hearing Review*, 19(4), 46–51.

BKL Electronic. (2019, April 07). bkl-electronic. Consulted at https://www.bkl-electronic.de/warengruppe/din-norm-steckverbinder.

Bonnet, F. (2019). Méthode de mesure individuelle de l'exposition sonore effective intra-auriculaire en milieu de travail [Doctoral dissertation]. Montreal. Unpublished.

Bonnet, F., Nélisse, H. & Voix, J. (2018a). Acoustical corrections to be used for improved in-ear noise dosimetry measurements. *The Journal of the Acoustical Society of America*, 143(3), 1910–1910. doi: 10.1121/1.5036222.

Bonnet, F., Nélisse, H. & Voix, J. (2018b). Individual in-situ calibration of in-ear noise dosimeters. *The Journal of the Acoustical Society of America*, 143(3), 1910–1910. doi: 10.1121/1.5036222.

Bonnet, F., Nélisse, H., Nogarolli, M. & Voix, J. (2019a). Individual in-situ calibration of in-ear noise dosimeters. *Applied Acoustics*, Submitted.

Bonnet, F., Nélisse, H., Nogarolli, M. & Voix, J. (2019b). In-Ear Noise Dosimetry under Earplug: Method to Exclude Wearer-Induced Disturbances. *IJIE (International Journal of Industrial Ergonomics)*, Submitted.

Campione, E. & Véronis, J. (2002). A Large-Scale Multilingual Study of Silent Pause Duration. *SP-2002, April 11-13, Aix-en-Provence*, pp. 199–202.

Canada Labour Standards Regulations. (2019). C.R.C., c. 986. Consulted at https://laws-lois.justice.gc.ca/eng/regulations/C.R.C.,_c._986/.

CCOHS. (2019, April 24). Canadian Center of Occupational Health and Safety. Consulted at https://www.ccohs.ca/oshanswers/phys_agents/exposure_can.html.

Christoph Gohlke. (2019, April 22). Unofficial Windows Binaries for Python Extension Packages. Version: 2.11-cp37-cp37m. Consulted at https://www.lfd.uci.edu/~gohlke/pythonlibs/#pyaudio.

Cirrus Research LLC. (2019, May 01). Dosebadge. Consulted at https://www.cirrusresearch.co.uk/products/dosebadge-noise-dosimeter/.

CSA. (2013). *Measurement of Noise Exposure*. CSA Z107.56-13. Mississauga, Canada: Canadian Standards Association.

École de technologie supérieure. (2018). *U. S. Patent Application n°62/669,177*. Alexandria, Virginia, USA: The United States Patent and Trademark Office.

EU-OSHA. (2003). *Occupational Noise Exposure - Occupational Health and Environmental Control e-CFR*. EU-OSHA Directive 2003/10/EC. Geneva, Switzerland: European Agency for Safety and Health at Work.

Feder, K., Michaud, D., McNamee, J., Fitzpatrick, E., Davies, H. & Leroux, T. (2017). Prevalence of Hazardous Occupational Noise Exposure, Hearing Loss, and Hearing Protection Usage Among a Representative Sample of Working Canadians. *Journal of Occupational and Environmental Medicine*, 92-113.

Formlabs. (2019, April 26). Formlabs printer and materials. Consulted at https://formlabs.com.

GitHub Developers. (2019, April 30). Python Acoustics. Consulted at https://github.com/python-acoustics/python-acoustics.

Honeywell. (2019, April 10). QuietPro QP400. Consulted at https://www.honeywellsafety.com/Products/Hearing/Intelligent_Hearing_Protection/QUIETPRO_QP400.aspx?site=/usa.

Howard-Leight by Honeywell. (2019, April 30). Quietdose. Consulted at https://www.howardleight.com/.

Hubert Pham. (2006, May 02). PyAudio Library. Distributed under the MIT License. Consulted at https://www.lfd.uci.edu/~gohlke/pythonlibs/#pyaudio.

IEC. (2002). *Electroacoustics - Sound level meters - Part 1: Specifications*. IEC 61672-1. Geneva, Switzerland: International Electrotechnical Commission.

Ipoweradd. (2019, April 26). Poweradd Pilot X7. Consulted at https://www.ipoweradd.com.

ISO. (1999). *Acoustics - Estimation of noise-induced hearing loss*. ISO 1999:1990. Geneva, Switzerland: International Organization for Standardization.

ISO. (2002). *Acoustics — Determination of sound immission from sound sources placed close to the ear — Part 1: Technique using a microphone in a real ear (MIRE technique)*. ISO 11904-1:2002. Geneva, Switzerland: International Organization for Standardization.

Knowles Corp. (2019, April 28). FG23652-P16. Consulted at https://www.knowles.com.

Larson-Davis. (2019, April 03). Spark Family of Noise Dosimeters. Consulted at http://www.larsondavis.com/Products/Dosimeters.

Mazur, K. & Voix, J. (2012). Development of an Individual Dosimetric Hearing Protection Device. *Inter-Noise 2012 : The 41st International Congress and Exposition on Noise Control Engineering*.

Microsoft. (2019, April 30). Windows Audio Session API (WASAPI). Consulted at https://docs.microsoft.com/en-us/windows/desktop/coreaudio/wasapi.

Mukerji, S., Windsor, A. M. & Lee, D. J. (2010). Auditory Brainstem Circuits That Mediate the Middle Ear Muscle Reflex. *Trends in Amplification*, 14(3), 170–191. doi: 10.1177/1084713810381771.

Nadon, V. (2015). *Development of a method and algorithms for the combined measurement – inside the ear with a hearing protector – of the noise exposure dose and the induced hearing fatigue as measured with otoacoustic emissions*. (Master's Thesis, École de technologie supérieure, Montreal).

Nadon, V. & Voix, J. (2018). Continuous Monitoring of Otoacoustic Emissions: A Tool to Prevent Hearing Loss. *National Hearing Conservation Association*, 59.

Nogarolli, M., Bonnet, F., Nélisse, H. & Voix, J. (2019). Design And Laboratory Validation Of An In-ear Noise Dosimetry Device. *26th International Congress of Sound and Vibration - ICSV26*.

NoiseMeters Inc. (2019, April 30). dBadge2 PRO Noise Dosimeter. Consulted at https://www.noisemeters.com/product/cel/dbadge/dbadge2-pro/.

NumPy Developers. (2019, April 19). NumPy Library. Consulted at https://www.numpy.org/.

Nélisse, H., Gaudreau, M.-A., Boutin, J., Voix, J. & Laville, F. (2012). Measurement of Hearing Protection Devices Performance in the Workplace during Full-Shift Working Operations. *Annals of Occupational Hygiene*, 56(2), 221–232. doi: 10.1093/annhyg/mer087.

Nélisse, H., Institut de recherche Robert-Sauvé en santé et en sécurité du travail & Direction des communications. (2010). *Étude de la transmission sonore à travers les protecteurs auditifs et application d'une méthode pour évaluer leur efficacité en milieu de travail: rapport*. Montréal: IRSST, Direction des communications.

OSHA. (2019a). *Occupational Safety and Health OSHA Technical - Noise and Hearing Conservation*. Appendix III:A Manual TED01-00-015, Chapter 5. Washington DC, USA: Occupational Safety and Health Administration.

OSHA. (2019b). *Occupational Noise Exposure - Occupational Health and Environmental Control e-CFR*. OSHA 1910.95. Washington DC, USA: Occupational Safety and Health Administration.

Randall, R. B. (1987). *Frequency analysis* (ed. 3). Naerum, DK: Brüel & Kjaer.

Real VNC. (2019, April 30). VNC Viewer. Consulted at https://www.realvnc.com/en/connect/download/viewer/.

Ryherd, S., Kleiner, M., Waye, K. P. & Ryherd, E. E. (2012). Influence of a wearer's voice on noise dosimeter measurements. *The Journal of the Acoustical Society of America*, 131(2), 1183–1193. doi: 10.1121/1.3675941.

Réseau de santé publique en santé au travail. (2019, April 11). Réseau de santé publique en santé au travail. Consulted at http://www.santeautravail.qc.ca/web/rspsat/dossiers/risques-physiques/bruit/lois.

Stinson, M. R. & Lawton, B. W. (1989). Specification of the geometry of the human ear canal for the prediction of sound pressure level distribution. *The Journal of the Acoustical Society of America*, 85(6), 2492–2503. doi: 10.1121/1.397744.

SVANTEK. (2019, March 12). SV102A+. Consulted at https://www.svantek.com/lang-en/product/5/sv_102_dual_channel_noise_dosimeter.html#about.

The Python Standard Library. (2019, April 30). Sound-playing interface for Windows. Consulted at https://docs.python.org/2.6/library/winsound.html?highlight=sound.

Theis, M. A., Gallagher, H. L., McKinley, R. L. & Bjorn, V. S. (2012). Hearing protection with integrated in-ear dosimetry: a noise dose study. *Proc. of the Internoise 2012/ASME NCAD meeting, August 19-22, New York*.

TSI Incorporated. (2018, April 01). The Edge 5. Consulted at https://www.tsi.com/products/noise-dosimeters-and-sound-level-meters/noise-dosimeters/the-edge-5-personal-noise-dosimeter/.

Tympan. (2019, March 30). Open source hearing aid development platform. Consulted at https://tympan.org/.

University of North Carolina at Chapel Hill, L. (2017, April 30). PyQtGraph Library. Consulted at http://www.pyqtgraph.org/.

Vigneault, J. (2007). Pour un meilleur support de la recherche au plan d'action 2006-2008 du réseau de santé publique en santé au travail.

Voix, J. & Laville, F. (2009). The Objective Measurement of Earplug Field Performance. *The Objective Measurement of Earplug Field Performance*, 3722-3732.

Welch, P. (1967). The use of fast Fourier transform for the estimation of power spectra: A method based on time averaging over short, modified periodograms. *IEEE Transactions on Audio and Electroacoustics*, 15(2), 70-73. doi: 10.1109/TAU.1967.1161901.